2006

Geochemical processes in deep water sediment cores from eastern Lake Erie.

Zhe Song
University of Windsor

Geochemical Processes in Deep Water Sediment Cores from Eastern Lake Erie

By

Zhe Song

A Thesis

Submitted to the faculty of Graduate Studies and Research through the Department of Earth Science in Partial Fulfillment of the Requirements for the Degree of Master of Science at the University of Windsor

Windsor, Ontario, Canada

2006

Your file Votre référence
ISBN: 978-0-494-17035-9
Our file Notre référence
ISBN: 978-0-494-17035-9

Abstract

Heavy metal pollution is particularly significant in Lake Erie. Sediments act as both sink and source for metal contaminants. Sediment core samples were collected in May and June, 2004, from the eastern basin of Lake Erie in order to assess the mobility of heavy metals in benthic ecosystems. Five extractions were applied to solid phase analysis including acetic acid, ascorbic acid, sodium dithionite, nitric acid/oxalic acid and total digestion.

Pore water and solid data revealed that mobility of heavy metals was influenced by redox reactions. Manganese, Fe and S were the crucial elements for Eh profiles. Distributions of trace metals were affected by the oxidization and reduction of Mn and Fe. Three zones were identified by the profiles of dissolved Mn and Fe: Mn oxidation, Mn reduction and Fe reduction. Cadmium had high mobility in the Mn oxide zone while Ni and Co were released with reducible Mn. Solid extractions indicated that anthropogenic pollution has improved in Lake Erie; reactive Mn and Fe oxides remobilize trace metals; the distribution of trace metal oxides are associated with the oxides of Fe, Al and Si. Comparison between ICP-OES and ICP-MS suggest that ICP-MS was much more suitable for trace element analysis, on the contrary, ICP-OES worked better for major element determinations; both methods suffered matrix effects.

Dedication

To my parents, wife and son

ACKNOWLEDGEMENTS

First and foremost, I would like to express my gratitude to my advisors, Dr. Brian Fryer and Dr. David Fowle, for all their advice and support during the time I spent at the University of Windsor.

I would like to thank my committee members Dr. Ali Polat and Dr. Ken Drouillard for their constructive comments and criticisms.

Special thanks and deep appreciation goes to Sean Crowe, Andrew O'Neil and Shuangquan Zhang for their valued advice and help.

A lot of thanks go to J.C. Barrette, Dr. Joe Gagnon, Dr. Zhaoping Yang, Ezra Kulczycki, Paul Kenword, Christina Smeaton, Melissa Price and Juan Carlos Ordonez Calderon for their patience and support in lab work.

Thanks to Dr. Jan Ciborowski, Carolyn Foley, Carl Yanch and Hans Bieberhofer for their help in field work.

Thanks to Crew of Canadian Coast Guard Ship LIMNOS for their help and hospitality.

Thanks for my family for love and continued encourage and to my friends Dr. Ilhami Yildiz, Mary Lou Scratch, Sonia Melacon, Carrol Hand, Diana Benz, Arne Sturm and Fujian Ma, who made me to feel like home here.

Last but not least, I want to thank Sharon Horne and Dr. Maria Cioppa for helping me through the bureaucratic network.

TABLE OF CONTENTS

LIST OF FIGURES

LIST OF TABLES

Chapter 1: Introduction

Freshwater remains one of the world's most precious commodities, as populations expand at ever increasing rates and with it, the need for this limited resource. North America possesses a significant fraction of this global resource in its Great Lakes. The formation of these lakes began nearly 14,000 years ago [Bolsenga, 1993] with the recession of the large ice sheets associated with major glaciations that impacted much of Canada and the upper Midwest of the United States. A vital economic, biologic and hydrologic link in the Great Lakes system, Lake Erie was the first of the Great Lakes formed as these glaciers retreated to the north [Bolsenga, 1993]. In its modern form it accepts water from Lakes Superior, Michigan, and Huron via the Detroit River and discharges it into Lake Ontario via the Niagara River (Fig. 1.1).

Lake Erie, the shallowest of the Great Lakes has a somewhat complex bathymetry that has led to classification of three distinct basins. The western basin which lies west of Pelee Island, Ontario is particularly shallow with an average depth of 7 meters [Bentley, 2000]. The average depth of the central basin, which stretches between Pelee Island and Long Point, Ontario, is 18 meters [Bentley, 2000]. East of Long Point lies the deep eastern basin, with an average depth of 36 meters and a maximum depth of 63 meters [Bentley, 2000]. The distinct morphology of the lake in turn leads to unique diagenetic behavior within the basins due to sediment focusing and organic matter deposition.

Lake Erie is an important regional, national, and international resource, as it is part of the 2,000-mile long Great Lakes system, which contains nearly 20 percent of the world's fresh surface water. Approximately 13 million people live in the Erie drainage

basin, and 39 percent of the Canadian shoreline and 45 percent of the United States shoreline is devoted to residential use. [Bentley, 2000; Bolsenga et al., 1993] Since Lake Erie's shores remain home to a heavy concentration of industry such as auto and steel production, it has received large anthropogenic inputs of metals, fertilizers, organic matter, sewage, and other contaminants from sources within and outside the watershed for years [Nariagu et al., 1996]. By the mid-twentieth century, Lake Erie had even been announced to be "dead" by several sources due to extreme eutrophication and the accompanying oxygen depletion at depth [Bentley 2000]. Among all of these of contaminants in Lake Erie, heavy metals have significant impacts in aquatic environments due to both their toxicity and their ability to bioaccumulate [Fangueiro et al., 2002]. Recent reports suggest Lake Erie ranks second in contamination by metals, in the Great Lakes [Bentley, 2000; Rossmann and Barres, 1988].

The introduction of metallic pollutants into aquatic ecosystems results from a variety of sources: atmospheric deposition, groundwater, surface runoff, direct injection or dumping and precipitation. Once introduced into the ecosystem, most metals are actively deposited into the sediments via sorption to particulate matter. With deposition in the sediments the metals are subjected to a number of early diagenetic processes resulting from the oxidation of organic matter and the transfer of electrons to terminal electron accepters (e.g. sulphate, iron oxides, nitrate). During the course of these diagenetic reactions metals are redistributed among a variety of solid reservoirs including: (1) bound to adsorptive and exchangeable phases (2) bound to carbonate phases (3) bound to oxides, (4) bound to organic matter and sulphides, and (5) bound to detrital or lattice metals (Gibs, 1973). However not all metals find irreversible deposition in the sediments

and instead can be accumulated by benthic organisms to toxic levels. Therefore both the bioavailability and subsequent toxicity of the metals have become the major research topic associated with sediments [Kemp and Swartz 1988, Berry et al 1996].

Recent advances in metal toxicity research recognize that the total metal concentration of sediment can not be strictly used to assess the impact of heavy metals on the aquatic ecosystem of interest. The potential health and environmental hazard of heavy metals instead depends on speciation of the metal and in particular the activity of free metal ion (although methylmercury is a notable exception) [Laxen and Harrison, 1981; Knight and McGrath, 1995; Parker and Pedler, 1997]. For example, metals such as lead, zinc and cadmium are actively cycled via microbial metabolism and their mobility depends strongly on their speciation rather than total element concentration e.g. sorbed, complexed by organics, or sequestered in a solid phase. [Galan et al., 2003, Garcia et al., 2005]. Specifically there are several factors that strongly affect the mobility of metals in the environment [Gabler, 1997; Ma, 2004; Garcia et al., 2005; Sahuquillo et al 2003]:

1. The mineralogic and chemical composition of the sediment.
    a. Chemical parameters include: pH, alkalinity, cationic exchange capacity (CEC), organic matter content and redox potential. For instance, reduction in redox potential may lead to changes in metal oxidation state, formation of new low-soluble minerals, and reduction of Fe, resulting in release of associated metals (Amrhein et al., 1994; Baumann et al., 2002; Masscheleyn et al., 1991); a decrease in pH (e.g., an effect of acid rain) may cause a release of metals from complexes and from solid matter surfaces by increased competition for sorption sites by the H^+ ion [Prokop et al 2003].

b. Physical parameters include: temperature, porosity, bioturbation, and sediment sorting. Sediment disturbance or dredging, can also lead to both the desorption and oxidation of contaminant and nutrient species (Morin and Morse, 1999; Bonnet *et al.*, 2000; Saulnier and Mucci, 2000)

2. The form of initial introduction of the metal: e.g. soluble or particulate.

3. Diagenetic processes, e.g. adsorption-desorption, precipitation, complex and ion-pair formation or microbial metabolism. (Klinkhammer 1980, Sawlan and Murray 1983, McKee et al 1989, Taylor et al 2003).

At present, organic matter as well as Fe and Mn oxyhydroxides are thought to be the most important reservoirs in freshwater sediments for the binding of metals [Wen et al., 1999]. Sulfide in sediments has been regarded as a crucial partitioning phase of metals in sediments [Di Toro et al., 1990; Ankley et al., 1991; Allen et al., 1993] although its influence in freshwater settings has not been well documented. Indeed, the relationship between the concentration of acid volatile sulfide (AVS) and that of the metals that are released from marine sediment has been used to predict metal bioavailability and toxicity in anoxic sediments.

Geochemists must therefore move forward to develop quantitative and reproducible methods to evaluate diagenesis and bioavailability in aquatic sediments. To date most of the work in this area has focused on functional chemical extractions to evaluate heavy-metal mobility in sediments. Various extractions have been developed to assess the mobility/availability of heavy metals in sediment samples; e.g. single extractions [Loring and Rantala, 1992; Tack and Verloo, 1996; Dassenakis et al., 2003] and sequential extractions [Tessier et al., 1979; Kersten and Forstner, 1986; Ure et al., 1993; Filgueiras

et al., 2002]. Comparison of the effectiveness of a variety of these extractions in evaluating sediment chemistry of Lake Erie will be a focus of thesis research presented here.

There have been several studies of metal geochemistry of sediments in Lake Erie, many of which had their focus on the western basin of Lake Erie which represents one of the most heavily impacted ecosystems in the Great Lakes Basin. Included in these studies are some studies of pore water geochemistry of heavy metals [Matisoff et al., 1980] and a study which combined pore water and hydrochloric acid-extractable data to interpret the mobility of trace and major metals in surficial sediments of western Lake Erie. [Lum et al., 1985] However, to date there has not been a study which combines pore water geochemistry and functional extractions to interpret heavy metal geochemistry in the eastern basin of Lake Erie.

For my thesis study, sediment samples and pore water chemistry were collected and measured respectively in the eastern basin of Lake Erie. Novel functional extractions and in situ pore water chemistry measurements were utilized to interpret the geochemistry of these sediments and to examine the differences between a series of extraction techniques. The specific objectives of our study include:

1. Analyze pore water geochemistry of sub-cores from the eastern basin as a function of depth to test the implicit assumption that the oxidation zone that occurs near the surface of sediment and the redox behavior of Mn and Fe affect the dissolution and mobility of trace metals in pore water, such as Ni, Co and Cd.

2. Evaluate metal mobility in sediments as function of depth through a series of different chemical extractions to determine the correlation of extracted fractions of various elements with major cations such as Mn and Fe and hence the role of processes such as redox, in metal sequestration.

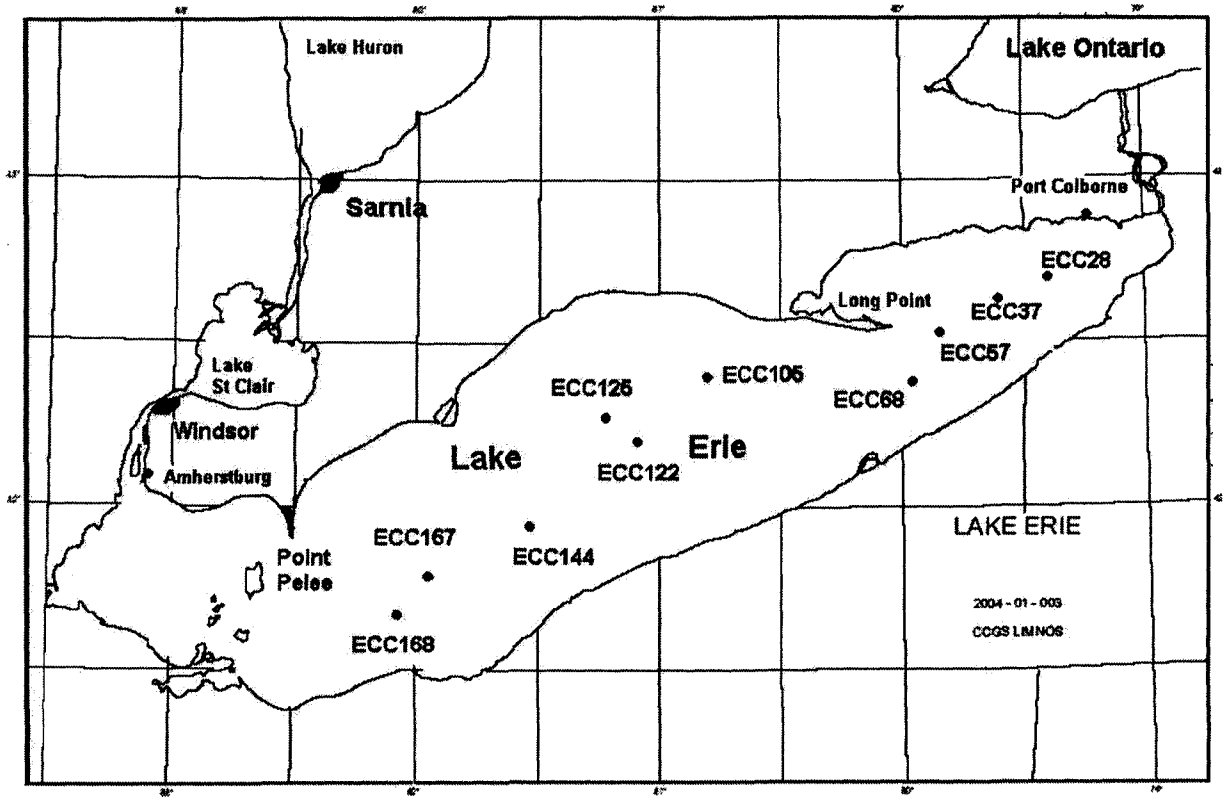

Figure 1.1: Geographic Setting of Lake Erie [Cruise Plan]

Chapter 2: Sampling and Methodology

2.1 Sampling

2.1.1 Sampling site selection

As the deepest basin in Lake Erie, the eastern basin of Lake Erie has unique characteristics when compared with the western and central basins. For example, the sedimentation rate in the eastern basin is higher; the bottom waters of the eastern basin are thicker and colder, and may maintain higher oxygen levels throughout the summer [Bolsenga et al 1993]. This is in contrast with the central basin where up to 90 percent of the bottom layer can become devoid of oxygen. In addition, the eastern basin may act as the catchment of contaminants coming from the central and western basins. Research focused on the eastern basin may help us to understand the fate and transport of contaminants in Lake Erie and in turn help in the efforts to remediate the whole Lake Erie ecosystem.

In this project, sediments were collected for geochemical and mineralogical analysis by box corer from Canadian Coast Guard's principal great lake research ship, Limnos in eastern Lake Erie during sampling cruises, June 2004. Sampling stations were selected around the central line of the eastern basin in Lake Erie where the deepest water occurs (Fig. 2.1). The goal for sampling station selection was to have sediment sampling sites in areas of fine-grained sediment accumulation [Mudroch and MacKnight, 1994; Mudroch and Azcue, 1995]. Fine-grained sediments (i.e. silt and clay) accumulate in areas of low energy due to energy-controlled processes. In most lakes, such an accumulation area is

usually found at the deepest points of the lake. Table 2.1 presents information on the sampling sites.

2.1.2 Samplers

Box cores are gravity cores that were designed for collecting large rectangular sediment cores in biological and geological studies at various water depths, variable penetration rates, and different sediment types. Due to these factors box cores are ideal for this study as the sediment-water interface is generally minimally disturbed by this sampling method. The box corer was operated from remotely on the vessel with a powered winch because of its heavy weight, and size. There are two basic designs of the closing mechanism of the box core: the Ekman design and the Reineck design [Mudroch and MacKnight 1994; Mudroch and Azcue 1995; Taft and Jones 2001]. An Ekman designed box corer was used to collect sediment samples at the bottom of Lake Erie in our sampling. It is composed of a stainless steel box with a pair of jaws and free-moving, hinge flaps. The spring-tension, scoop-like jaws are mounted on pivot points on opposite sides of the box. The jaws are held open by stainless steel bars and can be triggered and closed automatically when it reaches the bottom. After closure, the jaws meet tightly along the seams to prevent washout during retrieval. During descent through the water, the flaps are forced open by the pressure of water passing through the open-jawed box. The flaps cover the surface of the box during retrieval of the sample, preventing disturbance of the collected sediment. Fig. 2.2 is a picture of the box core.

2.1.3 Subsampling and sectioning

In our project, the sediments collected by the box corer were subsampled on board by inserting plastic core tubes (inner diameter 10cm, length 40cm) into sediment. The edge of core tubes were sharpened to minimize the compaction of the sediment upon driving the core tubes into the sediment. Water on the top of the retrieved sediment in the box corer was carefully siphoned off with plastic tubing without disturbing the sediment surface. The top of the core tubes had to be sealed by rubber stoppers to prevent the sediments from falling out during recovery of the cores from the box corer. The lack of disturbance of the sediment recovered in the box corer could be ascertained by sediment appearance. The length of the sediment cores obtained was approximately 30cm. The appearance of the sediment core was recorded prior to sectioning using digital photography, along with other features such as the length of the core; sediment color, texture etc.

Sediment cores were subsampled by extrusion from the core tubes and sectioning into 1-cm or 0.5-cm slices as soon as possible. By subsampling the sediment into larger sections, for example 3 to 10 cm thick, the information on the vertical distribution of contaminants could be lost [Mudroch and MacKnight., 1994; Mudroch and Azcue., 1995]. The cores were extruded by a piston-type extruder. The simple piston extruder is composed of a metal screw rod, piston and screw holder with a larger diameter than the piston. 1-cm and 0.5-cm spacers and a plastic cutter were also used for this sectioning (Figure 2.3). Extruding and sectioning cores using the simple type of extruder involves the following steps:

1. Placing the sediment core on the extruder piston

2. Adjusting the position of holder then pushing the core tube down slowly until the surface of the sediment is at the upper end of the tube.

3. Screwing the holder down till the space between piston and holder was 0.5 or 1 cm thick (measured by spacer).

4. Pushing the core tube down slowly till the piston reaches the holder. Sediment cores were extruded by 0.5 or 1cm.

5. Sampling the exposed sediment core by using plastic cutter

After sectioning, the slices of sediment were divided into two parts, one was placed in a Ziploc plastic bag or wide-mouth vessel and stored frozen at -20°C for solid phase analysis, and the other was placed in a centrifuge tube for extraction of pore water.

2.1.4 Pore water extraction

Sediment pore water, also referred to as interstitial water, is defined as the water filling the space between sediment particles and not held by surface forces, such as adsorption and capillary source, to sediment particles. Sediment pore water acts as a linking agent between the bottom sediments and overlying water. The content of this water is related to the physical properties and mineralogical composition of the bottom deposits. The sediment pore water chemistry may provide clues regarding the types and extent of diagenetic processes ongoing within the sediment. Specifically, the sampling and analysis of sediment pore water can provide valuable information on chemical changes occurring in the sediment, on the equilibrium reactions between the sediment solid phases and the water, on the transport and fluxes of contaminants into the

sediment/water interface and overlying water, and on the availability of nutrients and toxic chemicals to the biota [Mudroch and MacKnight, 1994; Mudroch and Azcue, 1995].

Most fine-grained deposits become anoxic at shallow depths (a few millimeters) but become rapidly oxidized upon exposure to air. The oxidation of sediments brings about rapid changes in redox-sensitive chemical species dissolved in the sediment pore water. To obtain a pore water sample approximating the natural sediment environment, exposure of the sediment and sampled pore water to the atmosphere must be mimized by employing oxygen-free conditions during the entire processing period. This can be accomplished by using an inert gas such as argon, nitrogen, helium [Mudroch and MacKnight, 1994; Mudroch and Azcue, 1995].

Major techniques of pore water extraction include squeezing, centrifugation, dialysis, and suction. In our project, centrifugation was chosen because of its advantages: simplicity, amount of sediment available, and ease of obtaining large volumes [Mudroch and MacKnight, 1994; Mudroch and Azcue, 1995].

Sediment pore water sampling was done in an anaerobic chamber full of nitrogen. Sediment fractions were placed in 50ml centrifuge tubes with caps screwing tightly and centrifuged at 6000 rpm for 15 to 30 min. After centrifugation, the supernatant was filtered into polyethylene containers using plastic syringes with syringe filters (pore size 0.45μm, diameter 30mm). The pH and redox potential were determined via a solid-state pH electrod and a platinum electrode respectively while on board the Liminos. Pore water samples were frozen and transported to the laboratory in GLIER. Alkalinity was determined by UV-Vis spectrophotometer. Sulfate, nitrate, nitrite and phosphate were determined by Ion Chromatography; ICP-MS was used to determine trace elements e.g.

Co, Mo, U, Tl, Ce, Cu, Cd, Pb, Zn, Cr; ICP-OES was used for the analysis of major elements e.g. Fe, Mn, Al, Ca, Na, Mg.

2.2 Experiment methods for pore water analysis

2.2.1 pH and Eh measurement

pH is determined by pH meter (VWR SP20); Eh is measured by using a pH meter in ion selective mode and using a platinum electrode. The electrode was calibrated using ZoBell's solution (VWR SP20).

2.2.2 Alkalinity measurement

The method is adapted from Sarazin et al. (1998). Reagent was prepared by mixing 10mmol/L formic acid and 50 mg/L bromophenol blue. Apparatus is UV-Visible spectrophotometer (Thermospectronic G20)

Although described in detail in Sarazin et al., 1998, here I provide a brief summary of the technique. For alkalinity values between 1-20mmol/L, 200 μL of standard solution or pore water sample was added into1 ml of the reagent then mixed and measured by UV-Vis at 590nm. Sodium bicarbonate was used as standard. Distilled water, deaerated with nitrogen, was used as a blank. Fig. 2.4 is a representative standard curve for alkalinity measurement.

2.2.3 NO_2^-, NO_3^-, SO_4^{2-} and PO_4^{3-} determination

NO_2^-, NO_3^-, SO_4^{2-}, PO_4^{3-} and Cl were determined by Ion chromatograph (IC) (Dionex As 50). Calibration standards utilized include sodium nitrite, sodium nitrate,

sodium sulfate and potassium dihydrogen phosphate. Sodium nitrite was treated by the following procedure before making solution: 2 g of sodium nitrite was placed in a 125 ml beaker and dried to constant weight (about 24 hours) in a desiccator containing concentrated sulfuric acid. Standards and samples were prepared in an anaerobic environment. Standard curves for IC analysis are presented in Fig. 2.5

2.2.4 ICP-OES determination

Pore water samples were diluted by a factor of 10 in 1% HNO3 for ICP-OES (IRIS#701776, Thermo Jarrell Ash Corporation) analysis. The following major and minor elements were quantified (Mn, Fe, Si, S, Na, Mg, Al, K, Ca) and some trace metals (V, Zn, Ni, Cr). Calibration was undertaken by measurement of a series of mixed element standards.

2.2.4.1 Principle of ICP-OES [Botes, 2003]

The ICP-OES is an efficient source of atomic and ionic emission, which can be applied in principle for the determination of all the elements other than argon and helium. The principle of the method is to excite the atoms into the higher energy levels by employing optimal conditions. This state is only temporary, because of the atom's natural tendency to return to the ground state. For the atom to change back to the ground level state the additional energy must be released. This energy can be observed as emission radiation, which is characteristic to the element emitting. A single element has a number of emission lines that can be used for analytical determination. However, the most

commonly used lines for an element, depend on the sensitivity of the line and possible interferences.

2.2.4.2 The various components of an ICP-OES [Botes, 2003]

A typical ICP-OES system is comprised of the following components (Fig. 2.6).

- A sample introduction system

The main function of the sample introduction system is to generate a fine aerosol of the sample so that it can be effectively ionized in the analytical plasma. The sample introduction system consists of the peristaltic pump for sample uptake, nebulizer to aspirate the sample and generate an aerosol and the spray chamber to separate the smaller and bigger droplets because the plasma discharge is inefficient at dissociating large droplets.

- The plasma, ICP torch and gas supply [Calderon, 2005; Botes, 2003]

An ICP is formed during the coupling of free electrons from a suitable gas (usually argon) to the energy radio frequency (RF) magnetic field, which is produced by a radio frequency generator. The gas is contained in a plasma torch, which consists of three concentric tubes made of materials that are resistant to high temperature (usually quartz). These three concentric quartz tubes are arranged to provide suitable gas flow geometry. The magnetic field is generated by a radio frequency (RF) coil surrounded the top of the torch.

In ICP-OES there are three gas flows (usually argon), which are necessary for plasma formation and instrument operation. Firstly, the coolant gas flow is used to avoid

melting of the torch. Secondly, the main function of the auxiliary or intermediate gas is to lift plasma. The third and central gas flow is called the injector or nebulizer gas. This is the gas flow that is needed to drive the nebulizer and to transport the sample to the plasma.

An inductively coupled plasma (ICP) is formed when some electrons of the argon atoms are stripped off by a high-voltage spark applied to the gas flowing at the end of the torch. These electrons are accelerated in the electromagnetic field generated by the RF coil and collide with other argon atoms stripping off more electrons. This collision induced ionization of the argon continues in a chain reaction, breaking down the argon gas into ions and electrons forming high energy plasma.

An ICP has a temperature gradient between 8000 ^{o}K at the base of the plasma to 6000 ^{o}K at the end. Sample aerosol enters the plasma via the sample injector. As the sample passes through these different temperature zones, it undergoes several physical changes before it becomes ionized. The first change involves desolvation of the droplets with water molecules stripped away turning the aerosol into solid particles. As the sample moves further into the plasma, the solid particle changes first into a gaseous form and then into ground-state atoms. The ionization of the atoms is achieved mainly by collisions of the argon electrons with the ground-state atoms. The ionized sample emerges from the plasma and is directed into the interface region of the mass spectrometer.

- Transfer optics and an optical spectrometer

The function of the spectrometer is to select a given line in the emission spectrum and isolate it from the other lines. The most important features the spectrometer must

provide are the following: high resolution, light throughput and stability. The other factor that must be taken into account is to minimize the factor for spray light in the spectrometer. It is, however, not always possible to have high light throughput and high resolution, and a compromise between the two is often necessary.

• Detectors and other electronics

One of the detection devices that are becoming more popular recently is the charge transfer device (CTD). These devices have high sensitivity and large dynamic range. There are two main types: Charged Coupled Device (CCD) and the Charged Injection Devices (CID). The CCD which is used in our equipment has the highest efficiency and very low noise levels. It can be thought of as a large number of photodetecting analog shift registers. After the photon-generated charges have been stored, they are recorded horizontally, row-by-row, through a high-speed shift register to a preamplifier. A computer stores the resulting signal. Conversely for the CID, the light strikes a row-column structure of discrete pixels, each of which is composed of a pair of semi-conductor capacitors.

• Computerized instrument control and data collection unit

The currently used data collection system is that of a microprocessor computer with the manufacturer's software package installed which is developed exclusively for the particular ICP-OES. This software controls the spectrometer's raw data storage. The system must provide the ability to require data fast and effectively. The software usually provides the capabilities to reprocess data, as well as do background and drift correction.

In many cases the removal of interferences are possible from the raw data. The processing unit must also make it possible to calibrate, standardize and use the calibration values to calculate the concentration of the elements of interest.

2.2.4.3 Interferences in ICP-OES

There are several sources of possible error in the determination of an analyte in solution. The main contributors to this error can be categorized into classes, namely: Matrix and spectral interferences. The matrix effects are divided into physical, chemical and ionization interferences. The spectral interferences are associated with the capabilities of the spectrometer used.

- **Matrix Effects**

a. Physical interference

Changes in the acid concentration or dissolved solids content and sample solution can lead to changes in the nebulization rate. This rate change is due to changes in the density, viscosity and surface tension of the solution. These effects can change the droplet size, which can have an influence on the sensitivity of the measurement. Significant amounts of sulphuric or phosphoric acid can suppress the analyte signal. Some elements introduced in the plasma can have an effect on analyte lines with high excitation potentials. These elements are mainly alkali elements.

b. Chemical interference

Chemical interference occurs when a compound is formed that prevents quantitative atomization of the element. In ICP-OES, however, this is generally not important due to the extreme conditions in the plasma.

c. Ionization interference

This interference causes a reduction in sensitivity, which depends on the following:

I. Temperature of the plasma

II. Ionization potential of the element

III. Concentration of the element.

d. Incomplete atomization interference [Olesik, 1991]

This matrix effect happens in flames and furnaces, and is particularly important for refractory species such as oxides. It can be minimized by operating in a more inert environment and at higher temperatures.

- **Spectral overlap**

Spectral overlap is one of the biggest problems of ICP-OES. This is a direct result of the high temperatures required to maximize the emission. As many species are injected into the plasma, high levels of interference can be expected. In the case of major elements it is not that significant, but in the case of trace or weakly emitting elements, the wavelength is dependant on other spectral features near to that wavelength. There is an average of 294 lines emitted per element, and overall there are more than 100000 wavelengths. The abundance of these lines can cause the following spectral line overlap: Direct spectral and wing overlap.

a. Direct overlap

Direct overlap occurs when two elements emit light at exactly the same wavelength. An increase in resolution will not solve the problem. These lines would not be able to be resolved.

b. Wing overlap

Wing overlap occurs through Doppler broadening, caused by the high temperatures of the plasma. This overlap can be rectified through the use of a high-resolution spectrometer. In other cases the selection of an alternate analytical line will be necessary. One example of this type of interference is the influence of Ca (393.37 nm and 396.85 nm) on the analytical lines of Al (394.4 nm or 396.2 nm). Ca will severely affect the analysis of Al in the mentioned example.

c. Continuum radiation

Throughout an ICP spectrum there is broad-band background beneath the line radiation. This adds to the offset of the signal measured. The continuum originates form a number of sources. These sources include: Electrons, argon gas and matrix species (both atomic and molecular). The operating parameters of the instrument also play role in the profile of the continuum and several levels of overlap can occur. Small changes in the argon gas flow can alter the background radiation considerably. This effect can be removed mathematically by using blanks, however it is often necessary to use a dynamic background correction method to eliminate this problem.

d. Stray light

Stray light is radiation that reaches the detector unintentionally. This stray light can have a number of causes. One of them is imperfections in the optical system and to a

greater extent, the grating. No optical system is perfect, but the manufacturers strive to minimize this effect through better-designed spectrometers. The ruled gratings have improved considerably, but the best grating to use in the spectrometer, to minimize the stray light effect, is a holographic grating spectrometer. Another cause of stray light are elements that have very intense emission lines (mainly alkaline earth elements). The light enters the spectrometer and in some cases can interfere with spectral lines of the analyte many band-passes away ("far-scatter"). There are a number of ways to try and minimize this problem such as the use of solar blind PMTs, which will not respond to radiation above 350 nm. The use of double monochromators and correction coefficients can also help to solve this problem..

e. Spectral lines and molecular bands from discharge atmosphere

I. Argon spectrum (Plasma gas)

Argon gas produces 294 lines in the region between 317 and 877 nm but there are no bright argon lines between 200 and 300 nm. The most intense lines are in the region of 420-440 nm and can play a role when analyzing for elements emitting in this region.

II. Hydrogen and oxygen spectra

The hydrogen and oxygen lines originate from atomic hydrogen and oxygen formed by the dissociation of water molecules. The hydrogen 397.07 nm line interferes with the Ca 396.85 nm line. Atomic oxygen lines interfere in the region of 436 and 845 nm.

III. Carbon and silicon spectra

The carbon lines that can play a role in the spectrum are the C 193.091, 199.362 and 247.856 nm lines. The carbon originates mainly from trace amounts of organic compounds in the compressed argon cylinders. The silicon lines are commonly found due

to erosion of silica torches, etching of glass spray chambers by hydrofluoric acid and/or solvent blanks. To eliminate these interferences silicon-free materials must be used in the analysis method.

IV. Molecular bands: OH, NO, N_2^+ and NH

Hydroxyl (OH) radicals resulting from the dissociation of water emit spectra in the 281 to 295 nm and 306 to 325 nm regions. The NO bands are most prominent at 195 to 300 nm and the N_2^+ from about 329-590 nm. The NH band at 336 and 337 nm are rather strong. Bands of molecules containing nitrogen can be eliminated by the use of extended torches. These are specially applied to measure the nitrogen concentration using the atomic nitrogen lines.

V. Absorption bands of O_2

In the air-path spectrometers the absorption O2 of is a major problem. The O2 band produces a background below 200 nm. The use of a vacuum system or purged nitrogen system will eliminate this background effect.

2.2.4.4 Calculation of instrument detection limit [GLIER SOP]

The instrument detection limit (IDL) is the most accurate way of assessing instrument detection capability. It is defined as three times the standard deviation of the calibration blank (C-Blk) run at each cycle. The average of 3 standard deviations of three replicate instrument readings are taken, the equation is as shown.

IDL = 3 x Average (C-BlkS.D.1, C-BlkS.D.2, C-BlkS.D.3)

2.2.5 ICP-MS determination

Inductively coupled plasma mass spectrometry (ICP-MS) is a significant technique with the capability to analyze trace elements at very low detection limits (ppb). Since standard ICP-MS requires the introduction of samples as a solution, solid samples must be dissolved in acids to be introduced into the ICP mass spectrometer. A sample is introduced as a fine aerosol that is ionized as it travels through the high temperature (8000 K) ICP plasma described in the ICP-OES section.

Pore water samples were dilute by a factor 10 using an Internal Standard Solution consisting of 1% HNO_3 and containing Be, In, Tl as internal standards. The ICP-MS utilized was a Thermo Elemental X7. The following elements were part of a typical ICP-MS run: Mn, Fe, Si, S, Na, Mg, Al, K, Ca, REE, V, Zn, Ni, and Cr. Calibration was undertaken by analysis of a series of certified mixed element standards which also contained the three internal standards for drift and matrix corrections.

2.2.5.1 Instrumentation [Calderon, 2005; Date 1989; Jarvis 2001]

- **The Ion Focusing System**

The ion focusing system, also known as the ion optics, is located between the skimmer cone and the mass analyzer. This system consists of one or more electrostatically controlled lenses. These are not traditional lenses but are made of metallic plates, barrels, or cylinders that have an applied voltage.

The role of the ion optics is to transport the maximum number of analyte ions from the interface region to the analyzer, while rejecting the matrix components, neutral

species and electrons. The sample is transported from the ion optics into the mass analyzer as a positively charged ion beam.

- **The Mass Analyzer**

The mass analyzer is located between the ion optics and the detector and is kept at a vacuum of 10^{-6} Torr with a second turbomolecular pump. This is the device of the ICP mass spectrometer that separates the ions of interest, according to their mass/charge ratio, from all other nonanalyte, matrix, solvent and argon-based ions.

There are four kinds of commercial mass analyzer: quadrupole mass filters, double-focusing magnetic-sector, time-of-flight, and collision-reaction cell technology. Of these, the quadrupole mass analyzer is the most commonly used in ICP-MS. It consists of four cylindrical or hyperbolic metallic rods of the same length and diameter. By placing a direct current (dc) field on one pair of the rods and a radio frequency (rf) field on the opposite pair, ions of a selected mass are allowed to pass through the middle of the four rods to the detector where they are converted to an electrical pulse. The other ions are ejected from the quadrupole. This scanning process is then repeated for another ion of different mass/charge ratio until all the analytes in a multielement analysis have been measured.

- **The Ion detectors**

The detector converts the ions emerging from the mass analyzer into electrical pulses, which are then counted by its integrated measurement circuit. The magnitude of the electrical pulses corresponds to the number of analyte ions present in the sample.

Trace element quantification of an unknown sample is then carried out by comparing the ion signal with known calibration or reference standards.

2.2.5.2 Analytical problems [Calderon, 2005]

The main problems that can influence the quality of the ICP-MS analyses include interferences, drift, memory and background. They are often interrelated and can occur as a result of operating conditions, or due to spectral interferences.

- **Interferences**

Interferences in ICP-MS can be divided broadly in two categories: a) spectral interferences in which overlapping mass peaks add to the analyte signal. These are the most serious interferences in ICP-MS, and b) Non-spectral interferences or matrix effects due to changes in signal intensity not related to the presence of a spectral component. High concentrations of some components in the solvent, reagents and sample can suppress or enhance the signal intensity.

a. Spectral interference

I. Polyatomic ions interference: This is the most common type of interference, which is produced by the combination of two or more atomic ions. These species are formed in the plasma from reactions among ions forming the plasma (argon), the matrix components in the solvent and sample, analyte elements, and entrained oxygen, nitrogen and other gases from the surrounding air. The elements prone to form these interfering species are the most abundant ions present, such as Ar, O, N, C and H.

II. Refractory oxide ions: These species occur when elements in the sample combine with ^{1}H, ^{16}O, $^{16}O^{1}H$ either from water or air to form molecular hydride, oxide and hydroxide ions. Interferences occur as the result of an incomplete dissociation of the sample matrix or from reactions in the cooler zone of the plasma immediately before the interface. Elements contributing with this type of interference include Al, Ba, Mo, P, REE, Si, Ti, Zr, and Hf. Light REE (LREE) form oxides interfering with heavy REE (HREE).

III. Doubly charged ions: Most of the ions formed in the plasma are singly charged (M^{+}) but some elements such as Ba and the REE produce a small proportion of M^{2+} ions. These ions may interfere with singly charged analyte isotopes that have the same mass/charge ratio (m/z) but half of their mass number.

IV. Isobaric interferences: This interference is caused by an isobaric isotope of another element in the sample, contributing to the analyte signal.

b. Matrix effects

This is a type of interference in which the sensitivity (counts per second) of the analyte can be suppressed or enhanced by concentration of the other elements present in the solvent or sample (the matrix). This group of interferences can be divided into two categories: a) physical effects resulting from the dissolved or undissolved solids present in a solution; and b) analyte suppression or enhancement.

I. Dissolved solid effects: For nebulization, samples must be free of particles that can cause physical blockage to the nebulizer. High levels of dissolved solids can be deposited in the sampling cone orifice causing severe signal drifts, usually loss in sensitivity, over short periods of time and a reduction in precision. Elements that form

refractory oxides (Al, Si, Zr) are prone to buildup in the sampler cone orifice. Those elements must be kept at concentrations much below 0.1-0.2 wt% and the total amount of less refractory elements much below 1-2 wt% to avoid blockage of the interface region. Residual organic matter can be deposited on the nebulizer, spray chamber, and torch walls leading to memory effects. At high levels of organic content, carbon can destabilize and extinguish the plasma torch as it is deposited as carbon in the sampler cone.

II. Suppression and enhancement effects: High concentrations of certain elements suppress or enhance the analyte signal. Instrument parameters such as RF power, plasma gas flow, and ion lens settings affect non-spectral interferences. In general, lighter masses are more suppressed than heavier masses, and for a given analyte, a heavier matrix element causes more suppression than a lighter one. Nearly all matrix elements will cause some degree of signal suppression or enhancement if they are present at a high enough concentration. These effects depend more upon the absolute concentration of the matrix element rather than the relative concentration of matrix and analyte. One of the most problematic matrix elements is sodium. Suppression of the analyte signal increases with increasing sodium concentrations. To solve this problem, samples (particularly sea water) should always be diluted to reduce the level of Na to less than about 1%, prior to the analyses. Higher concentration of acids can also result in severe suppression of the analyte signal.

c. Drift, memory, and blank effects

Drift is the gradual change of the instrument sensitivity with time for a given analyte. Drift often occurs as a loss in sensitivity with time, though increases can occur at the beginning of a run.

Memory effects are caused by previous sample material either remaining in the tubing, nebulizer, spray chamber and torch, or being deposited on and later eroded from the sampler and skimmer cones. These effects generally enhance the analyte signal. Blank problems (background) can arise due to contamination with reagents and the environment.

2.2.5.3 Data acquisition [Calderon, 2005]

To obtain quality ICP-MS data it is necessary to deal with several considerations: preliminary semiquantitative analysis of the samples, assessment of potential spectral overlaps, examination of possible matrix effects, selection of optimal instrument settings and methodologies to minimize spectral interferences and matrix effects, as well as the selection of a robust calibration methodology.

a. Calibration techniques

Three important types of calibration are available for chemical analyses:

I. External calibration: This calibration method compares the signal intensity of a standard solution containing a known amount of an element to the intensity in the unknown sample solution. With this method drift correction can be performed but matrix effects cannot be corrected.

II. Internal standardization: This method is used to correct for changes in analyte sensitivity caused by variations in the concentration and type of matrix components found in the sample as well as correcting for sensitivity drift with time. The internal standard is a nonanalyte isotope that is added to the blank solution, standards and samples before the analyses. It is typical to add three or more internal standards in the unknown sample to

cover the mass range of the analyte elements of interest. Elements included in the internal standard are not present in significant amounts in the sample. Concentration in the unknown samples is then calculated by comparing the intensity values of the internal standard in the unknown sample to those in the calibration standards. Calibration standards represent a range in concentrations likely to be found in the unknown samples. Bi, In and Tl are commonly used for internal standards.

III. Standard addition: This calibration requires one measurement of the unknown and another measurement on a spiked split of the unknown. The spike consists of an element or combination of elements of known concentrations. Drift is not corrected but any matrix effect is corrected to a high degree of accuracy.

b. Data processing

The ICP mass spectrometer detects the analytes as they hit the dynodes producing electric pulses. The number of counts of these electric pulses is proportional to the element concentration. However, some corrections have to be done because spectral interferences, sensitivity drift, and background effects can affect analyte signals. Mathematical corrections have been successfully used to compensate for these problems.

2.2.5.4 Instrument detection limit [Calderon, 2005]

For a 99% confidence level, instrument detection limit is typically defined as 3 times of standard deviation (SD) of replicate measurements of the sample blank. It can be presented by the following equation:

$$IDL = \frac{3 \times \text{S.D. of background signal}}{\text{Analyte intensity- background signal}} \times \text{Analyte concentration}$$

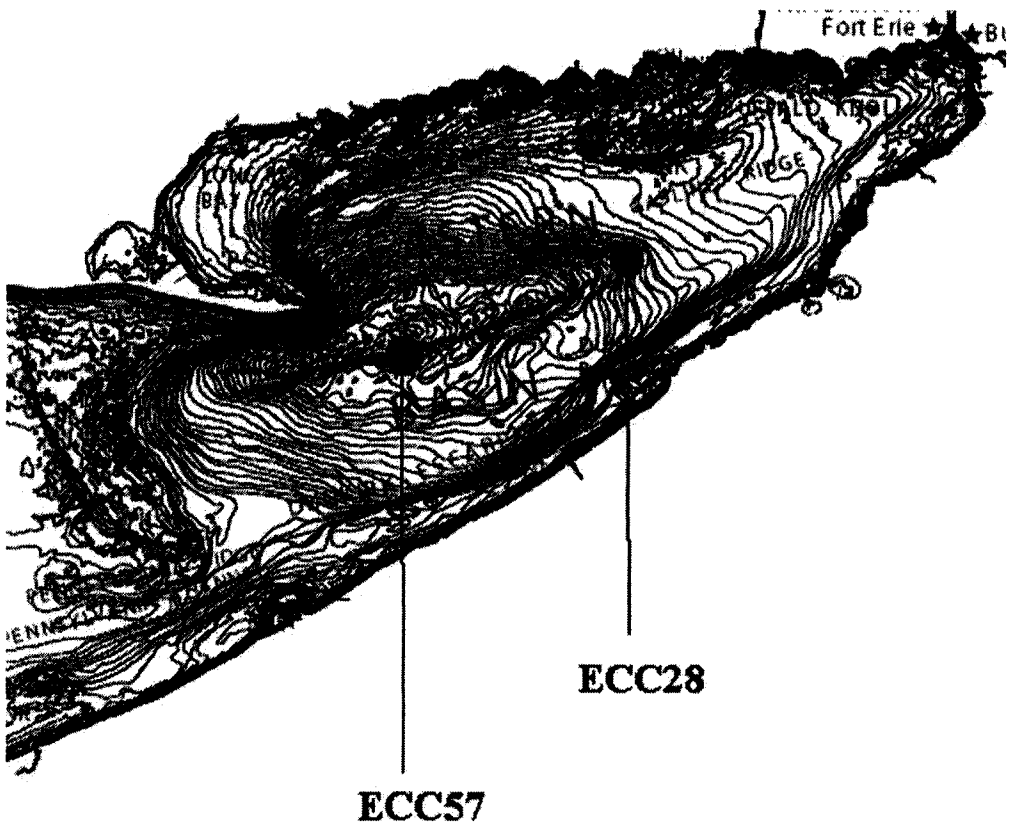

Figure 2.1: Bathymetry map of Lake Erie illustrating sampling sites (Modified from www.ngdc.noaa.gov)

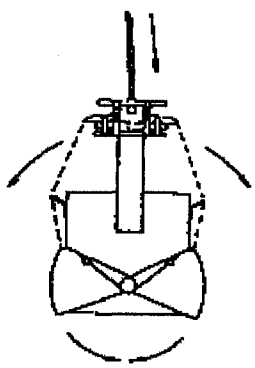

Figure 2.2 Ekman designed box core

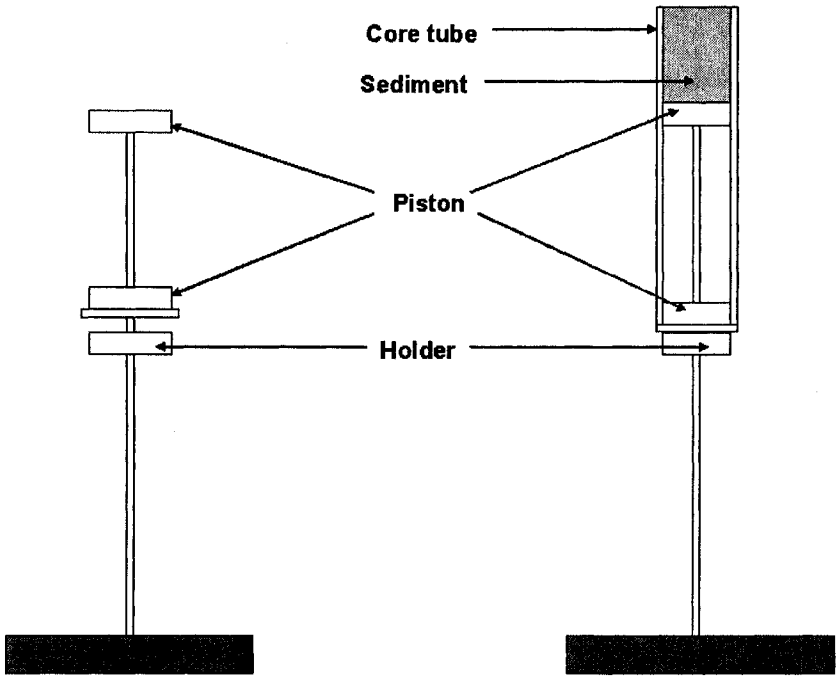

Figure 2.3 Tools for sediment core sectioning

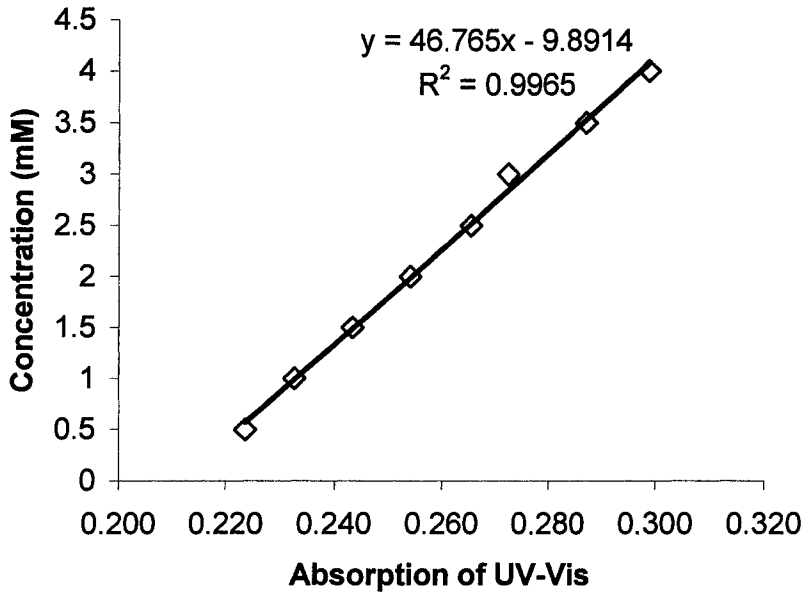

Figure 2.4 standard curve for alkalinity measurement

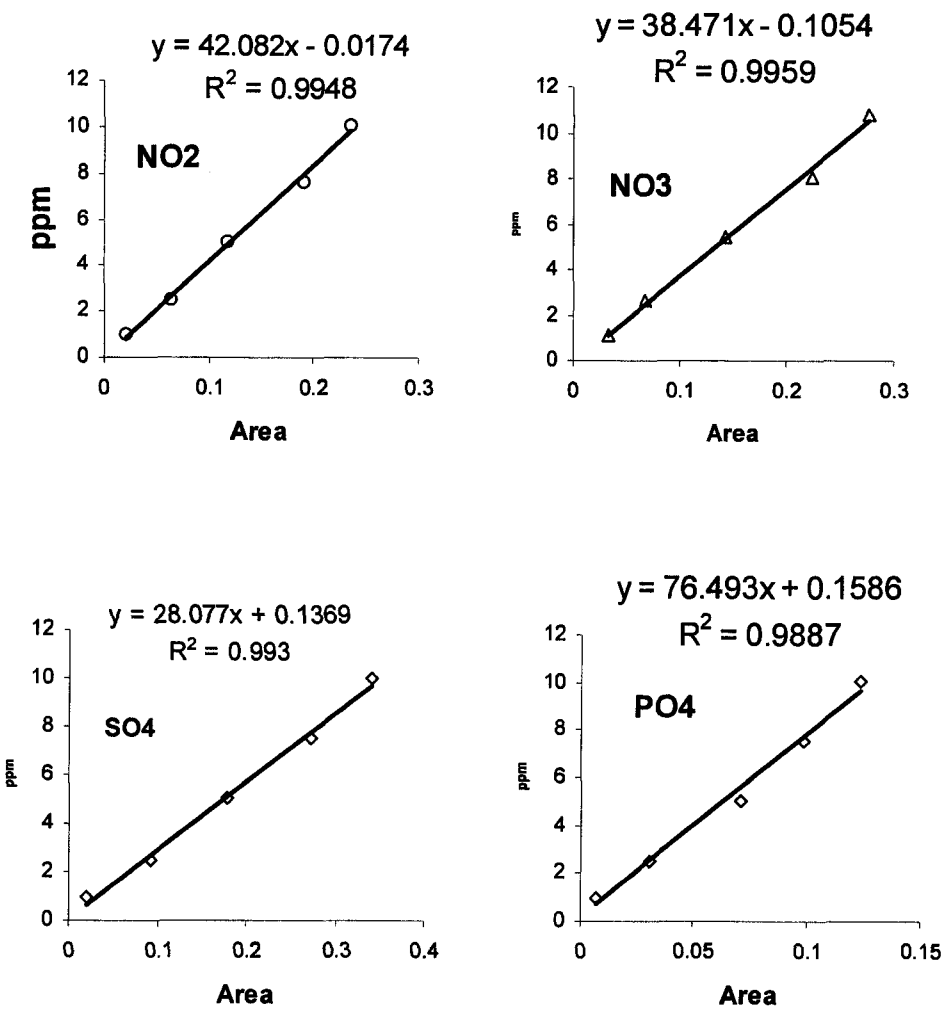

Figure 2.5: Standard curves for IC analysis

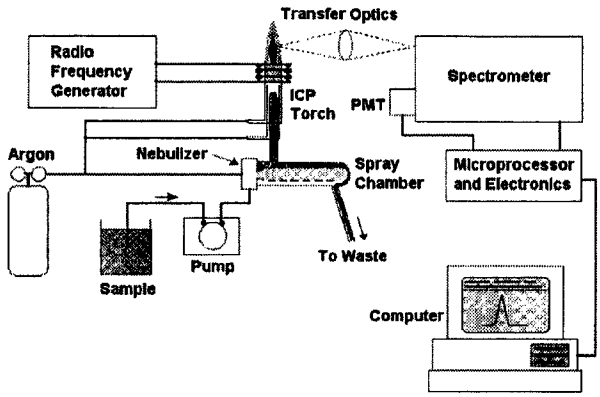

Figure 2.6: ICP-OES schematic diagram [Botes, 2003]

Table 2.1: Sample site location, and physical and chemical parameters

Site Number	Latitude	Longitude	Depth m		T°C Surface	T°C Bottom
ECC28	42.3716N	79.3012W	35.1		16.34	6.7
ECC57	42.2848N	79.5830W	60.5		16.6	4.5
Site Number	DO (mg/L) Surface	DO (mg/L) Bottom	pH Surface	pH Bottom	Cond Surface	Cond Bottom
ECC28	10.21	12.46	8.37	7.98	309	312
ECC57	11.59	13.2	8.34	8.00	282	311

Chapter 3: Pore Water Geochemistry of Heavy Metals in Sediments from Eastern Lake Erie

3.1 Introduction

The release of sediment-bound heavy metals can have a significant influence on lake water quality. Variation in environmental conditions can mobilize heavy metals which are concentrated in river sediment, allowing them to re-enter the overlying water resulting in increased bioavailability. Both pH and redox potential in the sediment/water system are significant parameters influencing the mobility of metals. It can be expected that changes between reducing and oxidizing conditions may increase or reduce the mobility of metals, for example, changing from reducing to oxidizing conditions can increase the mobility of Zn, Pb, Cu and Cd; on the contrary, the mobility is characteristically lower for Mn and Fe under oxidizing conditions. It has been reported that Fe and Mn are two of the most important elements in redox processes of sediments. This is not only due to their chemical reactivity, but also to their abundance in natural sediments. Many researchers have suggested that Mn and Fe reduction in sediment play crucial roles in the biogeochemical cycles of many elements, including carbon, sulphur, phosphorus and several trace metals [Burdige, 1993, Kostka et al., 1993].

During early diagenesis, the chemical, physical and microbiological changes that occur in the upper few centimetres of sediments, can influence mobilization of trace metals as well. Since the composition of pore water is the most sensitive indicator of the types and the extent of reactions that take place between chemicals on sediment particles and the aqueous phase which contacts them, pore water metal concentrations and

gradients enable us to estimate the fluxes of metals from the sediments to the overlying water and between the various layers within the sediments themselves.

3.2 Results and Discussion

3.2.1 pH and alkalinity profiles

Profiles of pore water pH and alkalinity in the two sediment cores are shown in Fig. 3.1 and 3.2.

High pH values appear near the sediment surface in both cores. Individual pH values remain steady around a value of 8.0 before small breaks happen at depths of 3.5cm for ECC28 and 2.5cm for ECC57 where pH drops from 8.0 to 7.8 in both cores. The pH values remain relatively stable over depths of 3.5cm to 8.5cm for ECC28 and 2.5cm to 10.5cm for ECC57 before suddenly decreasing. Steadily lower pH values are found after 10.5cm and solution tends toward neutral (pH$\approx$7.2). Core ECC57 has increasing pH after 23.5cm and reaches maximum at 26.5cm before droppings lower.

Alkalinity exhibits a completely reverse vertical profile to pH in both cores. ECC28 values sharply increase from 1.0, near the water-sediment interface, to 4.8mmol/L at 2.5 cm, then shows a slightly increasing trend in values For ECC57, alkalinity increases from 0cm to 15.5cm depth then slightly decreases after 22.5cm (where the small peak happens in pH).

Generally, most sediment contains large concentrations of calcium carbonate which can provide a buffer system for the pH in sediment pore water and also influence the concentration of bicarbonate and carbonate ions. The influence of pH on alkalinity can be measured by the following model:

According to the definition of alkalinity, alkalinity can be expressed by the following equation [DiToro, 2001]:

$$[\text{Alkalinity}] = [HCO_3^-] + 2[CO_3^{2-}] + [OH^-] - [H^+] \quad (5.1)$$

In the pH range is typical of the sediment pore waters, pH=7-8, and for large enough alkalinity, [Alkalinity] > 0.1mmol/L, the alkalinity is essentially all bicarbonate

$$[\text{Alkalinity}] \approx [HCO_3^-] \quad (5.2)$$

The deprotonation reaction for bicarnonate which yields carbonate is

$$HCO_3^- \leftrightarrow CO_3^{2-} + H^+ \quad (5.3)$$

And the mass action equation is

$$K_2 = [CO_3^{2-}][H^+] / [HCO_3^-] \quad (5.4)$$

Where K_2 is the equilibrium constant for the deprotonation reaction for bicarbonate.

Replacing Using $[HCO_3^-]$ by [Alkalinity]:

$$K_2 = [CO_3^{2-}][H^+] / [\text{Alkalinity}] \quad (5.5)$$

The equation that determinate the solubility of calcium carbonate is

$$K_{S1} = [Ca^{2+}][CO_3^{2-}] \quad (5.6)$$

Where K_{S1} is the solubility product of calcium carbonate. Replacing $[CO_3^{2-}]$ by $[Ca^{2+}]$, the following equation can be obtained:

$$[\text{Alkalinity}][Ca^{2+}] = K_{S1}[H^+] / K_2 = K_{CaAlk} \quad (5.7)$$

As a conditional constant, solubility constant, K_{CaAlk} is a function of pH. The effect of decreasing pH, which increases $[H^+]$, increases the solubility constant.

According to the hydrolization reaction of carbonate:

$$[CO_3^{2-}] + [H_2O] \leftrightarrow [HCO_3^-] + [OH^-] \quad (5.8)$$

With pH decreasing (pH.7), [OH^-] reduces and the reaction prefers to move toward right side, meantime [HCO_3^-] may increase. However, alkalinity is controlled by the balance among concentration of calcium, pH and alkalinity, the relationship between pH and alkalinity sometimes cannot be determined without considering the concentration of calcium.

3.2.2 Eh profiles

Profiles of pore water Eh in the two sediment cores are shown in Fig. 3.3.

For ECC28, Eh decreases between 0cm to 2.5cm; then Eh increases to a maximum at a depth of 5cm; Eh then decreases steadily before settling to stable values after 11.5cm.

For ECC57, Eh gradually declines till the depth of 7cm; a small rebound appears between 7cm to 9cm then Eh values descend sharply and stay at low levels after 10.5cm.

3.2.3 Nitrate, nitrite and sulphate profiles

Profiles of pore water NO_2^-, NO_3^- and SO_4^{2-} in the two sediment cores are shown in Fig. 3.4 and 3.5.

Enrichment of NO_3^- and SO_4^{2-} are found near the surface. Their concentrations decrease with depth. Since NO_3^- and SO_4^{2-} are two of the most important oxidants in sediments, their decreasing concentrations with depth may contribute to the decreasing Eh values as function of depth.

As a reduced compound, NO_2^- shows low concentrations in the surface sediments where high Eh values appear. Its concentration increases with decreasing Eh as function of depth.

3.2.4 Manganese and iron profiles

Profiles of dissolved pore water Mn and Fe in the two sediment cores are shown in Fig. 3.6. For both cores, low concentrations of dissolved Mn exist near the sediment-water boundary because the sediments are oxidized and Mn oxides have low solubility; an abrupt increase in soluble manganese appears immediately below the sediment surface where a sharp decrease of Eh values is found (For ECC28 0-2.5cm; for ECC57 0-3.5cm); soluble manganese then increases gently as function of depth; soluble Mn decreases in ECC57 after a depth of 20cm.

Pore water Fe concentrations remain low and constant above a depth of 10.5cm then sharply increase between 10.5cm to 20cm where Eh is at low levels.

Vertical profiles of soluble Mn and Fe suggest that the upper 20 cm of sediment can be divided into three zones: 1) Mn oxidation (above the depth of 2.5cm); 2) Mn reduction (between 2.5cm and 10.5cm); and 3) Fe reduction (after 10.5cm).

3.2.5 Mobility of trace metals

Cadmium (Fig 3.6): dissolved Cd sharply decreases in concentration from the surface over the first few cm depth. Below 2-5 cm depth, dissolved cadmium concentrations remain constant at low levels and is non detectable at some depths. The depth profiles of soluble cadmium indicate a complex set of responses during diagenesis which contrasts with the relatively simpler redox reactions of Mn and Fe. The high dissolution taking place in the uppermost zone of the sediment is accompanied by the large Eh value in the top sediment layers. Cd may have high mobility in near surface oxidizing conditions because the formation of Cd sulphide may be restricted. The

coincident decrease in pore water Cd concentrations with decreasing sulphate also suggests that the increase in dissolved Cd may be the result of sulphide oxidation [Song et al 2005]. Another possible explanation relates to high contents of organic matter and the only 1mm penetration of oxygen. An oxygen dependent dissolution reaction might be taking place such as the aerobic degradation of the organic matter to which the Cd is initially bound, followed by the migration of the dissolved Cd upward into overlying water or downward into the sediment (Gobeil et al. 1987). The irregular Cd profiles below 2-5.0cm may be related to redissolution of an initially precipitated solid Cd phase. Although dissolved sulphur profiles are similar to those of Cd, it is not clear whether this redissolution is controlled by soluble sulphide, because we can not determine out how much dissolved sulphide is present in the pore water.

Cobalt (Fig. 3.7): the similar geochemical behaviour for Co and Mn is well-known. They are believed to have similar oxidation mechanisms (Moffet and Ho, 1996). Fig. 3.5 shows the profiles of pore water Co (and Fe and Mn). General similarities exist for the profiles of pore water Co and Mn, especially the spikes in pore water Co concentrations within a zone of Mn reduction which suggest that Co may be incorporated in Mn oxyhydroxides and released as they are reductively dissolved.

Nickel (Fig. 3.8): Profiles of pore water Ni are presented in Fig. 3.6. Discrete spikes appear within the zone of Mn reduction and may be the result of microenvironments that develop around local enrichments in organic matter. The similarity between dissolved profiles of pore water Co and Ni may suggest that Ni is also released during the reductive dissolution of Mn oxides.

3.3 Conclusion

Mobility of trace metals in sediments can be influenced by both pH and Eh. Since pH of our cores only varies over a narrow range (7.0 to 8.0), it does not contribute significantly to the mobility of metals such as Mn, Fe. The profiles of pore water Eh data indicate that a strong oxidizing environment exists around sediment-water boundary, with increasing depth , Eh decreases and a reduction zone appears. Profiles of pore water sulphate reveals that sulphur is reduced as a function of depth. According to the vertical profiles of dissolved Mn and Fe, the upper 20 cm of sediment can be divided into three zones: 1) Mn oxidation; 2) Mn reduction; and 3) Fe reduction. Reduction of manganese, iron and sulfur may affect the mobility of trace metals differently. Cd has a high availability in the oxidizing environment which is the reverse of Mn. Behaviour of Ni and Co in the Mn zone area may suggest that their mobility depends on the reduction of Mn.

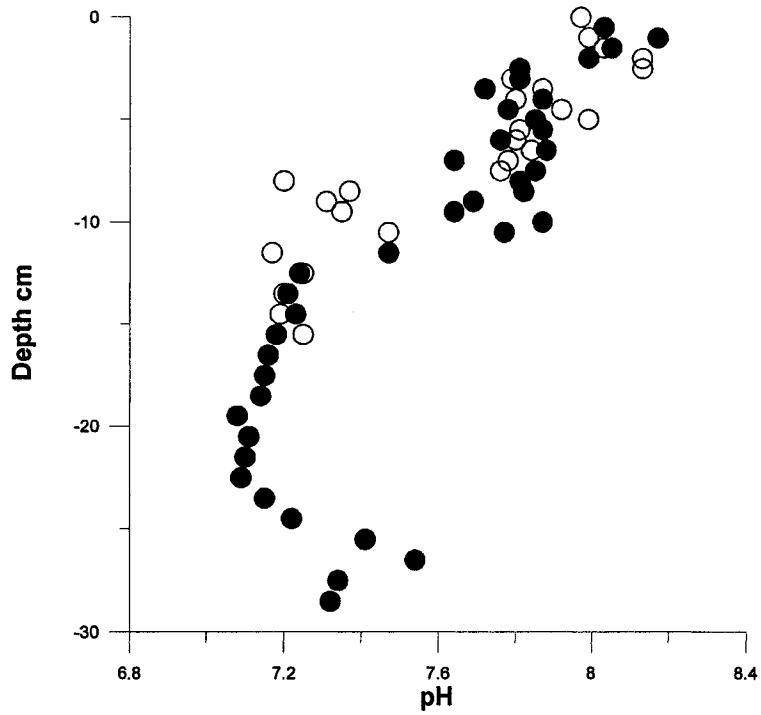

Figure 3.1 Profiles of pore water pH (○ ECC28 • ECC57)

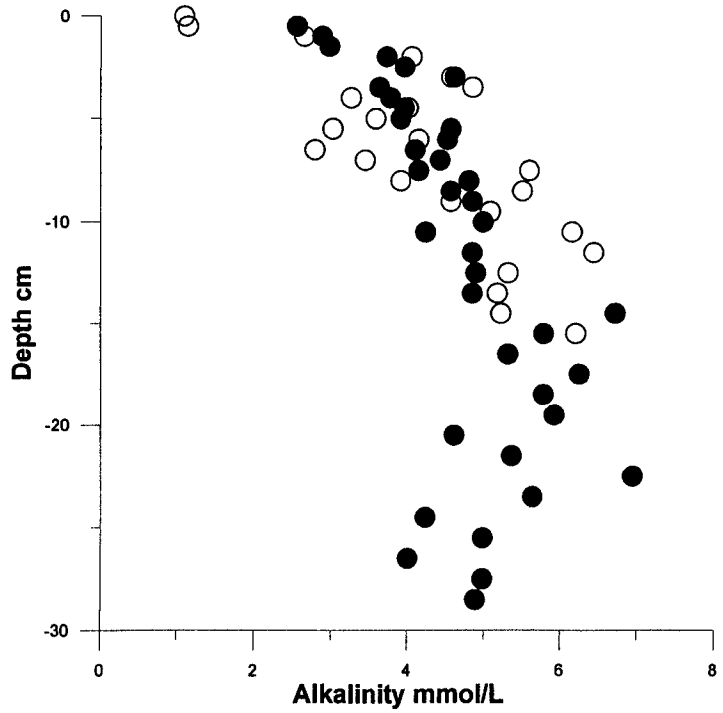

Figure 3.2 Profiles of pore water alkalinity (○ ECC28 • ECC57)

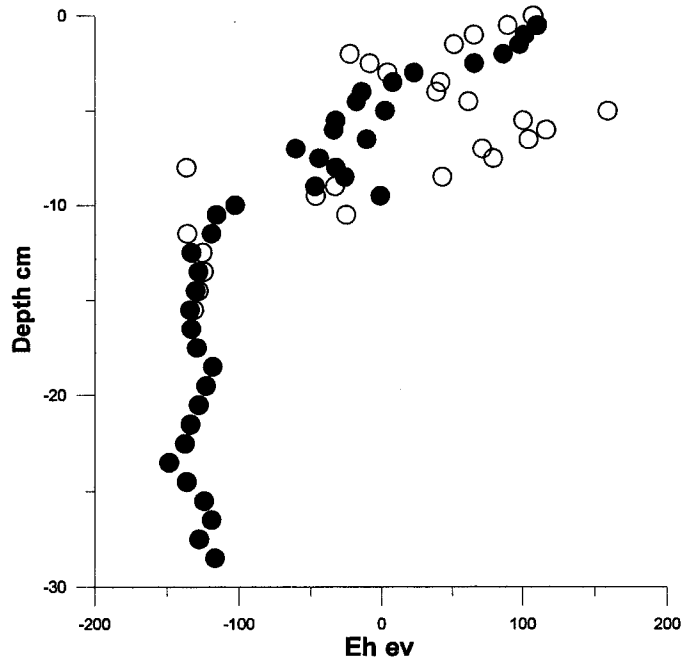

Figure 3.3 Profile of pore water Eh (○ ECC28 ● ECC57)

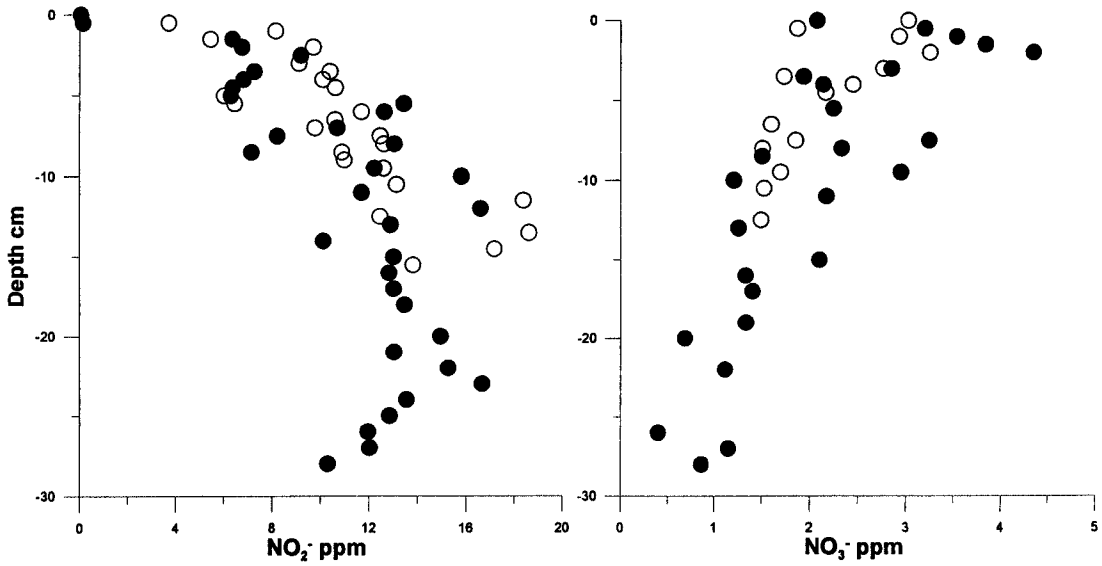

Figure 3.4 Profile of pore water NO_2^- and NO_3^- (○ ECC28 ● ECC57)

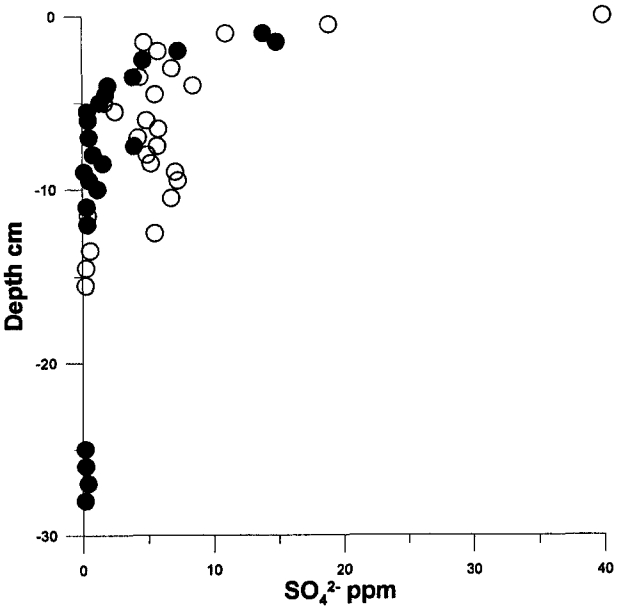

Figure 3.5 Profile of pore water SO_4^{2-} (○ ECC28 ● ECC57)

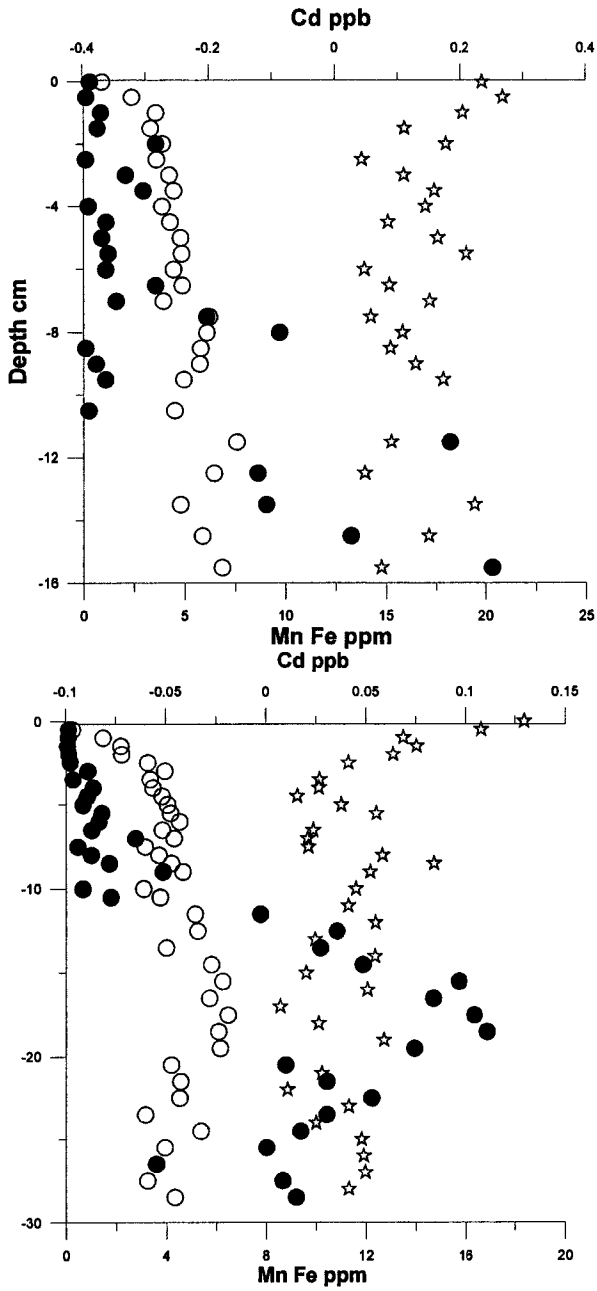

Figure 3.6: Cd pore water concentration profiles. Left ECC28, right ECC57 (☆Cd ○Mn ●Fe)

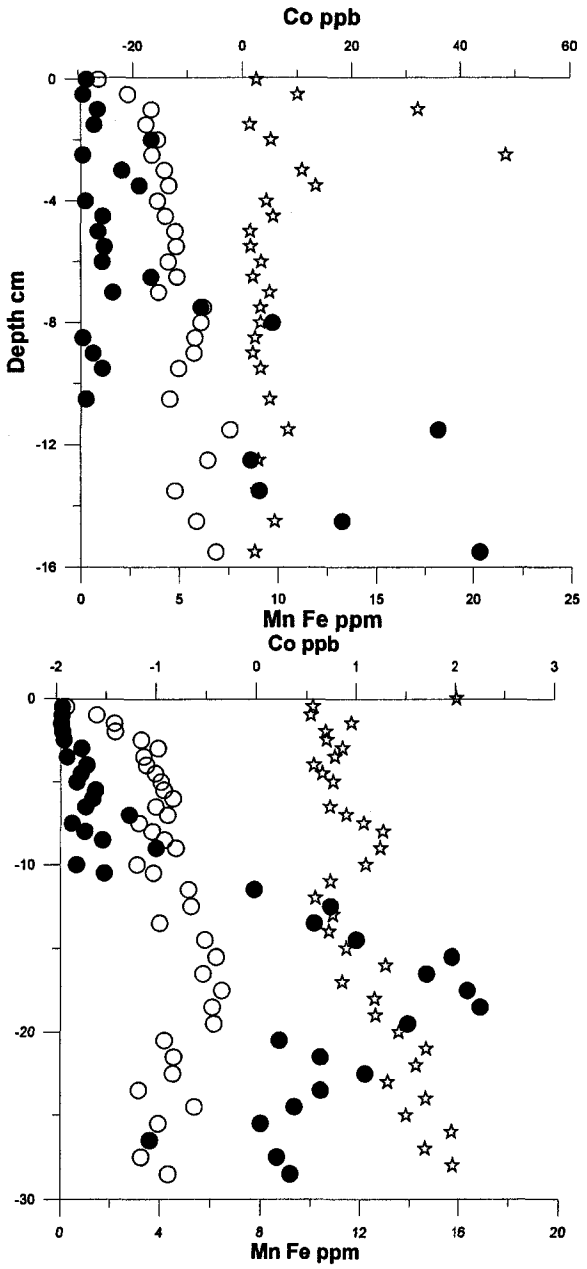

Figure 3.7: Co pore water concentration profiles. Left ECC28, right ECC57 (☆Co ○Mn ●Fe)

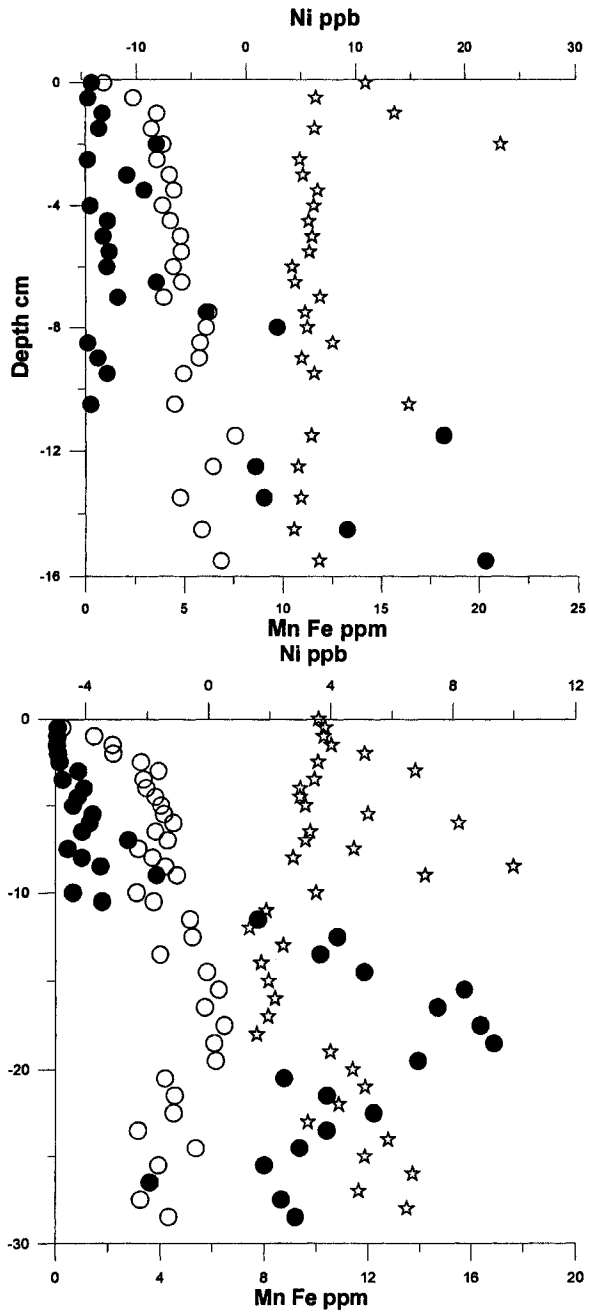

Figure 3.8: Ni pore water concentration profiles. Left ECC28, right ECC57 (☆Co ○Mn ●Fe)

Chapter 4: Comparison of Different Selective Extractions by ICP-OES Analysis

4.1 Introduction

The easiest and the most often used approach to evaluate heavy-metal mobility in sediments is laboratory extraction experiments. These experiments are designed to assess heavy-metal speciation, which controls heavy-metal mobility.

If the background or geochemical composition is known, the total metal concentration in sediments may provide important information about pollution levels. However, when analyzing the possible mobility of heavy metals in sediments and the environmental impact of contaminated sediments, the analysis of the total heavy metal content is insufficient. The chemical form which the metal is in can affect its behaviour and hence mobility and bioavailability within the environment (Hickey and Kittrick, 1984: Ajayi and VanLoon, 1989; Jardao and Nickless, 1989; Wallman et al., 1993, Stead-Dexter, 2004). In order to ascertain the mobility and bioavailability of these heavy metals in sediment, various chemical extractions have been used to assess the mobility/availability of heavy metals in sediment samples, involving both single extractions (Loring and Rantala, 1992; Tack and Verloo, 1996; Dassenakis et al., 2003) and sequential extractions (Tessier et al., 1979; Kersten and Forstner, 1986; Ure et al., 1993; Filgueiras et al., 2002). For single extractions, the methods commonly used are: (1) Total digestion; (2) strong acid digestion, and (3) moderate or weak acid extractions [Loring et al., 1992].

Five single extractions including partial and total digestion have been investigated in this project. Compared with sequential extraction techniques based initially on Tessier et al. (1979), the use of single extractions enables information about extractable metal content to be obtained more simply than by sequential extraction, at the expense of using larger amounts of sample [Filgueiras et al., 2002].

4.2 Methodology of Solid Phase Analysis

4.2.1 Freeze-drying

Wet sediment samples were put in wide-mouth plastic beakers. The mouths of the beakers were sealed by Kimwipe and elastic bands. Beakers were then set up in a Freeze-dryer (ThernoSavant ModulyoD-115) and were freeze-dried at -40°C. Samples were weighed before and after freeze-drying. These data were used to calculate the moisture of sediments.

4.2.2 Organic matter determination

The method is cited from Standard Operating Procedure – GLIER Metals Lab. 1.0 g of freeze dried sediment sample was weighted into a 15 ml glass beaker and muffled at 450°C for 24 hours. The total organic content was determined using the following formula:

Organic content (%) = [(B-C)/B] x 100

Where: B = weight of dry sediment before muffling (g)

C = weight of dry sediment after muffling (g)

4.2.3 Total digestion (HNO3/HF/HCl/Oxalic)

In the total decomposition method, hydrofluoric acid is used in combinations with a concentrated oxidizing acid such as nitric acid and aqua regia to release the total metal concentrations of sediments [Rantala etal., 1989; Loring et al., 1992]. Hydrofluoric is necessary in this digestion because it is the only acid which completely dissolves the silicate lattices and releases all the associated metals such as Al and Fe [Loring et al., 1988; Loring et al., 1992]. With the hydrofluoric treatment, accuracy can be assessed by analyzing reference materials certified for total metal content [Loring et al., 1992]. Generally, the reference materials are certified for total metal contents only. Therefore, they can only be used as an accuracy check of the metal concentrations determined in a solution obtained from HF dissolution of the sample [Loring et al., 1992]. In the method of this project [GLIER SOP], hydrofluoric acid, nitric acid and aqua regia were used to release the total metal content from sediments into solution in sealed Teflon bombs. The advantages of Teflon bomb digestion are: (1) to digest samples rapidly; (2) to reduce risk of contamination; (3) to require small volume of acid [Loring et al., 1992].

a. Reagents:

50% non boiling distilled nitric acid, 50% non boiling distilled hydrofluoric acid, 50% (v/v) non boiling distilled hydrochloric acid, 0.2N oxalic acid, ultra pure water

b. Equipment:

Hotplate, 30ml screw top Teflon digestion bomb (washed by 10% nitric acid and rinsed by MQ water)

c. Procedure:

In the laboratory, approximate 0.1 g of dry sediment was weighed into a 30 ml Teflon digestion bomb, then 2 ml 50% HF and 2 ml 50% HNO_3 were added in. Tube cap was loosened to allow any gases to evolve. The cap was closed tightly after 10 minutes. The solution was placed on the hot plate at 100-150°C for 3 days. The solution in the digestion bomb was then evaporated to dryness after 3 days, then 4ml aqua regia (3:1 HCl : HNO_3) was added. The digestion bomb was closed tightly and heated at 100-150°C overnight. The solution in bomb was evaporated to dryness the next day, then 2 ml 50% HF and 2 ml 50% HNO_3 were added. The bomb was closed tightly and heated on hot plate at 100-150°C for an additional 3 days. The solutions in digestion bomb were evaporated to dryness after 3 days, then 4ml 50% HNO_3 was added in, then evaporated to dryness. The residue was reconstituted in mixed 1%HNO_3, 0.2Noxalic. The solution was diluted to approximate 50ml with 1% HNO_3 and accurately weighed. This solution could be used directly for ICP-OES analysis. For ICP-MS analysis, the solutions were further diluted 100 times with the internal standard solution (Be, In, Tl).

4. 2.4 Acetic acid extraction

Generally, the proportion of the total metal concentration removed by this extraction is operationally defined as the non-detrital acid soluble metal fraction of the sediment [Loring et al., 1992]. The proportion of a metal remaining in the residual fraction is operally defined as the detrital acid insoluble fraction of the material [Loring et al., 1992].

Measurement of total sediment or particulate metal concentrations is a poor method of determining the source and pathways by which the major and trace metals have

entered the aquatic environment [Loring et al., 1992]. Selective chemical methods have been developed and used to partition the total metal concentrations into their loosely bound (non-detrital) and residual (detrital) phases. As one of the weakest acids, acetic acid has been widely used as either single selective extraction or a step of sequential extraction. Dilute acetic acid can be used to separate detrital and non-detrital fractions from carbonate rocks [Chester et al., 1967]. The acetic acid extraction has been chosen to remove effectively the weakly bound part of the total metal concentrations from sediments without releasing elements from structural positions or those strongly complex with organic matter [Loring, 1978; Loring et al., 1988; Loring et al., 1992]. This method removes metals held in ion exchange positions, easily soluble amorphous compounds of iron and manganese, carbonates and those metals weakly held in organic matter [Loring et al., 1992]. It leaves the silicate lattices intact and does not disturb the resistant iron and manganese minerals or organic compounds. The method used in this project is cited from Standard Operating Procedure – GLIER Metals Lab [GLIER SOP].

a. Reagent:

5% acetic acid (aristar grade), Dilution water (Ultra-pure water)

b. Equipment:

50ml centrifuge tube (Washed by 13% nitric acid and rinsed by distilled water), shaker

c. Procedure:

In the laboratory, approximate 0.5 g of dry sediment was weighed into a 50ml centrifuge tube, then 20 ml of 5% acetic acid were added in. Tube cap was loosen to allow any gases to evolve. The cap was closed tightly after 10 minutes. The solution was

shaken on at room temperature for 24 hour. After 24 hours, the solution was centrifuged at 5000 R.P.M. for 10 minutes, then filtered by filter paper. The solution was diluted to approximate 50ml by ultra pure water. This solution could be used directly for ICP-OES analysis. For ICP-MS analysis, the solutions were further diluted 50 times by internal standard solution (Be, In, Tl).

4.2.5 Nitric acid / Oxalic acid extraction

The method belongs to strong acid digestion. Strong acid digestion is probably the most commonly used decomposition technique for the determination of heavy metal concentrations of soil and sediment due to low cost, readily available inorganic acids and the low salt content of the digested solutions [Wong et al., 2003]. In general, strong acid digestion requires the use of concentrated inorganic acids to decompose and dissolute the soil or sediment matrix into a solution form in conjunctions with high temperatures and, sometimes, high pressure [Wong et al., 2003]. The strong acid digestions without HF result in incomplete digestions because silicates and other resistant phases are not dissolved [Loring et al., 1992]. The method in this project is cited from Standard Operating Procedure – GLIER Metals Lab [GLIER SOP].

a. Reagent:

50% no-boiling distilled nitric acid, 0.2N Oxalic Acid, Dilution water (Ultra pure water)

b. Equipment:

Hotplate, 30ml screw top Teflon digestion bomb (washed by 13% nitric acid and rinsed by distilled water)

c. Procedure

In the laboratory, approximate 0.1 g of dry sediment was weighed into 30ml Teflon digestion bomb, then 2 ml 50% HNO_3 were added in. Tube cap was loosen to allow any gases to evolve. The cap was closed tightly after 10 minutes. The solution was placed on the hot plate at 100°C for 4 hours. The solution in digestion bomb was evaporated down at 70°C overnight, then 5ml 1% HNO_3 and 1ml 0.2N oxalic were added in. The solution was centrifuged at 5000 R.P.M. for 10 minutes, and then filtered by filter paper. The solution was diluted to approximate 100g by 1% HNO_3 and accurately weighed. This solution could be used directly for ICP-OES analysis. For ICP-MS analysis, the solutions were further diluted 100 times by internal standard solution (Be, In, Tl).

4.2.6 Ascorbic acid extraction

This technique is one of the extractions which involve the use of reducing agents. Arrhenius and Korkish (1959) indicated that ferro-manganese nodules contain a reduceable fraction, consisting of the oxides of manganese, which can be separated using a reducing agent [Chester et al., 1967]. Experiments show that a buffered ascorbate solution used in conjunction with citrate ion (as a chelator) can rapidly dissolve freshly precipitated iron oxides (ferrihydrite) while not significantly dissolving crystalline or resistant iron oxides or iron monosulfides [Ferdelman et al., 1991]. Although it is calibrated for iron phases [Kostka et al., 1994], and much less for Mn phases [Chester et al., 1967], it can be applied to both Mn and Fe [Van der Zee et al., 2004]. For Mn oxides analysis, the ascorbic acid dissolution is used to quantify the Mn oxide reactivity, because

it combines proton-assisted and reductive dissolution [Van der Zee, 2004]. The extraction used in this project is cited from Ferdelman's method [Kostka et al., 1994].

a. Reagent:

Extraction reagent: 50g sodium citrate and 50g sodium Bicarbonate were added to 1000ml of ultra pure water; this mixture was deaerated with nitrogen, and then 20g ascorbic acid was added into the solution in anaerobic chamber (For final pH of 8.0)

Dilution water (Ultra pure water)

b. Equipment

50ml centrifuge tube (Washed by 13% nitric acid and rinsed by distilled water), shaker, anaerobic chamber

c. Procedure

In an anaerobic chamber, approximate 0.25 g of wet sediment was weighed into 50ml centrifuge tube, then 10 ml of extraction reagent were added in. The tube cap was loosen to allow any gases to evolve. The cap was closed tightly after 10 minutes. The solution was shaken at room temperature for 24 hour. After 24 hours, the solution was centrifuged at 5000 R.P.M. for 10 minutes, then filtered by filter paper in the anaerobic chamber. The solution was diluted to approximate 50ml by 1% 1% HNO_3. This solution could be used directly for ICP-OES analysis. For ICP-MS analysis, the solutions were further diluted 50 times by internal standard solution (Be, In, Tl).

4.2.7 Sodium dithionite extraction

This technique is one of the extractions which involve the use of reducing agents. Sodium dithionite is a strong reducing extraction reagent, which is widely used for

extracting total contentsof iron and manganese oxides [Postma, 1993; Raiswell et al., 1994; Dong et al., 2000]. It has been concluded that dithionite quantitatively extracts the iron oxide/oxyhydroxide phases with only relatively small amounts extracted from iron silicates [Canfield, 1989; Raiswell et al., 1994; Raiswell et al., 1996]. The technique used in this project is cited from Canfield's method [Kcstka et al., 1994].

a. Reagent:

Extraction reagent: 1000ml of 0.35M sodium acetate / 0.2M sodium citrate was deaerated with nitrogen, and then 50g sodium dithionite was added into the solution in anaerobic chamber (For final pH of 4.8)

Dilution water (Ultra pure water)

b. Equipment

50ml centrifuge tube (Washed by 13% nitric acid and rinsed by distilled water), shaker, anaerobic chamber, water bath

c. Procedure

In an anaerobic chamber, approximate 0.25 g of wet sediment was weighed into a 50ml centrifuge tube, then 10 ml of extraction reagent were added in. Tube cap was loosen to allow any gases to evolve. The cap was closed tightly after 10 minutes. The solution was shaken in a water bath at 60°C for 4 hours. After 4 hours, the solution was centrifuged at 5000 R.P.M. for 10 minutes, then filtered by filter paper in an anaerobic chamber. The solution was diluted to approximate 50ml by 1% 1% HNO_3. This solution could be used directly for ICP-OES analysis. For ICP-MS analysis, the solutions were further diluted 50 times by internal standard solution (Be, In, Tl).

4.3 Instrumentation

Analyses were carried out by an Inductively Coupled Plasma – Optical Emission Spectrometry (ICP-OES) (IRIS#701776, Thermo Jarrell Ash Corporation). The instrumental parameters used for the analyzed elements are shown in Table 4.1.

4.4 Results and Discussion

. The results of partial and total metal concentration in sediments of ECC28 and ECC57 at 0–30 cm depths are presented in Figures 4.1 to 4.9.

4.4.1 Total metal concentrations in sediments

The accuracy of the analytical procedures and the quality of data for total metal determination were checked with a reference material, Mess-3, a marine sediment reference material for trace metals and other constituents, National Research Council Canada. The total metal concentrations of Zn, Cr, Ni, Cu, Fe, V and Mn in Mess-3 and the certified reference values are presented in Table 4.2. The duplication of extraction results are presented in Table 4.3.

It is evident from the data of Table 4.2 that the concentrations of heavy metals determined in the standard reference material Mess-3 generally agreed with certified values. Some of the profiles show significant high metal concentrations at the very top. Since these samples were collected near the boundary between water and sediment where the richness of suspended particulate matter (SPM) exists, this significance may due to SPM involvement. The similarity of Mn and Co profiles (Fig. 4.10) may provide further

indication that releasing of Co to pore water may be affected by the reductive dissolution of Mn.

4.4.2 Comparison of total and nitric acid/oxalic soluble metal concentrations in sediments

Nitric acid can dissolve metals held at ion-exchange positions, compounds of iron and manganese, carbonates, and metals bound to organic matter; oxalic acid is an efficient reagent for the digestion of crystalline oxides. Nitric acid/oxalic acid extraction, therefore efficiently removes most bound fractions of heavy metal in solid phases except from stable crystalline lattice. For many metals, this method may be considered as a pseudo total heavy metal fraction while there are not significant quantities of resistant crystalline materials in the sediments.

In order to estimate the efficiency of nitric acid/oxalic digestion, a comparison of data was made with total metal concentrations (Fig 4.11 to 4.12). The efficiency of leaching for Fe ranged from 65–100%, Mn from 60-100%, Cu from 50-100% and Cr from 40–75%. Successful leaching of sediments is achieved for Fe, Mn and Cu (in general from 90–100%) at some depths, but a significantly lower efficiency of leaching is found for Ni (6–20%) and Zn (15-50%). For ECC57, the efficiency of leaching for Mn ranged from 60–100%, Zn from 60-100%, Ni from 50-80%, Cr from 40–75%, Fe from 50-75%, Cu from 50-80%. Successful leaching of sediments is also achieved for Mn and Zn (in general from 90–100%) at some depths. For the elements which could not be dissolved in nitric acid /oxalic acid, they are probably bound to silicates or other

refractory materials which cannot be dissolved without hydrofluoric and aqua regia treatment.

Residual heavy metal concentrations are calculated by total extraction minus nitric acid/oxalic acid extraction. The residual concentration of Fe demonstrates some correlation with Mn and Ni as presented in Figure 4.19 (For ECC28: R (Fe-Mn) =0.89, R (Fe-Ni) = 0.94, R (Mn-Ni) =0.85; for ECC57: R (Fe-Mn) =0.78, R (Fe-Ni) = 0.65, R (Mn-Ni) = 0.71). The relationship among these elements suggests that they are associated with similar resistant phases.

It can be concluded that the proportion of metals dissolved is variable and that it depends on the matrix and on the element analyzed. Since the nitric acid/oxalic acid digestion seriously underestimates the amounts of some metals in sediments, it is not an appropriate method for total metal content determinations in sediments such as ECC28 and ECC57, but it could be considered as one of the step sequential methods to determine the fraction of metal bound to both Fe and Mn oxides and organic matter.

Cd has particularly interesting spatial distributions. Generally, dissolution of Cd can be increased in oxidizing environment. The sharp increase in the concentration of solid phase Cd at the base of surface layer where a strong oxidizing zone exists has been found in both cores (Fig. 4.1). It is accompanied by decreasing concentrations of pore water Cd, and may be caused by the downward migration and precipitation of the Cd released from the oxidizing zone. This migration and precipitation may cause the accumulation of Cd in deeper sediments. In ECC57, however, decreasing of HNO3/oxalic determined Cd happens after the sharp increase then remains depleting with depth. Since no total

extractable data are available for Cd, the leaching rate of HNO3/oxalic can not be calculated for Cd.

4.4.3 Acetic acid extractable metal concentrations in sediments

Acetic acid extraction (5% v/v) efficiently removes from particulate matter, the weakly bound fraction of heavy metals held at ion-exchange positions, easily soluble amorphous compounds of iron and manganese, calcium carbonates, and metals weakly bound to organic matter (Scancar et al 2000). The extractant does not disturb silicate lattices, resistant iron and manganese minerals, or organic compounds. The method is used to estimate the extent of contamination with heavy metals originating from anthropogenic activities (Loring and Rantala, 1992; Scancar et al 2000). Leaching rates of acetic acid extraction calculated by divide total soluble data (Fig 4.13 to 4.14)indicates that about 1% of Cr, 5% of Fe, 10% of Ni and Zn, 25-35% of Cu, 40-60% of Mn in ECC57, 3% of Cr, 5-10% of Fe, 10-20% of Ni, 20-30% of Zn, 30-40% of Cu and 40-70% of Mn in ECC28 are soluble in 5% v/v acetic acid. Comparing the partitioning of heavy metal between ECC28 and ECC57 exhibit that a high level of acetic acid leaching of Cr, Cu, Fe, Mn, Ni, Zn appears in ECC28.

Some data for Cu and Zn may indicate a high level (about 30-40%) of anthropogenic pathways by which these elements entered sediments. For Ni the anthropogenic portion is in general lower than 20%. Ni soluble in acetic acid also shows a strong relationship with Fe as seen in Figure 4.20 (ECC28: R=0.82; ECC57: R=0.81). It should be stressed that a high proportion (only 1-3%) of the total amount of Cr in sediments from both ECC28 and ECC57, is not extracted. This may happen since Cr in these sites is bound

predominately in silicates and in crystalline iron and manganese oxides and 5% v/v acetic acid does not dissolve these compounds from sediments.

All acetic acid extractable data show a slight increase as a function of depth and increasing alkalinity, this may reflect the metals which are bound to carbonate. Most elements have peak concentrations around the depth of 10-15cm for ECC28 and 25cm for ECC57. Combined with sedimentation rate (2000g m^{-2} $year^{-1}$ which equates to a thickness of about 0.3 cm for ECC28, 1000g m^{-2} $year^{-1}$ for ECC57, Bolsenga and Herdendorf 1993), the temporal variability indicates that these peaks reflect the contamination rush in Lake Erie during 1950s to 1960s.

4.4.4 Ascorbic acid extractable metal concentrations in sediments

Ascorbic acid extraction is widely used for determination of iron and Mn oxide. Ascorbic acid extraction efficiently removes the most reactive iron oxide fraction (amorphous oxide). [Kostka and Luther III, 1994, Ferdelman et al 1991]. The extractant does not disturb silicate lattices, resistant iron and manganese minerals (crystalline oxide), acid volatile sulfide, or organic compounds. The method is used to assess iron and Mn oxide reactivity and crystallinity from dissolution rates. It is one of the most promising approaches for reactive fraction measurements (Christensen et al 2000).

The results for partitioning of heavy metals soluble in ascorbic acid in sediments of ECC28 are presented in Figure 4.15 and for sediments of ECC57 in Figure 4.16. For ECC28, 3-4% of Cr, 6-10% of Fe, 10% of Ni, 5-10% Zn and 20-40% of Mn are soluble in ascorbic acid; for ECC57, 3% of Cr, 4-7% of Fe, 5-10% of Ni, 5% Zn and 15-40% of

volatile sulfide [Kostka and Luther III 1994, Raisewell et al 1994]. The method is used widely to extract iron oxide from sediment samples. It can be employed to estimate the "reducible" oxides (e.q. goethite, hematite) [Poulton and Canfield 2005]. The results for partitioning of heavy metals soluble in sodium dithionite-sodium citrate-sodium acetate in sediments of ECC28 are presented in Figure 4.17 and for sediments of ECC57 in Figure 4.18. It can be seen from these data that about 10-15% of Cr, 20-30 of Cu, 30-50% of Fe, Ni and Zn, 70%-100% of Mn in ECC28 are extracted from the solid phases. For ECC57, 10-15% of Cr, 15-30% of Cu, 20-35% of Fe, Ni and Zn, 80%-100% of Mn are soluble in dithionite extraction.

Small leaching rate variations of Cr, Mn, Cu are shown in different sites, however, Fe, Ni, Zn show similar comparable large variations. Figure 4.21 presents the correlations among these elements. The Fe fraction displays a strong covariance with the Ni fraction in ECC28 (R=0.84) and ECC57 (R=0.88), as do Fe and Zn in ECC28 (R=0.91) and ECC57 (R=0.73). This may suggest that Fe oxide strongly influences the distribution of Zn and Ni.

With ascorbic acid, 15-25% of total Fe (amorphous Fe oxide, the most reactive Fe oxide) was extracted and 20-40% of the total Mn. This observation suggests Fe has a stronger crystallinity than Mn. Because of this, the mineralogy of manganese oxides in sediments are generally thought to be composed of more amorphous materials, and are often found as coating on inorganic (e.g., clays) or biogenic (e.g., siliceous tests) sedimentary particles [Burdige 1993]. They are also usually found in close association with sedimentary iron oxides. This association is shown in core of ECC28 in which Fe and Mn show a medium strong relationship (R=0.71).

70-100% of the total Mn of contents of the two sediment cores is associated with dithionite-soluble fraction (oxide phase), compared to only 20-50% for Fe. This observation implies that Mn may be more readily released from silicate minerals during weathering; this suggestion may be supported by the residual Mn contents after nitric acid/oxalic acid treatment.

Specific geochemical phases, such as oxide phases, which affect the binding and/or sorption of elemental substances to the sediments, are measured to determine the elemental mobility and availability. Fractions of Fe and Mn oxides can be digested by sodium dithionite extraction. Linear regressions have been calculated and plotted for the relationship of various elements to iron, aluminum, manganese and silicon and combinations of these independent variables (Table 4.4). One sample frequently appearing as an outlier is from ECC57. The correlation coefficients indicate that Fe, Al and Si are the dominant phases with which the elements listed in table are preferentially associated. No significant correlation has been found between any element and organic matter. The linear regression analysis of the elements may be used as a tool with which to assess the relative important of various phases / variables which are relevant to the problem of metal availability at least to benthic-feeding organisms. [Lum and Gammon 1985].

4.4.6 Comparison of Mn pore water and sediment results

As mentioned in Chapter 3, vertical profiles of soluble Mn and Fe suggest that the upper 20 cm of sediment can be divided into three zones: 1) Mn oxidation (above the

depth of 2.5cm); 2) Mn reduction (between 2.5cm and 10.5cm); and 3) Fe reduction (after 10.5cm).

With these redox changes in the sediments, the reduction of manganese and iron oxides results in the production of their reduced, and generally more soluble, forms [Burdige, 1993]. The dissolved Mn and Fe formed by these reactions may precipitate out of the sediment pore waters as sulfide, carbonate or phosphate phases [Burdige, 1993]. However, these reduction reactions generally also lead to pore water gradients across the redox boundary of the reduced forms of these metals. The resulting upward diffusion of these ions then leads to their re-oxidation and the formation of new oxides [Burdige, 1993]. For manganese, the steady-state distribution of dissolved Mn should generate a solid-phase peak just above the redox boundary [Burdige et al., 1983; Burdige, 1993; Froelich et al., 1979]. These peaks are indeed displayed in both ECC28 and ECC57 in total soluble fractions around the depth of 2.5 cm where the boundaries of the Mn oxidation zone and reduction zone appear (Fig. 4.22). The vertical profiles of ascorbic soluble Mn support the modeling of internal redox cycling. The dissolved Mn may diffuse a short distance to pass from the Mn reduction zone to the water column and then be re-oxidized. This re-oxidation may be one of the reasons which produce the richness of ascorbic acid soluble Mn near the water-sediment boundary.

4.4.7 Precision of ICP-OES for different solid extraction

Data for the ascorbic acid and acetic acid extractions are expressed in ppm as mean ± standard deviation in Figure 4.23. Large standard deviations appear in analyses of ascorbic acid extractions. Comparing the coefficient of variance (standard deviation

divided by mean) for acetic acid extraction and ascorbic acid extraction data, shows that acetic acid extraction results have a better precision than that of ascorbic acid extraction.

This may be caused by the matrix effects because in the acetic acid extraction the only extra elements introduced into the sample solution are carbon, hydrogen and oxygen, which generally have no significant influence in ICP-OES analysis; in the ascorbic acid extraction, however, high concentration of sodium (approximately 0.5%) has been introduced into the sample solution by the reagent of sodium citrate and sodium bicarbonate, and the sodium may have an effect on analyte lines with high excitation potentials after it is introduced into plasma. Since the standard deviations are not so large, the mean of the three repeat analyses may be regarded as credible.

As for individual elements, large standard deviations exist in ascorbic acid extractable Cd, Cr and Ni determinations and poor precision for V has been found in both ascorbic acid and acetic acid extractions.

4.5 Conclusions

Total acid dissolution including HF treatment, nitric acid/oxalic digestion, and extraction in 5% v/v acetic acid, ascorbic acid and sodium dithionite were applied in the determination of Zn, Cr, Fe, Mn, Ni and Cu in sediments of Lake Erie. The accuracy of total digestions was estimated by the certified reference material, Mess-3.

The efficiency of the nitric acid/oxalic digestion was measured by comparing with data from the total digestion technique. This extraction cannot be applied for total metal analysis for some elements (e.g. Ni, Cr and Zn) since it seriously underestimates the amounts of these metals in Lake Erie sediments from the eastern basin. Correlations of

residual concentrations after nitric acid/oxalic digestion for Fe, Mn and Ni reveals that these elements may be associated with similar resistant silicate phases.

An acetic acid extraction procedure was used to evaluation of the extent contamination of heavy metals possibly originating from anthropogenic activities. Analysis of sediments from ECC28 and ECC57 may indicate a reducing anthropogenic input of heavy metals in this area recently.

Ascorbic acid extraction provides information on reactive Fe and Mn oxides, which can be used to evaluate the mobility of heavy metals coupled with the pore water data. Enrichment of Mn oxide near the surface may come from nitrate oxidation.

Sodium dithionite extractions shows the covariance in oxide phase concentration of Fe, Mn, Ni, and Zn and suggests that Fe has a stronger crystallinity than Mn; Fe, Al and Si oxide act as a dominant role on the distributions of Ni and Zn.

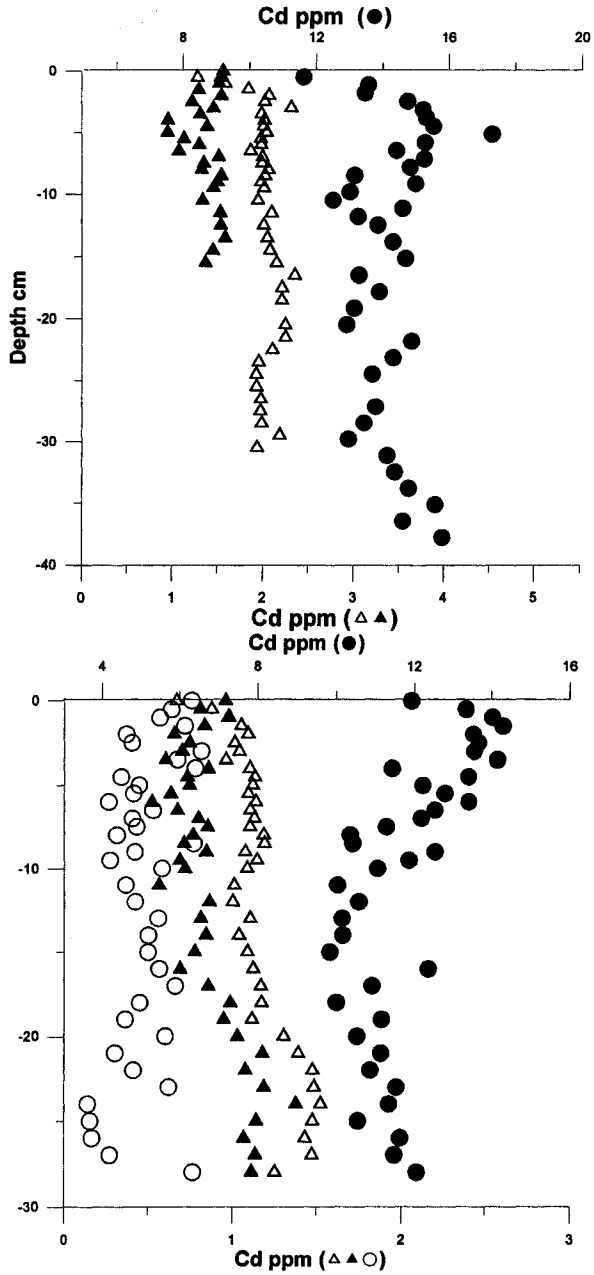

Figure 4.1: Cd solid phase concentration profiles. Left ECC28, right ECC57 (▲ ascorbic acid Δacetic acid ○ sodium dithionite ● HNO3/Oxalic)

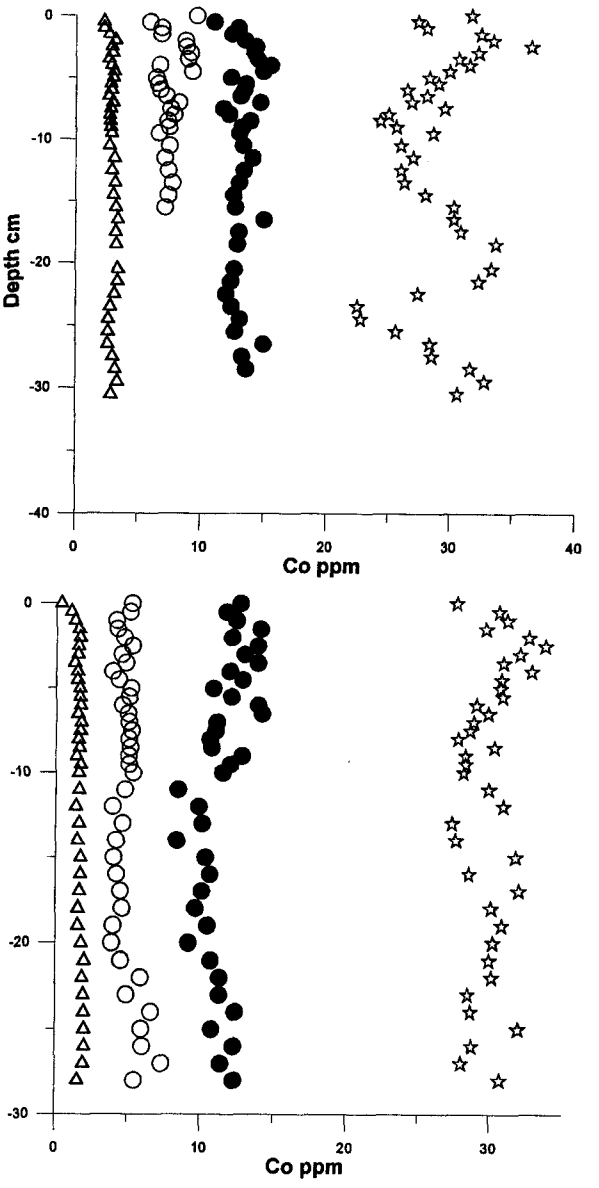

Figure 4.2: Co solid phase concentration profiles. Left ECC28, right ECC57 (Δacetic acid ○ sodium dithionite ● HNO3/Oxalic ☆Total)

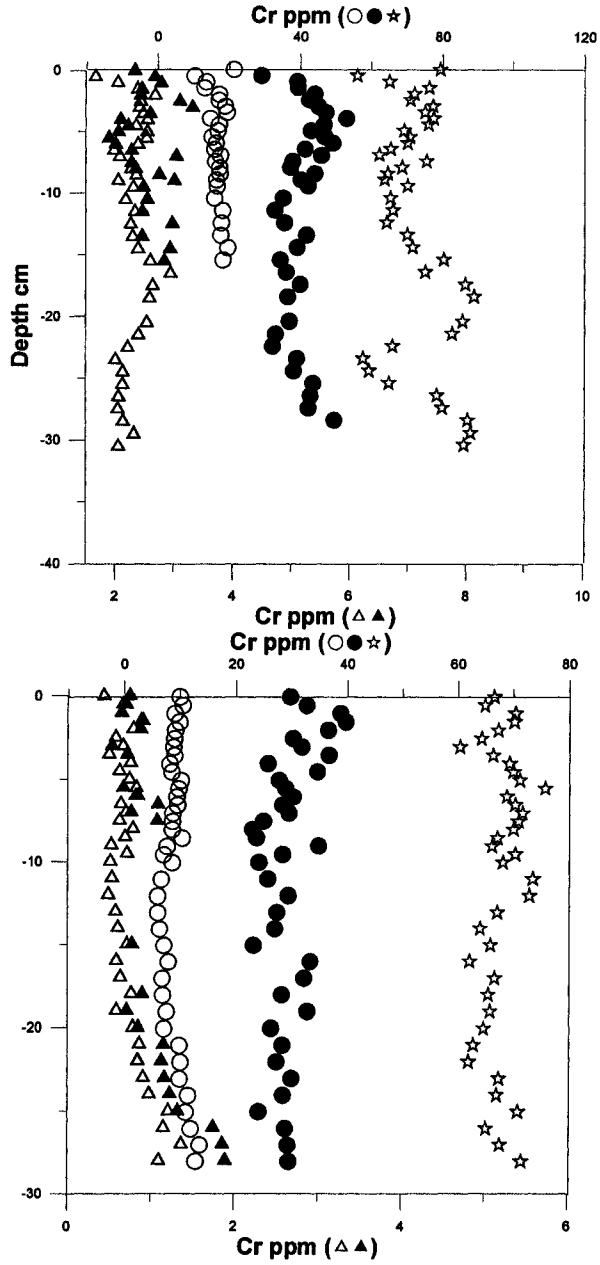

Figure 4.3: Cr solid phase concentration profiles. Left ECC28, right ECC57 (▲ ascorbic acid Δacetic acid ○ sodium dithionite ● HNO3/Oxalic ☆Total)

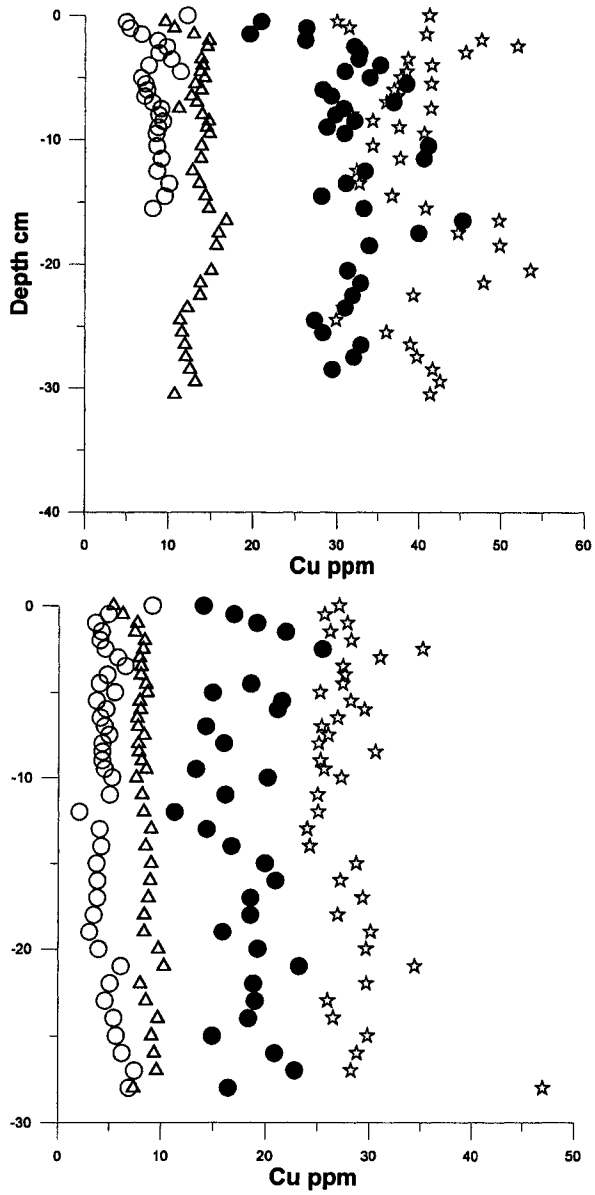

Figure 4.4: Cu solid phase concentration profiles. Left ECC28, right ECC57 (▲ ascorbic acid Δacetic acid ○ sodium dithionite ● HNO3/Oxalic ☆Total)

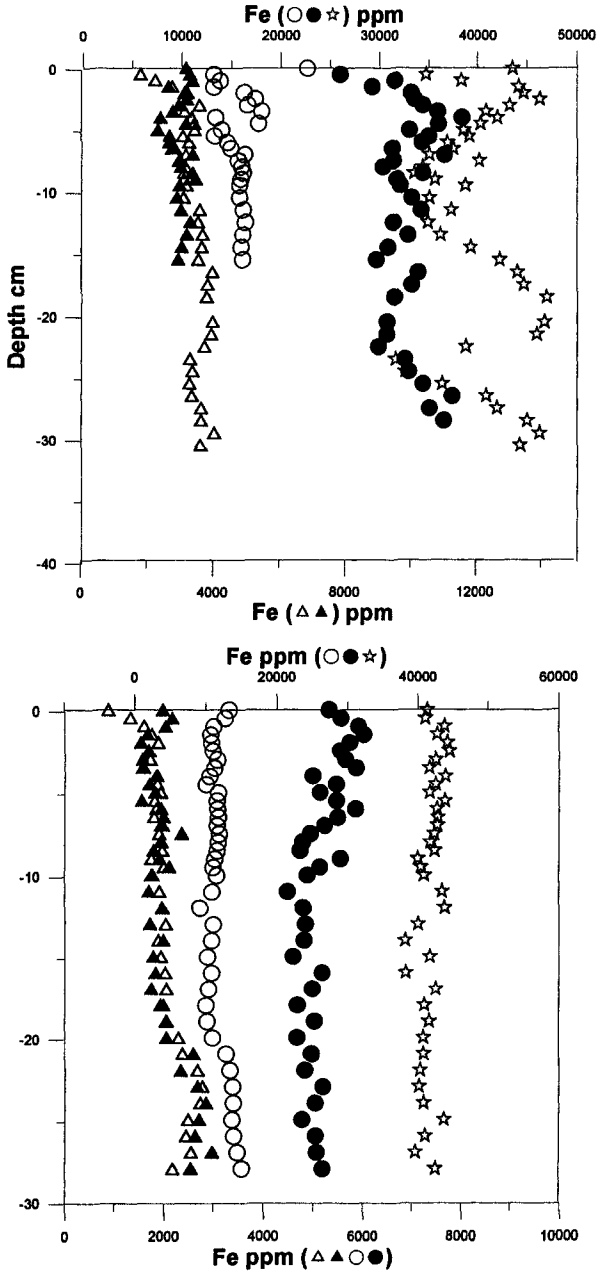

Figure 4.5: Fe solid phase concentration profiles. Left ECC28, right ECC57 (▲ ascorbic acid Δacetic acid ○ sodium dithionite ● HNO3/Oxalic ☆Total)

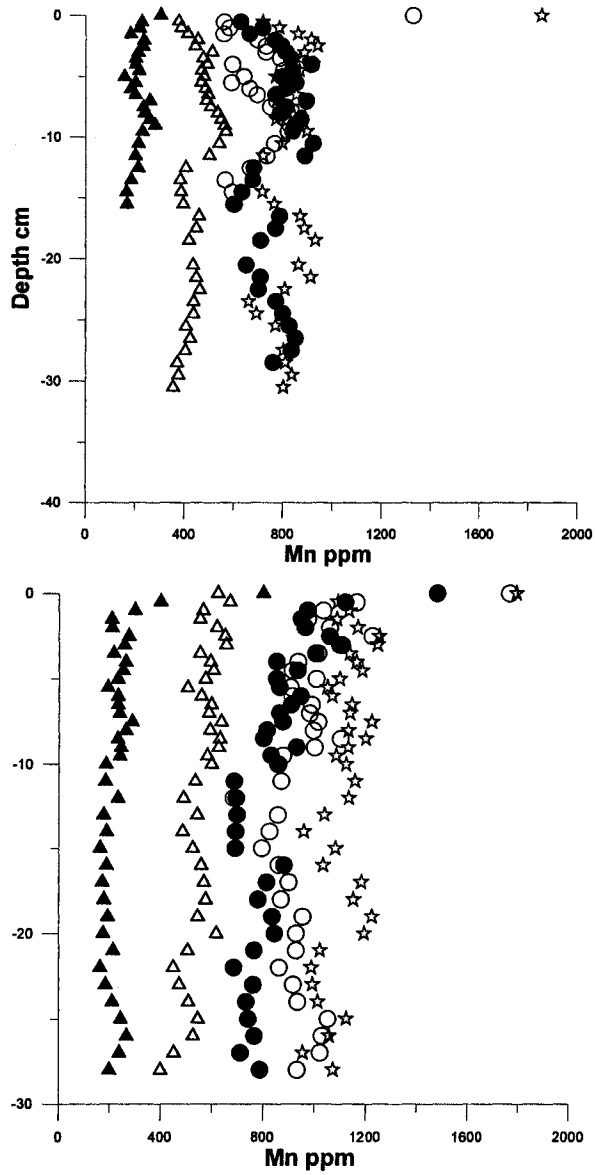

Figure 4.6: Mn solid phase concentration profiles. Left ECC28, right ECC57 (▲ ascorbic acid Δacetic acid ○ sodium dithionite • HNO3/Oxalic ☆Total)

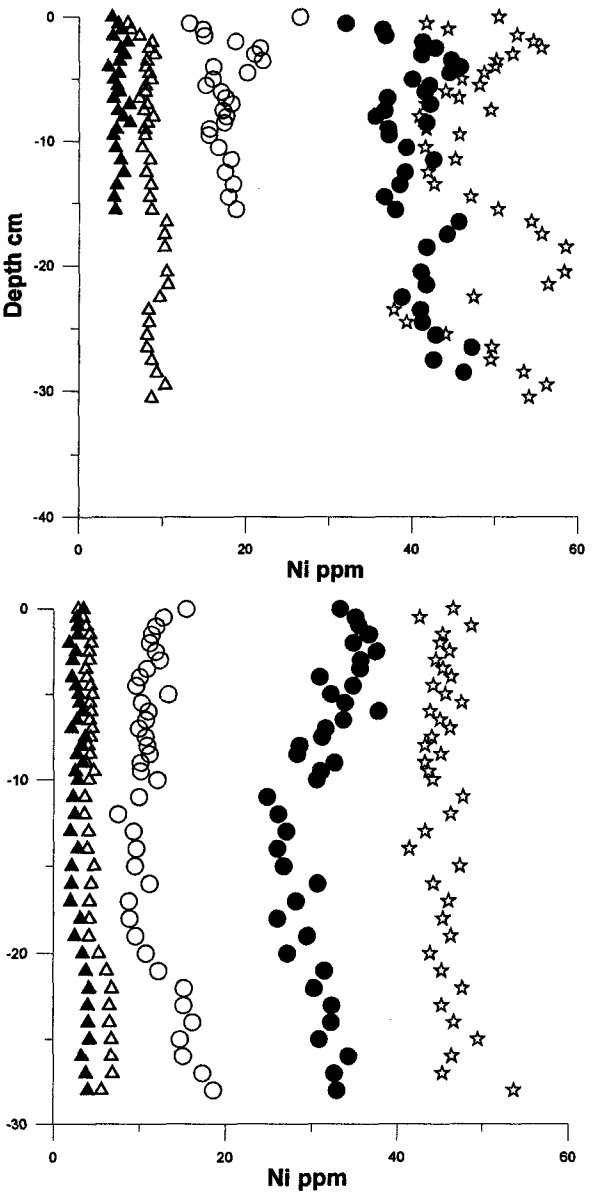

Figure 4.7: Ni solid phase concentration profiles. Left ECC28, right ECC57 (▲ ascorbic acid Δacetic acid ○ sodium dithionite ● HNO3/Oxalic ☆Total)

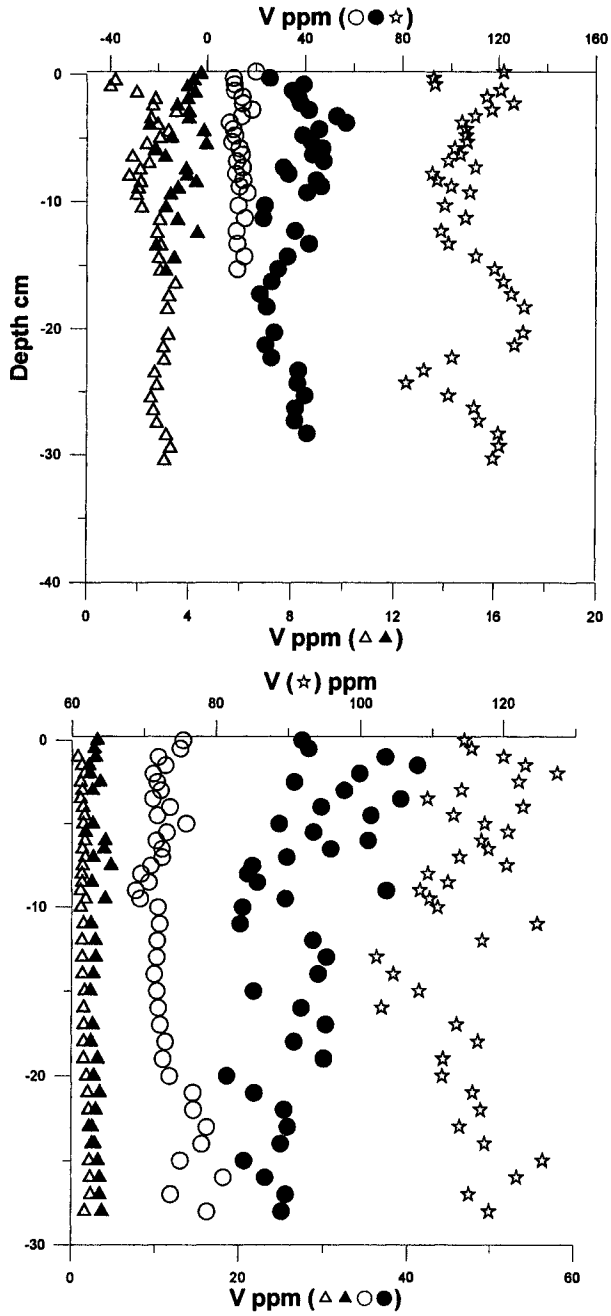

Figure 4.8: V solid phase concentration profiles. Left ECC28, right ECC57 (▲ ascorbic acid Δacetic acid ○ sodium dithionite ● HNO3/Oxalic ☆Total)

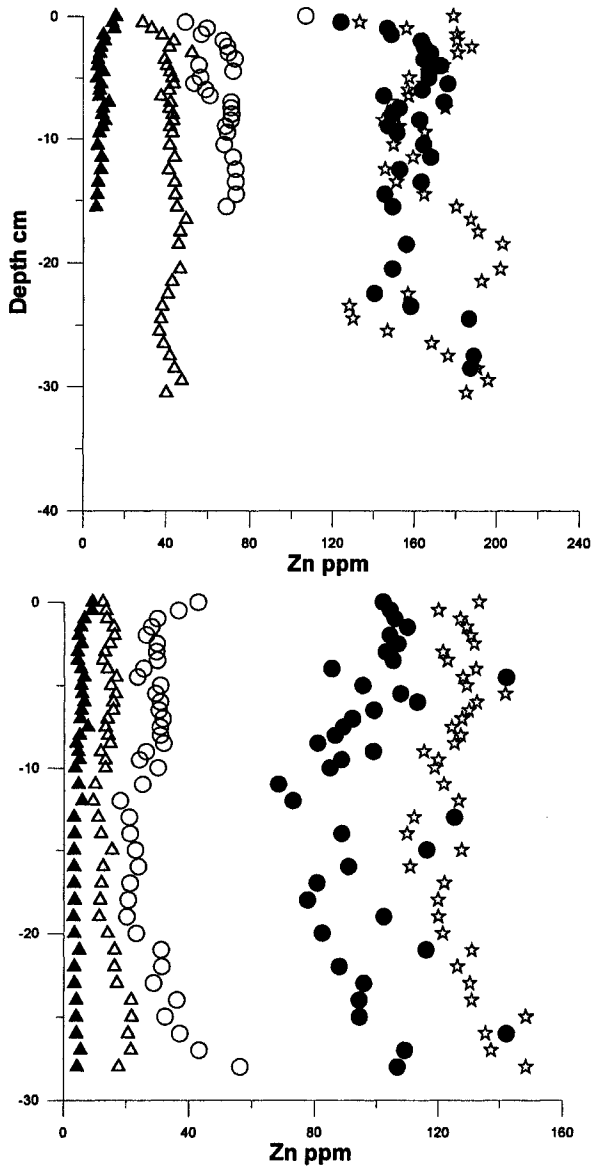

Figure 4.9: Zn solid phase concentration profiles. Left ECC28, right ECC57 (▲ ascorbic acid Δacetic acid ○ sodium dithionite • HNO3/Oxalic ☆Total)

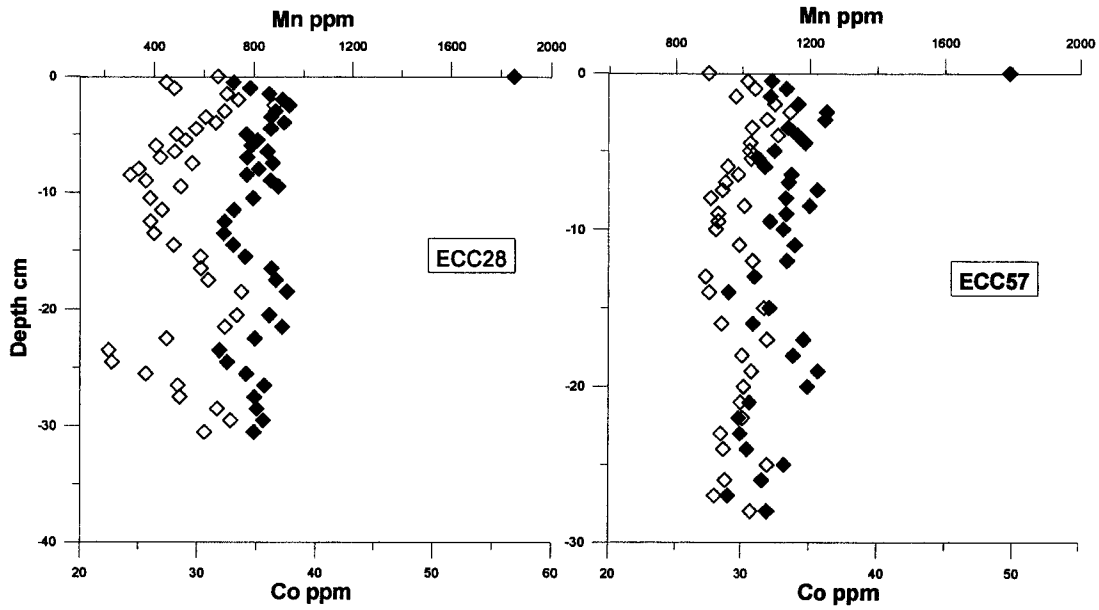

Figure 4.10: Total extractable Mn and Co concentration profiles. (◇Co ◆Mn)

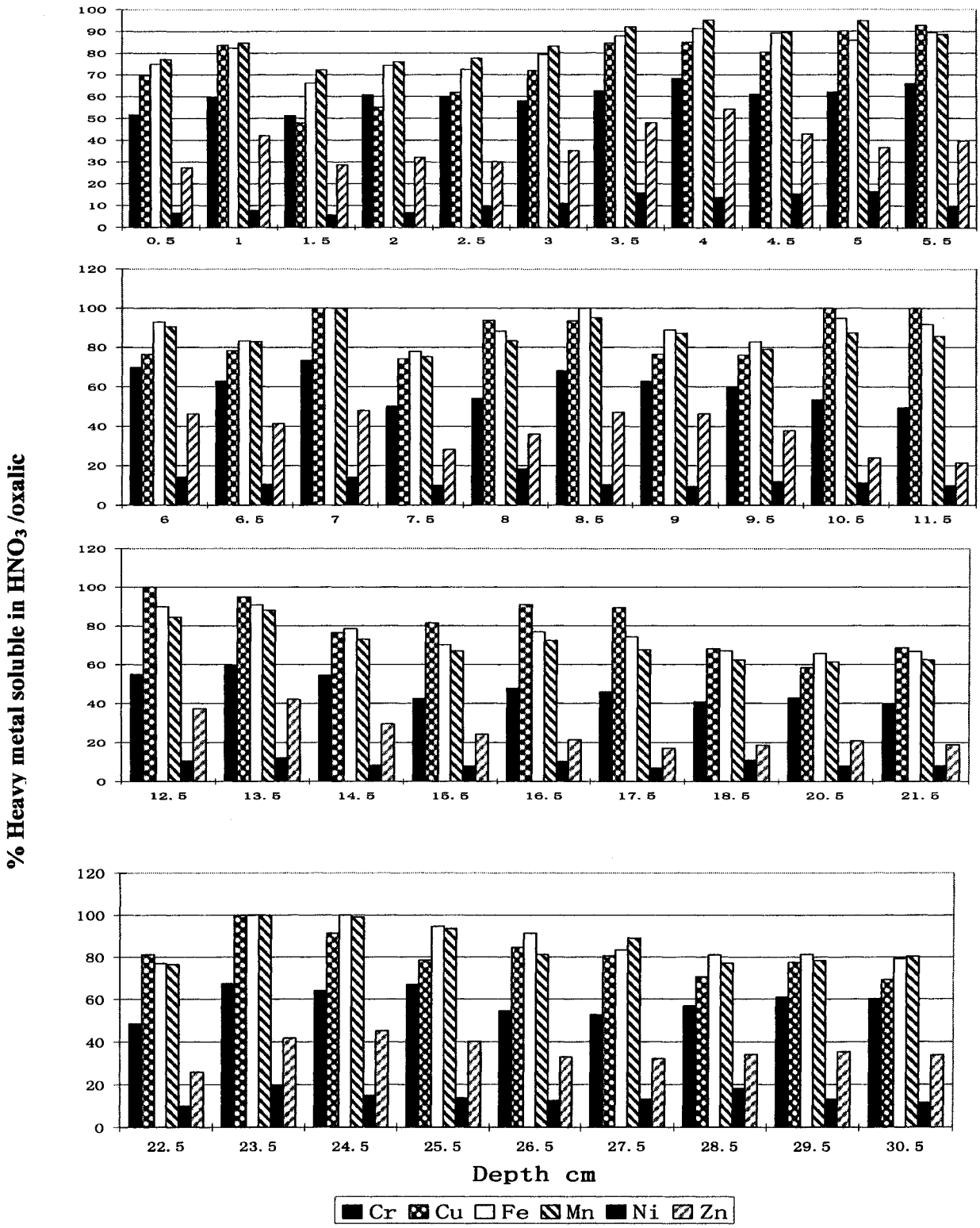

Figure 4.11: Percentage of heavy metals in HNO3/oxalic soluble fraction compared to total metal content found in sediment of ECC28

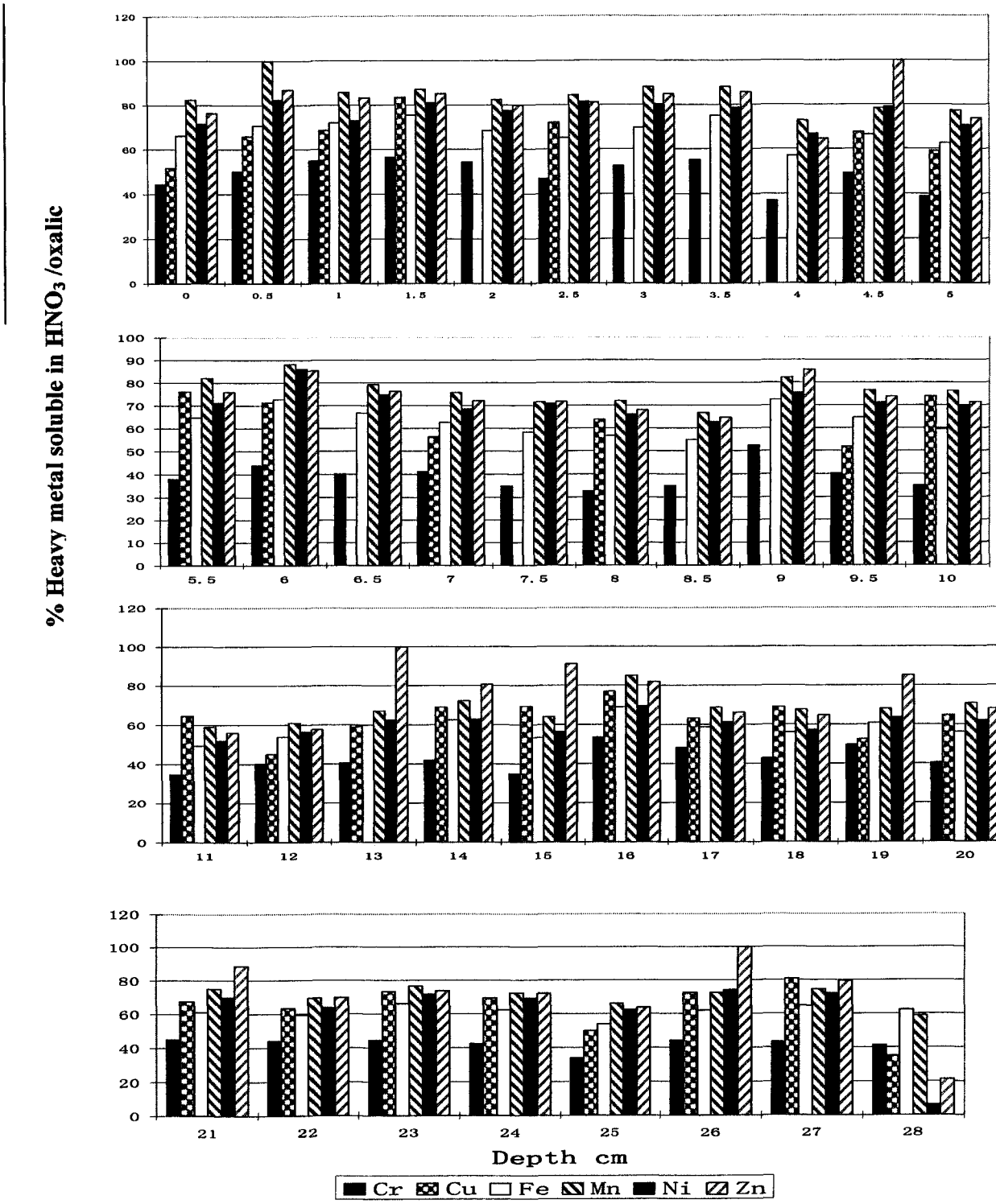

Figure 4.12: Percentage of heavy metals in HNO3/oxalic soluble fraction compared to total metal content found in sediment of ECC57

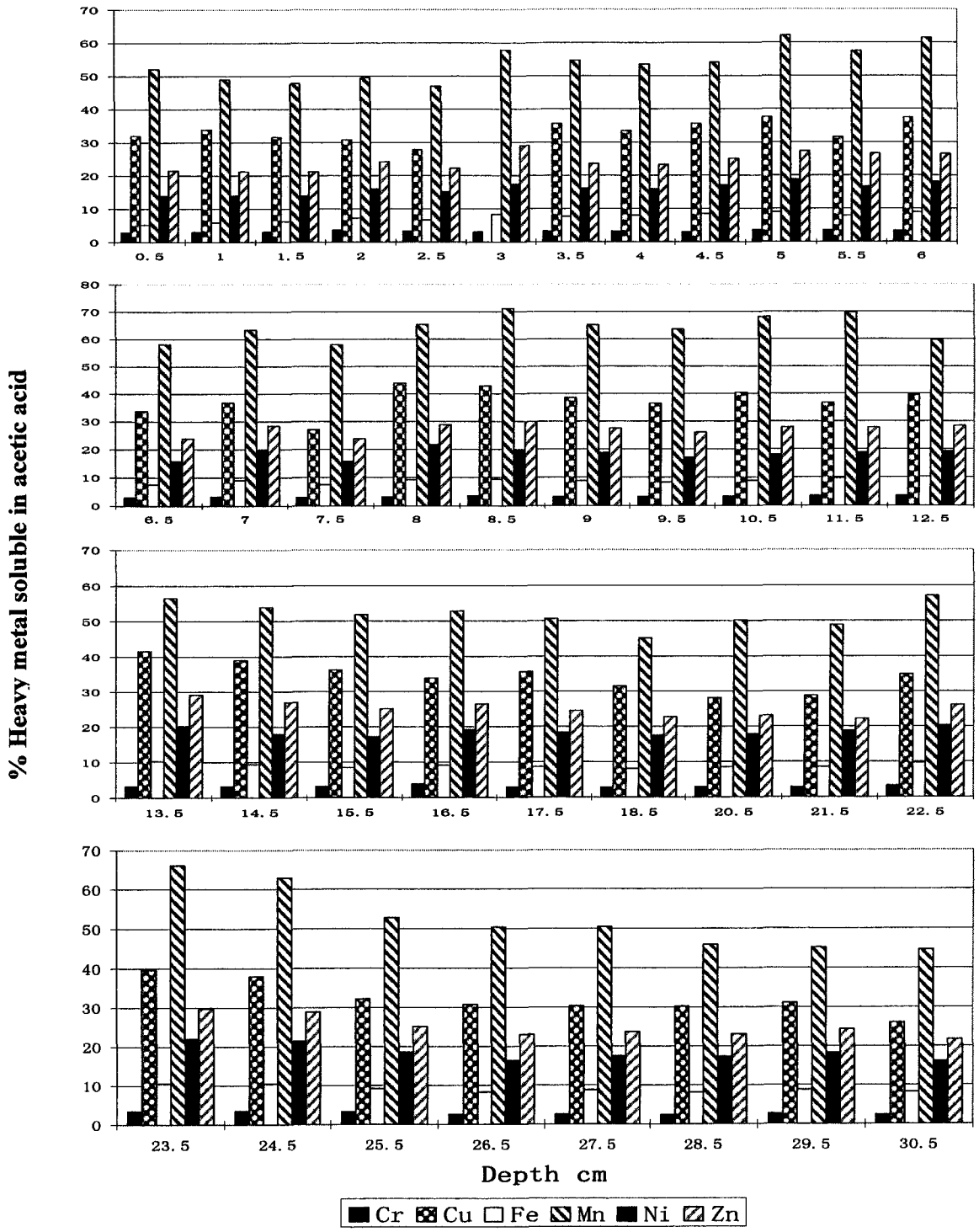

Figure 4.13: Percentage of heavy metals in acetic acid soluble fraction compared to total metal content found in sediment of ECC28

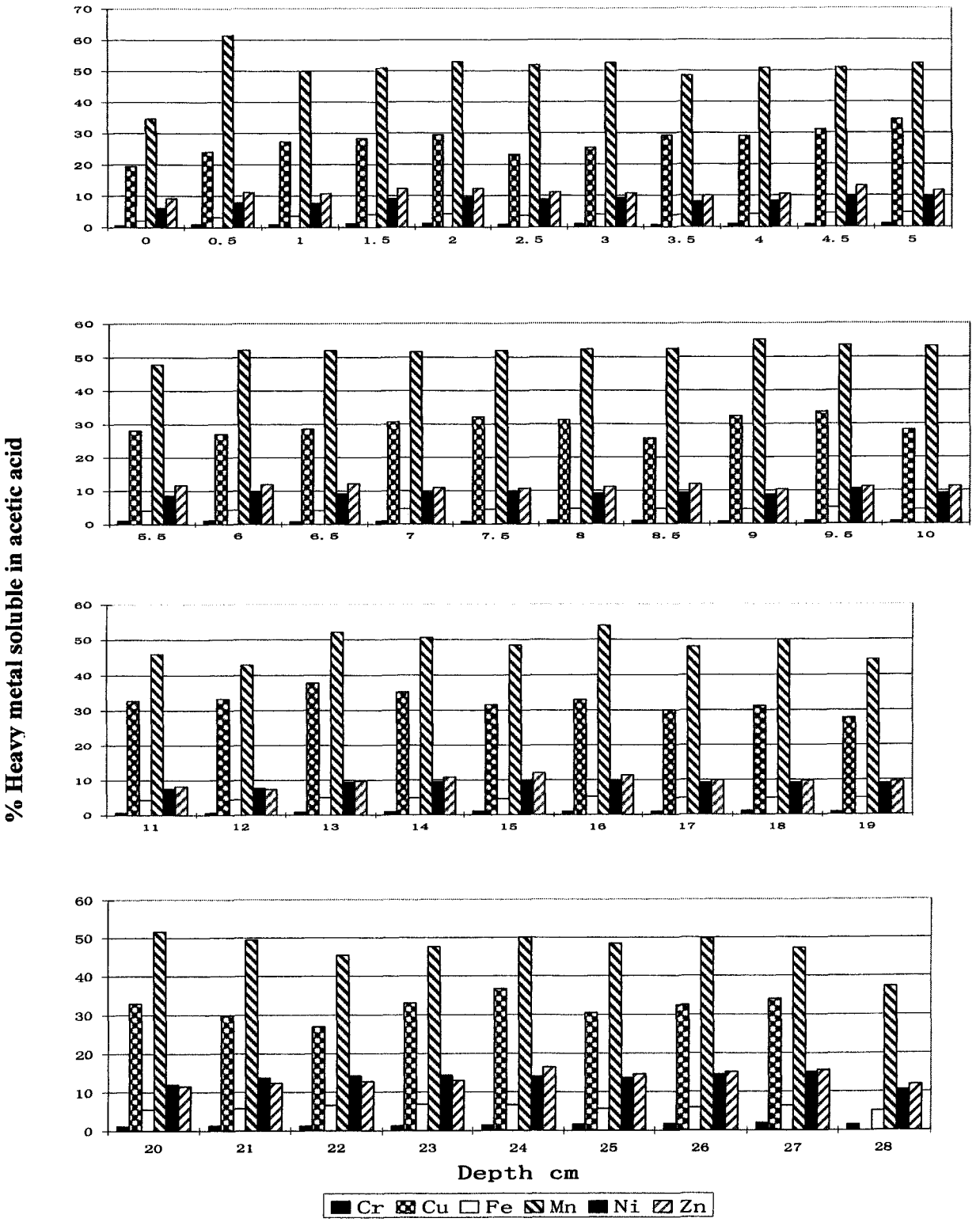

Figure 4.14: Percentage of heavy metals in acetic acid soluble fraction compared to total metal content found in sediment of ECC57

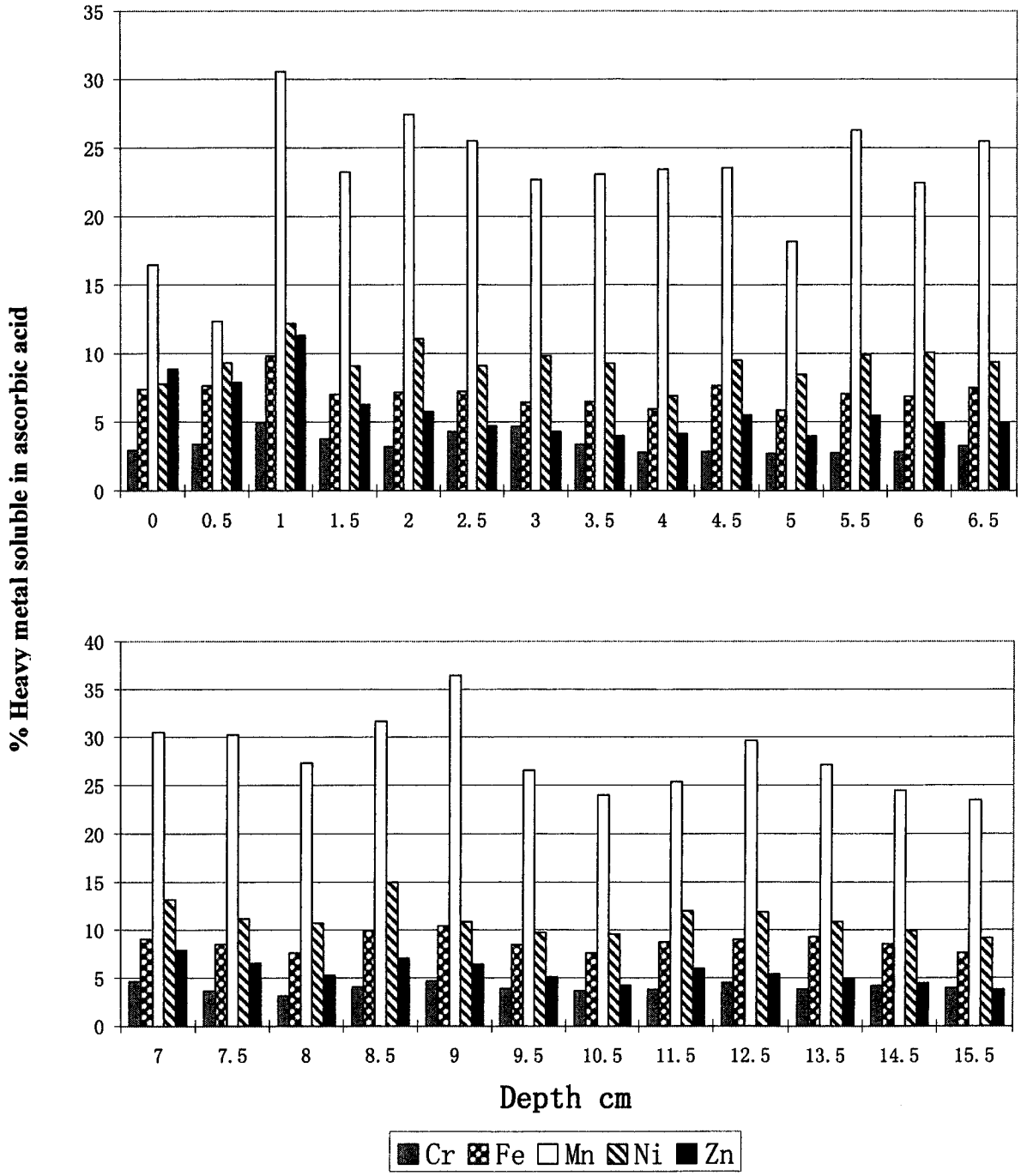

Figure 4.15: Percentage of heavy metals in ascorbic acid soluble fraction compared to total metal content found in sediment of ECC28

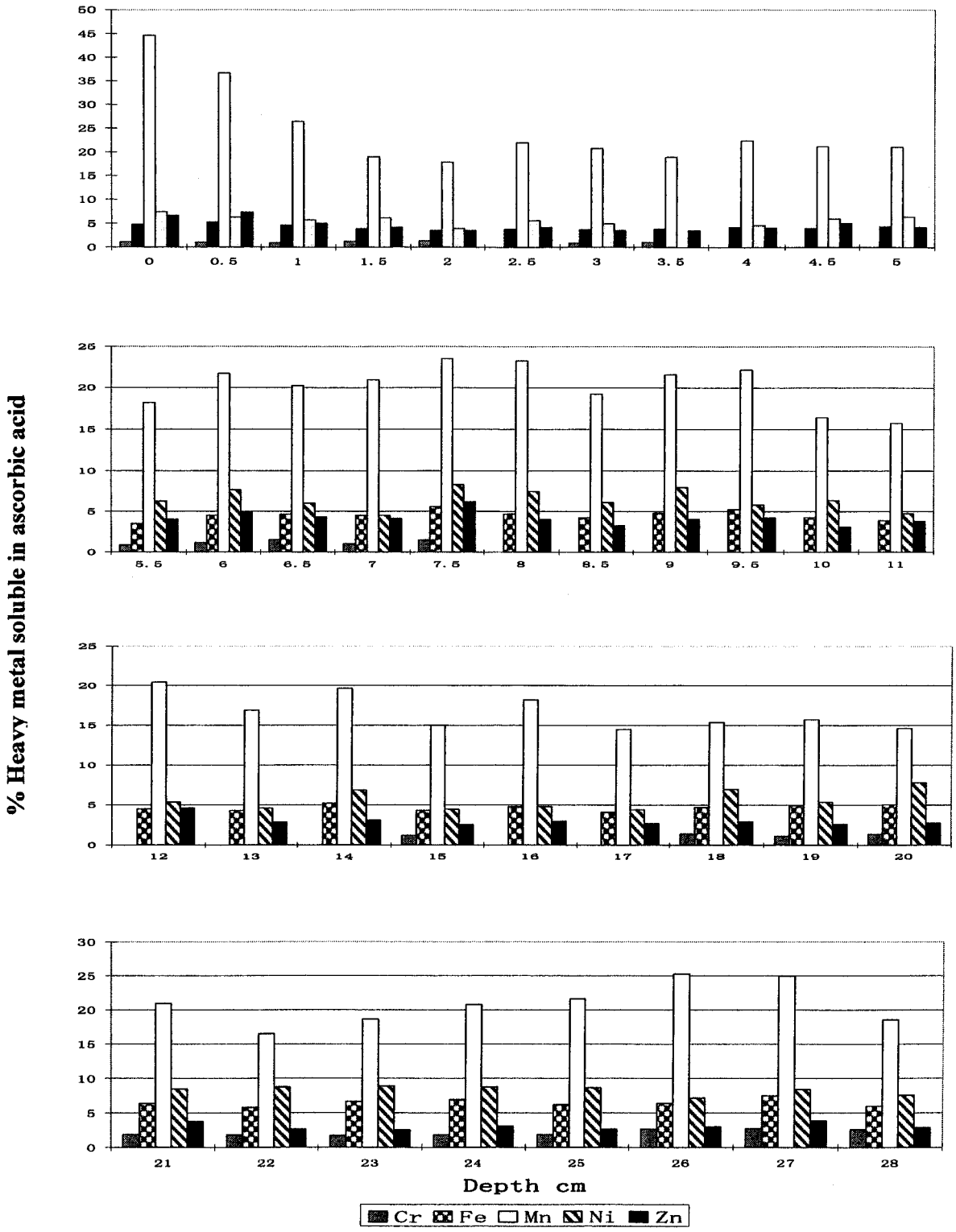

Figure 4.16: Percentage of heavy metals in ascorbic acid soluble fraction compared to total metal content found in sediment of ECC57

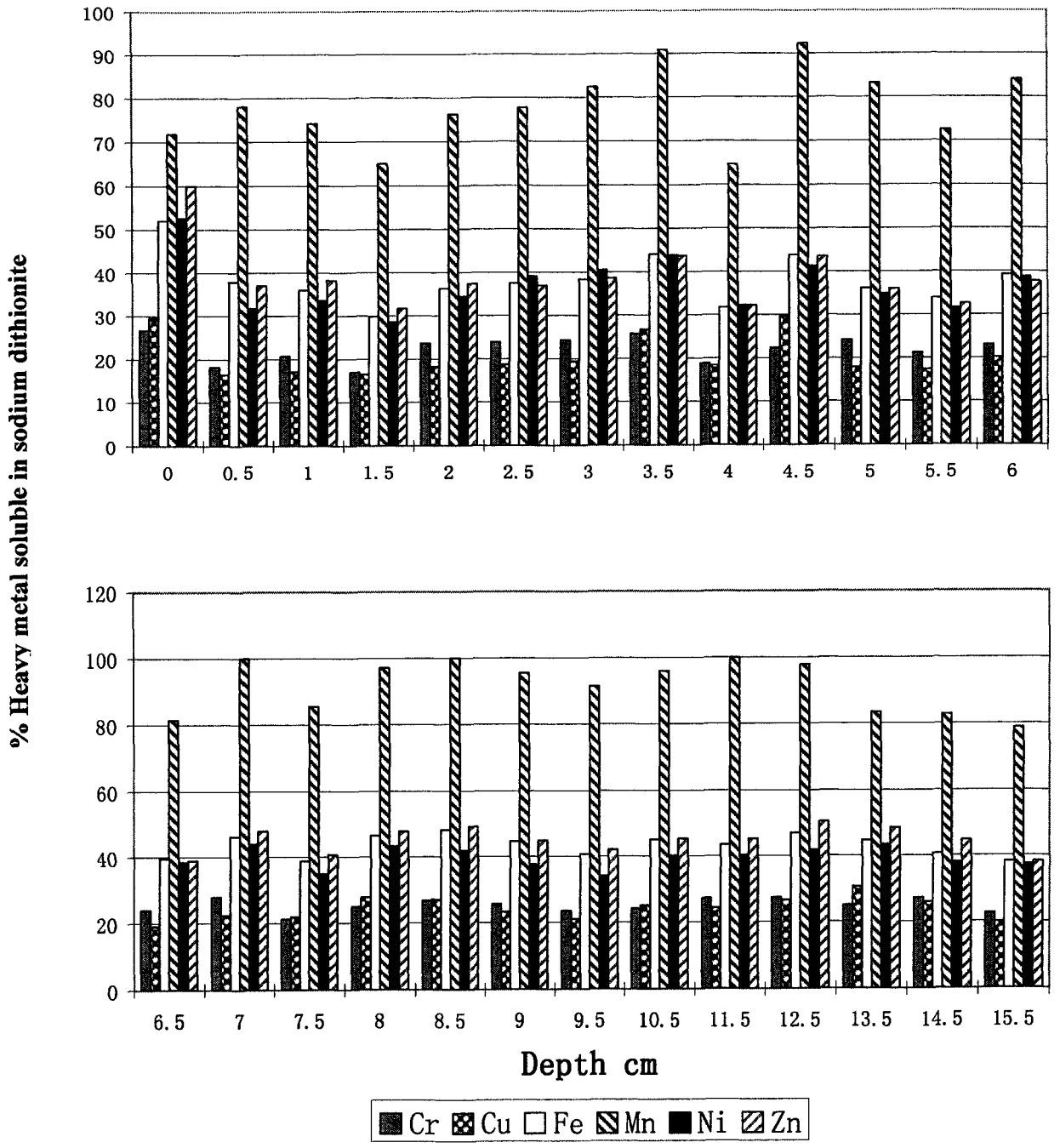

Figure 4.17: Percentage of heavy metals in sodium dithionite soluble fraction compared to total metal content found in sediment of ECC28

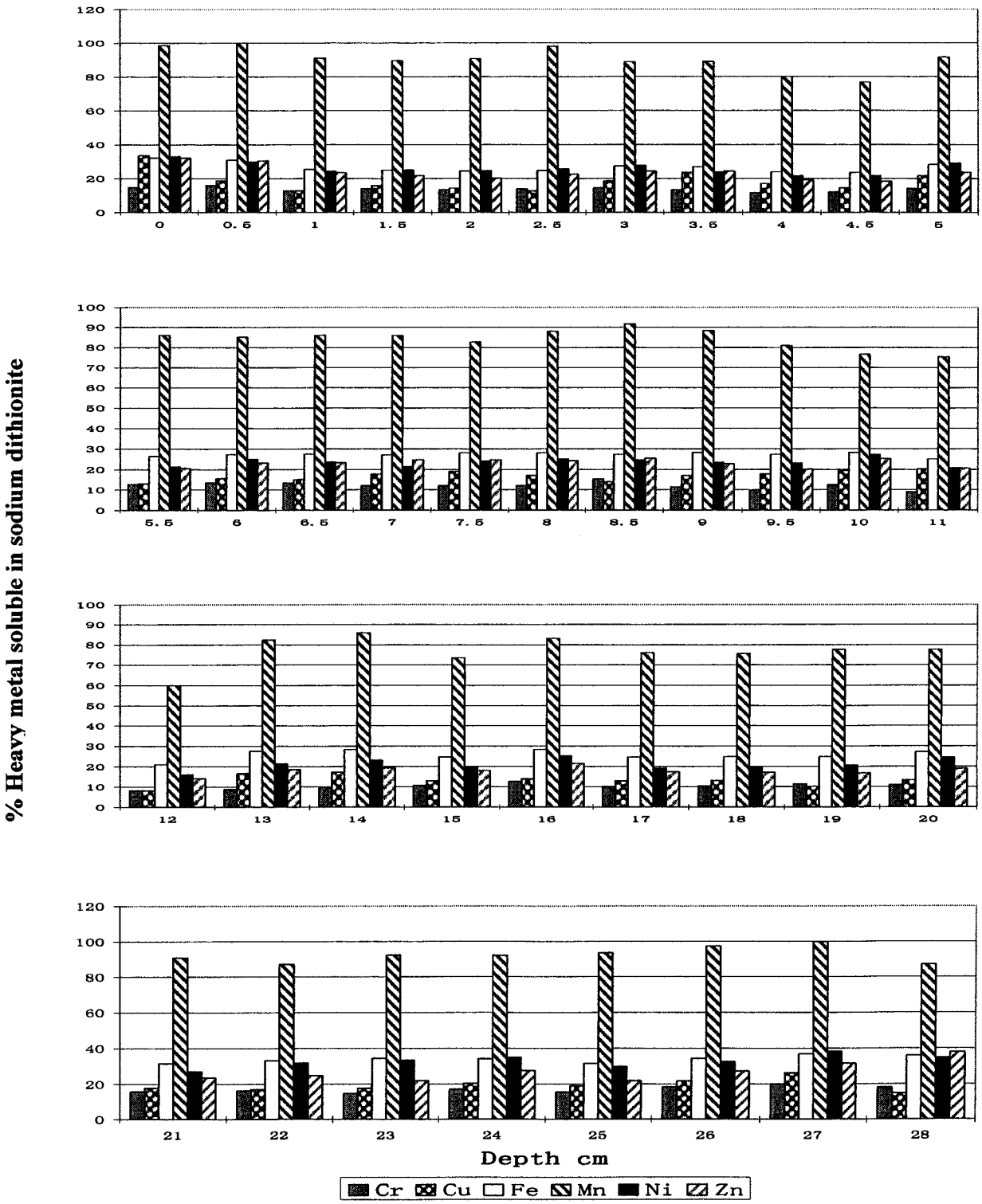

Figure 4.18: Percentage of heavy metals in sodium dithionite soluble fraction compared to total metal content found in sediment of ECC57

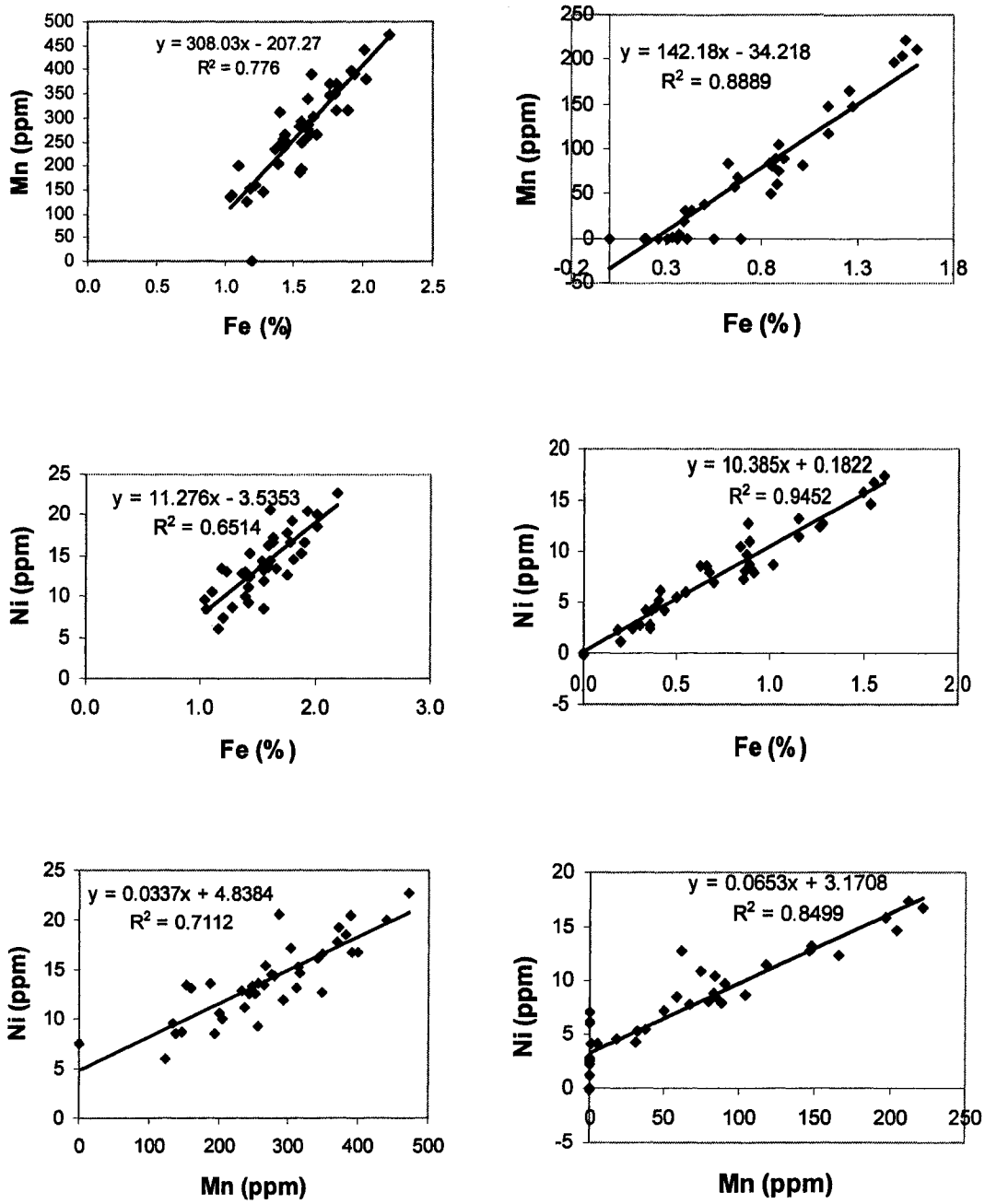

Figure 4.19: Relationship between residual Fe, Mn and Ni after HNO_3/oxalic treatment (Left ECC28, right ECC57)

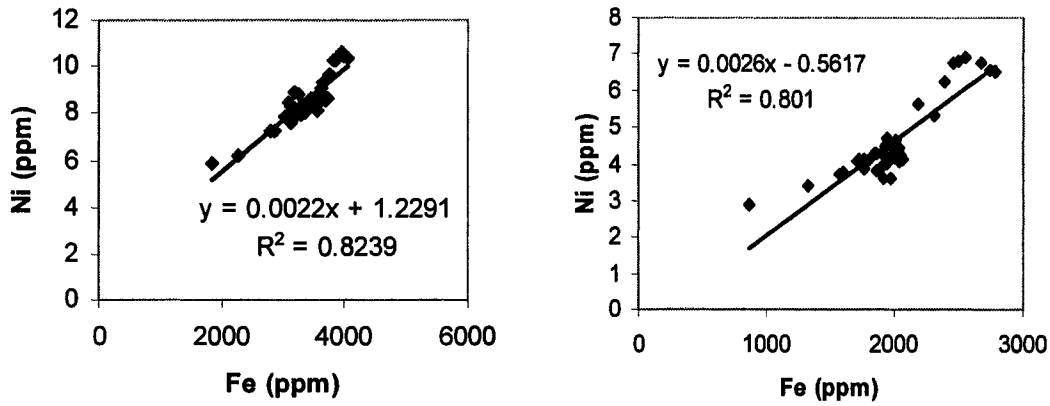

4.20: Relationship between acetic acid soluble Fe and Ni (Left ECC28, right ECC57)

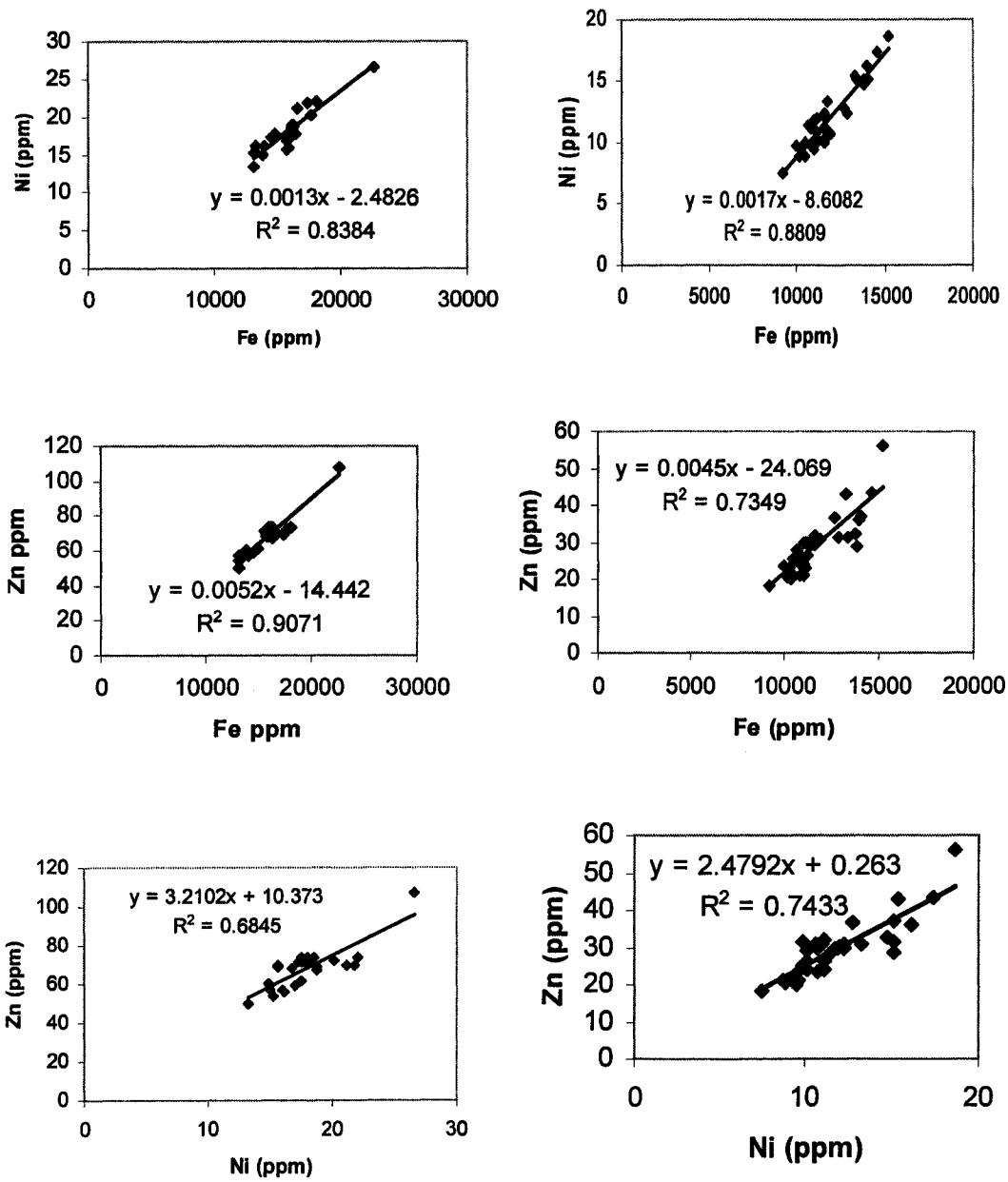

Figure 4.21: Relationship between sodium dithionite soluble Fe, Ni and Zn (Left ECC28, right ECC57)

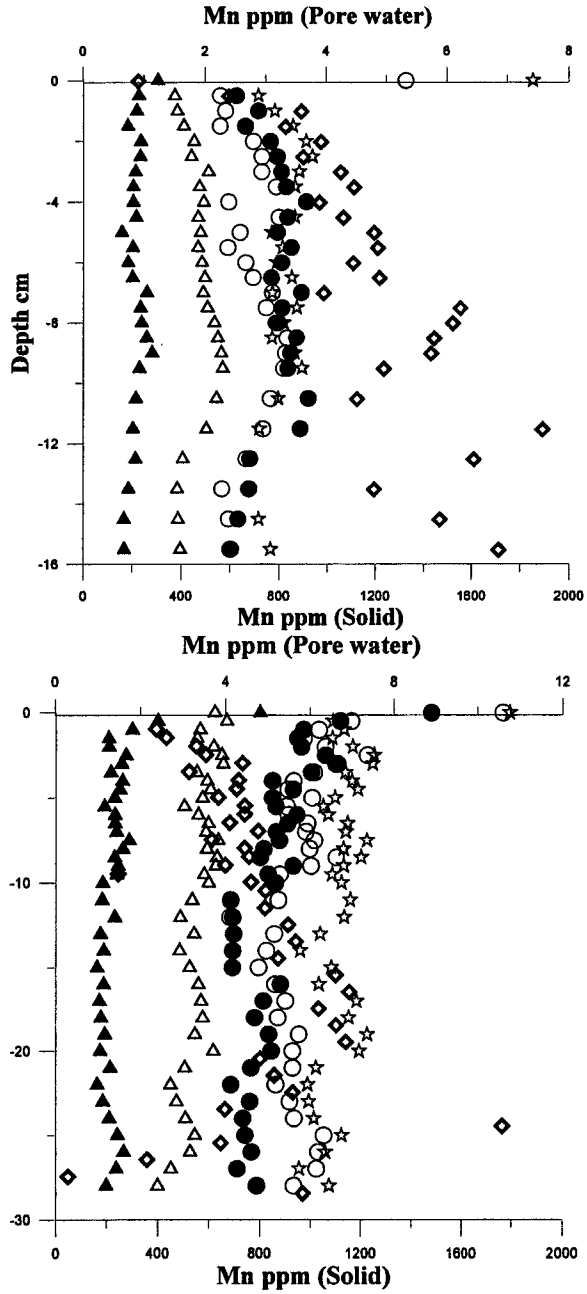

Figure 4.22: Vertical distribution of solid-phase Mn and pore water Mn. Left ECC28, right ECC57 (◇pore water ▲ ascorbic acid Δacetic acid ○ sodium dithionite ● HNO3/Oxalic ☆Total)

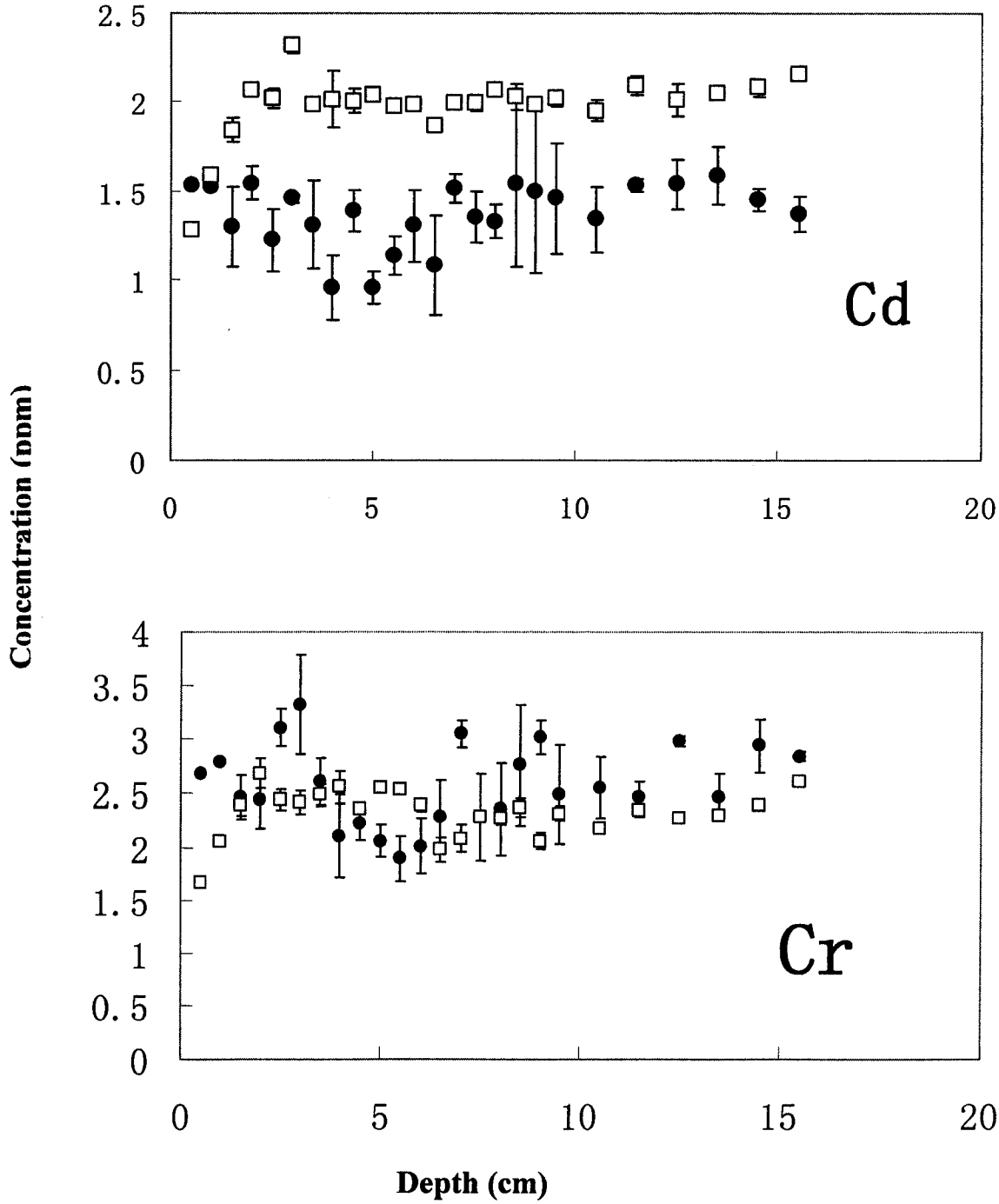

Figure 4.23: Standard deviation of acetic acid (upper) and ascorbic acid soluble metals in sediment of ECC28 (□ acetic acid • ascorbic acid)

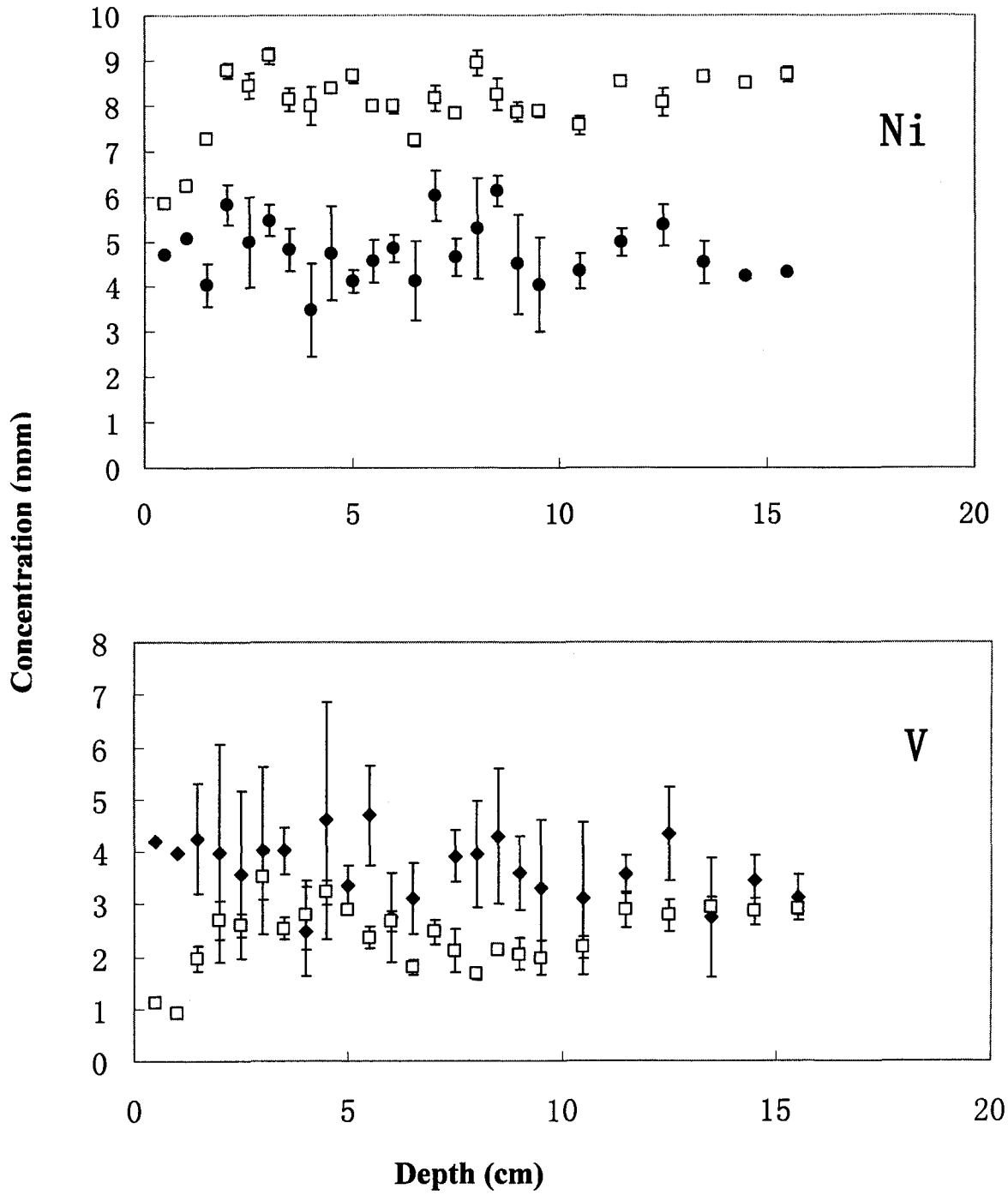

Figure 4.23: Standard deviation of acetic acid (upper) and ascorbic acid soluble metals in sediment of ECC28 (□ acetic acid • ascorbic acid) (Continued)

Table 4.1: Operational parameters used for the determination of elements by ICP-OES

Parameter		Setting
Nebulizer type		Meinhard concentric glass
Spray chamber type		Cyclonic
Detector type		Themostatted charge injection device
RF power		1150 W
Auxiliary gas		Low
Nebulizer pressure		15.0 psi
Flush pump rate		100 rpm
Analysis pump rate		100 rpm
Relaxation time		0.0 sec
Sample flush time		40 sec
Delay time		15 sec
Number of Repeats		3
CID Max. Integration times	Low wavelength range	30.0 sec
	Long wavelength range	5.0 sec

Table 4.2: Results for the total metal content of Mess –3

Element	Found value (ppm)	Certified value (ppm)	Variance (%)
Cr	93.90	105 ± 4	10.57
Cu	28.51	33.9 ± 1.6	15.90
Fe	4.27 (%)	4.34 (%) ± 0.11	1.61
Mn	306.11	324 ± 12	5.56
Ni	46.27	46.9 ± 2.2	1.34
V	231.51	243 ± 10	4.94
Zn	149.33	159 ± 8	6.08

Table 4.3: Duplication of total extraction

Element	ECC28-3 (ppm)		ECC57-37 (ppm)	
	Original	Repeat	Original	Repeat
Cr	84.83	76.31	58.10	67.70
Cu	39.69	40.83	28.40	28.24
Fe	4.28 (%)	4.41 (%)	3.81 (%)	3.96 (%)
Mn	870.28	861.48	915.73	955.67
Ni	50.73	52.64	40.76	45.24
V	115.18	120.81	100.90	115.24
Zn	178.94	180.40	125.62	137.28

Table 4.4: Correlation coefficient for various element associations in the sodium dithionite soluble fraction of sediment from eastern Lake Erie (r^2 is significant at the 0.01 level when > 0.56)

	Fe		Al		Si		Mn	
	ECC28	ECC57	ECC28	ECC57	ECC28	ECC57	ECC28	ECC57
Co	0.67	0.47	0.70	0.53	0.80	0.63		
Cr	0.64	0.72			0.75			
Ni	0.84	0.88	0.88	0.78	0.72	0.58		
Mn					0.60			
P	0.69				0.56			
V								
Mo	0.82	0.55	0.80	0.53	0.70			
Cu			0.67	0.63	0.76	0.67		
Y	0.63	0.79	0.70	0.57	0.70			
Ca								
La	0.77	0.71	0.89	0.63	0.74	0.65		
Ce	0.78	0.75	0.88	0.57	0.75	0.58		

	Fe		Al		Si		Mn	
	ECC28	ECC57	ECC28	ECC57	ECC28	ECC57	ECC28	ECC57
Pr	0.80	0.78	0.90	0.59	0.76	0.65		
Nd	0.78	0.81	0.88	0.55	0.75	0.50		
Sm	0.77	0.72	0.85	0.44	0.76			
Eu	0.79	0.69	0.82	0.38	0.73			
Gd	0.69	0.72	0.77	0.42	0.67			
Tb	0.76	0.66	0.80	0.39	0.71			
Dy	0.66	0.75	0.74	0.46	0.60			
Ho	0.59	0.70	0.68	0.39	0.54			
Er	0.62	0.68	0.73	0.37	0.61			
Tm	0.60	0.68	0.68		0.52			
Yb			0.54	0.41				
Th			0.66					
Fe			0.76	0.65	0.78	0.87		

Reference

Ajayi S. O., VanLoon G. W., 1989. Studies on redistribution during the analytical fractionation of metals in sediments. Sci. Total Environ. 87/88:171– 187.

Allen, H. E., Fu, G., Deng, B., 1993. Analysis of acid-volatile sulfide (AVS) and simultaneously extracted metals (SEM) for the estimation of potential toxicity in aquatic sediments. Environ. Toxicol. Chem. 12:1441-1453.

Amrhein, C., Mosher, P.A., strong, J.E., Pacheco, P.G., 1994. Trace metal solubility in soils and waters receiving deicing salts. J. Environ. Qual. 23: 219-222.

Ankley, G. T., Phipps, G. L., Leonard, E. N. et al., 1991. Acid-volatile sulfide as a factor mediating cadmium and nickel bioavailability in contaminated sediments. Environ. Toxicol. Chem. 10:1299-1307.

Arcinas, A.. Overview of Inductively Coupled Plasma Optical Emission Spectroscopy (ICP-OES) for use in Barium concentration determination.

Baumann, T., Muller, S., Niessner, R., 2002. Migration of dissolved heavy metal compounds and PCP in the presence of colloids through a heterogeneous calcareous gravel and a homogeneous quartz sand - pilot scale experiments. Water Res. 36: 1213-1223.

Bentley, L., 2000. Biosphere 2000 project. Website: www.environmentaleducationohio.org.

Berry W. J., Hansen D. J., Mahony J. D., Robson D. L., Di Toro D. M., Shipley B. P., Rogers B., Corbin J. M. and Boothman W. S., 1996. Predictingthe toxicity of metalspiked laboratory sediments usingacid-volatile sulfide and interstitial water normalizations. Environ. Toxicol. Chem. 15, 2067–2079.

Birch, G., Siaka, M., Owens, C., 2001. The Source of Anthropogenic Heavy Metals in Fluvial Sediments of a Rural Catchment: Coxs River, Australia, Kluwer Academic Publishers

Birch, G.F., Taylor, S.E., Matthai, C., 2001. Small-scale spatial and temporal variance in the concentration of heavy metals in aquatic sediments: a review and some new concepts. Environ. Pollution 113, 357-372.

Bolsenga, S., Herdendorf, C., 1993. Lake Erie and Lake St. Clair Handbook. Wayne State University Press, Detroit.

K. Das, A.R. Chakraborty, M.L. Cervera, M. de La Guardia, 1995. Metal speciation in solid matrices. Talanta 42, 1007-1030.

Bonnet C., Babut M., Ferard J. F., Martel L., Garric J., 2000. Assessing the potential toxicity of resuspended sediment. Environ. Toxicol. Chem. 19: 1290–1296.

Botes, P. J.. 2004. Investigation of mobility of trace elements in river sediments using ICP-OES. Magister Scientiae degree Thesis, University of Pretoria.

Burdige, D. J., 1993. The biogeochemistry of manganese and iron reduction in marine sediments. Earth-Sci. Rev., 35: 249-284.

Calderon, J. C. O., 2005. Inductively coupled plasma mass spectrometry. Earth Science, University of Windsor.

Canfield, D.E., 1989. Reactive iron in marine sediments. Geochim. Cosmochim. Acta 53: 619-632.

Casas, J.M., Rosas, H., Sole, M., Lao, C., 2003. Heavy metals and metalloids in sediments from the Llobregat basin, Spain. Environ. Geology 44, 325-332.

Clarka, M. W., Davies-McConchieb, F., McConchiea, D., Birchb, G.F., 2000. Selective chemical extraction and grainsize normalisation for environmental assessment of anoxic sediments: validation of an integrated procedure. Sci. Total Environ. 258: 149-170.

Chester, R., Hughes, M.J., 1967. A chemical technique for the separation of ferro-manganese minerals, carbonate minerals and adsorbed trace elements from pelagic sediments. Chem. Geol. 2: 249-262.

Christensen, T. H., Bjerg, P. L., Banwart, S. A., Jakobsen, R., Heron, G., Albrechtsen, H-J, 2000. Review article: characterization of redox conditions in groundwater contaminant plumes. J. of Contam. Hydrol. 45.165–241.

Cotton, F., Wilkinson, G. and Gaus, P. L., 1987. Basic Inorganic Chemistry, Second edition, John Wiley & Sons, New York.

Cruise Plan: Cruise Plan of Lake Erie Benthic Survey, 2004. Department of Environment, National Water Research Institute.

Dassenakis, M., Andrianos, H., Depiazi, G.,Konstantas, A., Karabela, M., Sakellarei, A. and Scoullos,M., 2003. The use of various methods for the study of metal pollution in marine sediments, the case of Euvoikos Gulf, Greece. Appl. Geochem. 18: 781–794.

Date, A. L., 1989. Applications of inductively coupled plasma mass spectrometry. Blackie, Glasgow and London.

Di Toro, D. M., Mahony, J. D., Hansen, D.J. et al., 1990. Toxicity of cadmium in sediments: the role of acid volatile sulfide. Environ Toxicol Chem 9:1487-1502.

Di Toro, D.M., 2001. Sediment flux modeling, A John Wiley & Sons, Inc..

Fangueiro, D., Bermond, A., Santos E., Carapuça, H., Duarte, A., 2002. Heavy metal mobility assessment in sediments based on a kinetic approach of the EDTA extraction: search for optimal experimental conditions. Anal. Chim. Acta. 459: 245–256.

Dong, D., Li, Y., Zhang, B., Hua, X., and Yue, B., 2000. Selective chemical extraction and separation of Mn, Fe oxides and organic material in natural surface coatings: application to the study of trace metal adsorption mechanism in aquatic environments. Microchem. J. 69: 89-94.

Ferdelman, T. G., Church, T. M. and Luther III, G. W., 1991. Sulfur enrichment of humic substances in a Delaware salt marsh sediment core. Geochim. et Cosmochim. Acta Vol. 55: 979-988.

Filgueiras, A., Lavilla, I. and Bendicho, C., 2002. Comparison of the standard SM&T sequential extraction with small scale ultrasound-assisted single extractions for metal partitioning in sediments. Anal. Bioanal. Chem. 374: 103–108.

Flyhammar, P., 1997. Estimation of heavy metal transformations in municipal solid waste. Sci. Total Environ. 198: 123-133.

Forstner, U. 1989. Contaminated Sediments: Lectures on Environmental Aspects of Particle-Associated Chemicals in Aquatic Systems. Springer-Verlag, New York, New York.

Gabler, H., 1997. Mobility of heavy metals as a function of pH of samples from an overbank sediment profile contaminated by mining activities. J. geochem. Exploration 58: 185-194.

Garcia, G., Zanuzzi, A. L., Faz A., 2005. Evaluation of heavy metal availability prior to an in situ soil phytoremediation program. Biodegradation 16: 187-194.

Galan, E., Gomez Ariza J. L., Gonzalez, I., Fernandez-Caliani, J. C., Morales, E., Giraldez, I., 2003. Heavy metal partitioning in river sediments severely polluted by acid mine drainage in the Iberian Pyrite Belt. Appl. Geochem. 18: 409 - 421.

Gibs, R. J., 1973. Mechanisms of trace metal transport in rivers. Science 180: 71-73.

Gill G. A., Bloom N. S., Cappellino S., Driscoll C. T., Dobbs C., McShea L., Mason R., Rudd J. W. M., 1999. Sediment–water fluxes of mercury in Lavaca Bay, Texas. Environ. Sci. Tech. 33: 663–669.

GLIER SOP: Standard Operating Procedure-GLIER Metals Lab. Great Lakes Institute of Environmental Research, University of Windsor.

Gobeil C., Silverberg N., Sundby B. and Cossa D., 1987. Cadmium diagenesis in Laurentian through sediments. Geochim. et Cosmochim. Acta Vol. 51: 589-596.

Gomez Ariza, J. L., Giraldez, I., Sanchez-Rodas, I., Morales, E., 2000. Comparison of the feasibility of three extraction procedures for trace metal partitioning in sediments from south-west Spain. Sci. Total Environ. 246: 271-283.

Harrison R. M., Laxen D. P. H., Wilson S. J., 1981. Chemical association of Pb, Cd, Cu and Zn in street dusts and roadside soils. Environ. Sci. Technol. 15:1378– 1383.

Hickey M. G., Kittrick J. A., 1984. Chemical partitioning of cadmium, copper, nickel and zinc in soils and sediments containing high levels of heavy metals. J. Environ. Qual. 13:372– 386.

Kemp, P. F. and Swartz, R. C., 1988. Acute toxicity of interstitial and particle-bound cadmium to a marine infaunal amphipod. Marine Environ. Res. 26: 135-153.

Klinkhammer, G. P. 1980. Early diagenesis in sediment from the eastern equatorial Pacific, II. Pore water metal results. Earth and Planetary Sci. Let. 49: 91-101.

Kersten, M. and Forstner, U., 1986.Chemical fractionation of heavy metals in anoxic estuarine and coastal sediments. Water Sci. Technol. 18: 121–130.

Knight, B. and McGrath, S. P., 1995. A method to buffer the concentrations of free Zn and Cd ions using a cation exchange resin in bacterial toxicity studies. Environ. Toxicol. Water Q. 8: 223 - 230.

Kostka, J. E. and Luther III G. W., 1994. Partitioning and speiation of solid phase iron in saltmarsh sediments. Geochim. et Cosmochim. Acta, Vol. 58, No. 7:1701-1710.

Jardao C. P., Nickless G., 1989. Chemical associations of Zn, Cd, Pb and Cu in soils and sediments determined by the sequential extraction technique. Environ. Technol. Lett. 10: 743– 752.

Jarvis, K. E., 2001. Inductively coupled plasma-mass spectrometry. Blackie, Glasgow and London.

Lagerwerff J. V., Specht A. W., 1970. Contamination of roadside soil and vegetation with Cd, Ni, Pb and Zn. Environ. Sci. Technol. 4(7):583–596.

Laxen, D. P. H. and Harrison, 1981. The physicochemical speciation of Cd, Pb, Cu, Fe and Mn in the final effluent of a sewage treatment works and its impact on speciation in receiving river. Water Res. 15: 1053 - 1065.

Loring, D.H., 1978. Geochemistry of zinc, copper, and lead in the sediments of the estuary and Gulf of St. Lawrence. Can. J. Earth Sci., 15:757-772.

Loring, D. H. and Rantala, R. T. T., 1988. An intercalibration exercise for trace metals in marine sediments. Mar. Chem., 24: 13-28.

Loring, D. H. and Rantala, R. T. T.: 1992, Manual for the geochemical analyses of marine sediments and suspended particulate matter. Earth-Sci. Rev. 32, 235.

Lui, D.Y., Powell, J., Sykes, M., website of University of London, 2002
Scancar, J., Milacic, R. and Horvat, M., 2000. Comparison of various digestion and extraction procedures in analysis of heavy metals in sediments. Water, Air, and Soil Pollution 118: 87-99.

Lum, K. R., and Gammon K. L., 1985. Geochemical availability of some trace and major elements in surficial sediments of the Detroit River and Weatern Lake Erie. J. Great Lakes Res. 11: 328-338.

Ma, L. Q., Dong, Y., 2004. Effects of incubation on solubility and mobility of trace metals in two contaminated soils. Environ. Pollution 130, 301-307.

Ma L. Q., Rao G. N., 1997. Heavy metals in the environment: chemical fractionation of Cd, Cu, Ni and Zn in contaminated soils. J. Environ. Qual. 26:259–64.

Marques, M. J., Salvador, A., Morales-Rubio, A. E., de la Guardia, M., 2000. Trace element determination in sediments: a comparative study between neutron activation analysis (NAA) and inductively coupled plasma-mass spectrometry (ICP-MS). Microchemi. J. 65, 177-187.

Masscheleyn, P.H., Delaune, R.D., Patrick Jr, R.D., 1991. Effects of redox potential and pH on arsenic speciation and solubility in contaminated soil. Environ. Sci. Technol. 25: 1414-1419.

Matisoff, G., Lindsay, A.H., Matis, S., and Soster, F.M., 1980. Trace metal mineral equilibria in Lake Erie sediments. J. Great Lakes Res. 6 (4): 353-366.

McKee, J. D., Wilson, T. P., Long D. T., Owen R. M., 1989. Pore water profiles and early diagenesis of Mn, Cu, and Pb in sediments from large lakes. J. Great Lakes Res. 15 (1): 68-83.

Morin J, Morse JW. 1999. Ammonium release from suspended sediments in the Laguna Madre estuary. Marine Chem. 65: 97–110.

Mudroch, A., Azcue, J. M., 1995. Manual of Aquatic Sediment Sampling, Lewis Publishers.

Mudroch, A., MacKnight, S. D., 1994. Handbook of Techniques for Aquatic Sediments Sampling, second edition, Lewis Publishers.

Nirel P. M. V., Morel F. M., Pitfalls of sequential extractions. Water Res. 8:1055-1056. Nriagu, J.O., Lawson, G., Wong, H.K.T. and Cheam Ven. 1996. Dissolved trace metals in Lakes Superior, Erie, and Ontario. Environ. Sci. 30: 178-186.

Parker D.R. and Pedler J. F., 1997. Revaluating the free-ion activity model of trace metal availability to higher plants. Plant Soil 196: 223 - 228.

Postma, D., 1993. The reactivity of iron oxides in the sediments: a kinetic approach. Geochim. Cosmochim. Acta 57: 5027-5034.

Poulton, S. W. and Canfield, D. E., 2005. Development of a sequential extraction procedure for iron: implications for iron partitioning in continentally derived particulates. Chem. Geol. 214: 209-221.

Poulton, S. W., Raiswell, R., 2000. Solid phase associations, oceanic fluxes and the anthropogenic perturbation of transition metals in world river particulates. Marine Chem. 72:17–31.

Prokop, Z., Vangheluwe, P. A., Van Sprang, P.A., Janssen, C.R. and Holoubek, I., 2003. Mobility and toxicity of metals in sandy sediments deposited on land Ecotoxicol. and Environ. Safety 54: 65–73.

Raiswell, R., Canfield, D.E., Berner, R.A., 1994. A comparison of iron extraction methods for the determination of degree of pyritization and the recognition of iron-limited pyrite formation. Chem. Geol. 111, 101–110.

Rantala, R.T.T., Loring, D.H., 1989. Teflon bomb decomposition of silicate materials in a microwave oven. Anal. Chim. Acta, 220:263-267.

Rivera-Duarte I., Flegal A. R., 1997. Pore-water silver concentrations and benthic fluxes from contaminated sediments of San Francisco Bay, California, U.S.A. Marine Chem. 56: 15–26.

Rossmann, R., Barres, J., 1988. Trace element concentrations in near-surface waters of the Great Lakes and methods of collection, storage, and analysis. J. Great Lakes Res. 14 (2):188-204.

Sahuquillo A., Lopez-Sanchez J. F., Rubio R. et al., 1999. Use of a certified reference material for extractable trace metals to assess sources of uncertainty in the BCR three-stage sequential extraction procedure Anal. Chim. Acta. 382:317-327.

Sahuquillo, A., Rigol, A., Rauret, G., 2003. Overview of the use of leaching/extraction tests for risk assessment of trace metals in contaminated soils and sediments. Trends in Anal. Chem. 22: 154-159.

Salomons W., Forstner U., 1980. Trace metal analysis on polluted sediments. Part II: Evaluation of environmental impact. Environ. Technol. Lett. 1:506-517.

Sarazin, G., Michard, G. and Prevot, F., 1999. Arapid and accurate spectroscopic method for alkalinity measurements in sea water samples. Water Res. Vol 33, No. 1, pp290-294.

Saulnier I., Mucci A., 2000. Trace metal remobilisation following the resuspension of estuarine sediments: Saguenay Fjord, Canada. Appl. Geochem. 15: 191–210.

Sawlan, J. J., and Murray, J. W. 1983. Trace metal remobilization in the interstitial waters of red clay and hemipelagic marine sediments. Earth and Planetary Sci. Let. 64: 213-230.

Stead-Dexter, K., Ward, N. I., 2004. Mobility of heavy metals within freshwater sediments affected by motorway stormwater. Sci. Total Environ. 334-335: 271-277.

Song, Z., Crowe, S. A., O'Neil, A.H., Fryer, B. J., Fowle, D. A., 2005. The influence of early diagenesis on trace metal and phosphorus cycling in Lake Erie sediments. GAC annual meeting.

Tack, F. M. and Verloo, M. G., 1996. Imapct of single reagent extraction using NH4Oac-EDTA on the solid phase distribution of metals in a contaminated dredged sediments. Sci. Total Environ. 178: 29–36.

Taft, A., Jones, 2001. C. Sediment Sampling Guide and Methodologies, second edition, State of Ohio Environmental Protection Agency.

Taylor, K. G., Boyd, N. A. and Boult, S., 2003. Sediments, pore waters and diagenesis in an urban water body, Salford, UK: impacts of remediation. Hydrol. Process 17: 2049-2061.

Tessier A., Campbell P. G. C., Bisson M., 1979. Sequential extraction procedure for the speciation of particulate trace metals. Anal. Chem. 51(7):844– 851.

Tokalioglu, S., Kartal, S., Elci, L., 2000. Determination of heavy metals and their speciation in lake sediments by flame atomic absorption spectrometry after a four-stage sequential extraction procedure. Anal. Chim. Acta. 413: 33-40.

Tuzen, M., 2003. Determination of trace metals in the River Yesilırmak , sediments in Tokat, Turkey using sequential extraction procedure. Microchem. J. 74: 105–110.

Ure A. M., Quevauviller P., Muntau H., Griepink B., 1993. Speciation of heavy metals in soils and sediments. An account of the improvement and harmonization of extraction techniques undertaken under the auspices of the BCR of the Commission of the European Communities. Int. J. Environ. Anal.Chem.;51:135-151.

Van der Zee, C., Van Raaphorst, W., 2004. Manganese oxide reactivity in North Sea sediments. J. Sea Res. 52: 73-85.

Wallman W., Kersten M., Gruber J., Forstner U.. 1993. Artifacts in the determination of trace metal binding forms in anoxic sediments by sequential extractions. Int. J. Environ. Anal. Chem. 51: 187– 200.

Wen, X., Allen, H. E., 1999. Mobilization of heavy metals from Le An River sediment. Sci. Total Environ. 227: 101-108.

Widerlund A., 1996. Early diagenetic remobilisation of copper in near-shore marine sediments: a quantitative pore-water model. Marine Chem. 54: 41–53.

Wong, C., Li, X., 2003. Analysis of heavy metal contaminated soils.Pract. Periodical of Haz., Toxic, and Radioactive Waste Mgmt., 7:12-18.

Appendix: Comparison of ICP-OES and ICP-MS Analysis

1. Results and discussion

1.1 Comparison of total extracted sediment data obtained by ICP-MS and ICP-OES

Total digested sediment samples were analyzed by ICP-OES and ICP-MS, and the results obtained for ECC 28 are presented in Fig. A.1.

A general trend observed when comparing the ICP-OES and ICP-MS data is that the values for all the elements determined by both techniques are generally within 20% of each other except for K, Fe, Co and Zn where the ICP-MS values are always lower than those found by ICP-OES. Some elements like the rare earth elements cannot be detected by ICP-OES.

In general, when pooled and compared there is good agreement between both analytical techniques for the mean concentrations for Na, Mg, Ca, V, Cr, Cu, Cd and Mn in a subset of samples. However, for several other elements, such as Zn, K and Fe, there are large differences between the results obtained.

To evaluate the accuracy of methods employed, a certified sample (Mess-3) was analyzed by both techniques and data determined by ICP-OES and ICP-MS were compared with the certified values (Table A.1). Differences from -15 to 0% were obtained for ICP-OES except for Co and between -19 and 0% for ICP-MS except for K, Fe, Zn and Ni.

1.2 Comparison of pore water data obtained by ICP-OES and ICP-MS

Pore water samples were analyzed by ICP-OES and ICP-MS, and the results obtained for ECC 28 are presented in Fig. A.2.

Compared with sediment samples, pore water samples have lower matrix concentrations. This may reduce the matrix effects in ICP-MS analysis. However, as the concentrations of most trace metals in pore water are much lower than those in sediments, the utility of ICP-OES measurements will be limited by detection limits of this technique.

Broad trends observed when comparing ICP-OES and ICP-MS data include the distinctly different mean concentrations for the elements Fe, Mn and K are large. ICP-MS values for Fe are always higher than those found by ICP-OES; ICP-MS gives lower values for K.

2. Conclusions

In view of the results determined by both techniques, some issues can be considered:

- Sample pretreatment has a small influence on performance, as the samples must be dissolved for both techniques.
- Sample size requirements are similar in both ICP-OES and ICP-MS.
- The most often used reagent for dilution in ICP-OES is 1% nitric acid or distilled water while internal standard (Be, In, Tl dissolved in 1% nitric acid) must be added in the samples for ICP-MS analysis.

- The working range of ICP-MS has a ceiling (>100ppm) [Olesik, 1991], above which error escalates exponentially.
    - This may require larger dilution factors for ICP-MS treatments which can introduce new sources of error into the analysis.
- The detection limits acquired in both techniques are sample dependent. Generally, detection limits of ICP-MS are up to 3 orders of magnitude less than those in ICP-OES. For this reason, ICP-MS is considered the preferred technique for trace and ultra-trace analysis.
- Comparing the values found for the certified material Mess-3 obtained in ICP-OES and ICP-MS, a general trend can be observed that ICP-OES is the more appropriate choice for major elements analysis such as Na, K, Ca, Mn and Fe;
    - Ni and Zn present good accuracy in ICP-OES while poor accuracy is shown in ICP-MS.
    - Suppression of Ni and Zn signal in ICP-MS analysis may be caused by the high background concentration of Na in some matrices.
- Pore water data indicated that ICP-MS is the preferred technique for the elements V, Cr, Co, Ni, Cu and REE.

It remains complicated to determine the appropriate technique for the samples and elements of choice, ICP-OES or ICP-MS. In general terms, ICP-OES is often the better choice for the lower atomic weight elements, while ICP-MS is better for the higher atomic weight elements [Lui et al, 2002]. But confounding factors such as matrix effects and abundance of dissolved elements must be considered and quantified prior to the analysis of environmental samples analysis.

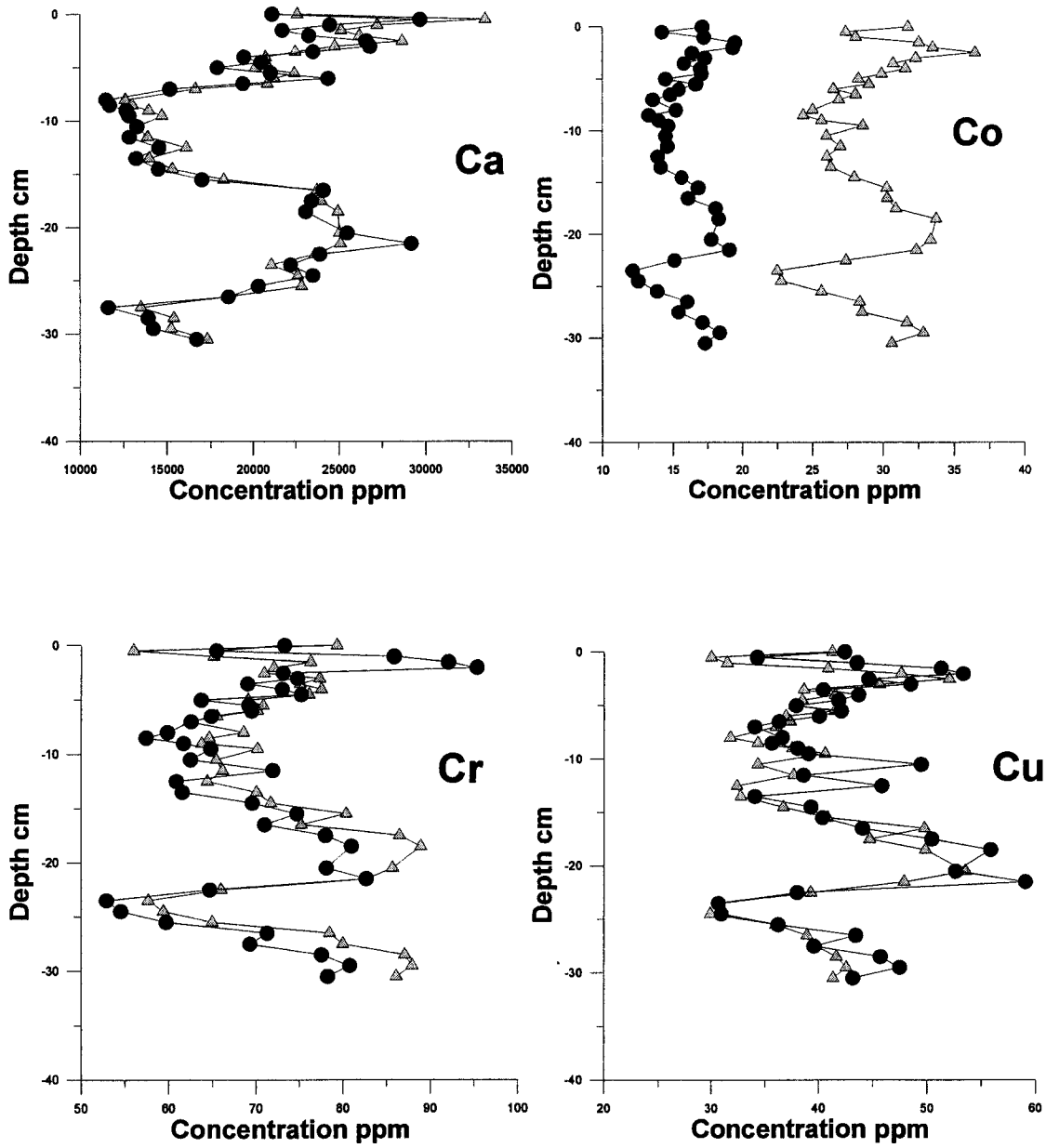

Figure A.1 Comparison of total digestion data obtained by ICP-OES and ICP-MS (△ ICP-OES, • ICP-MS)

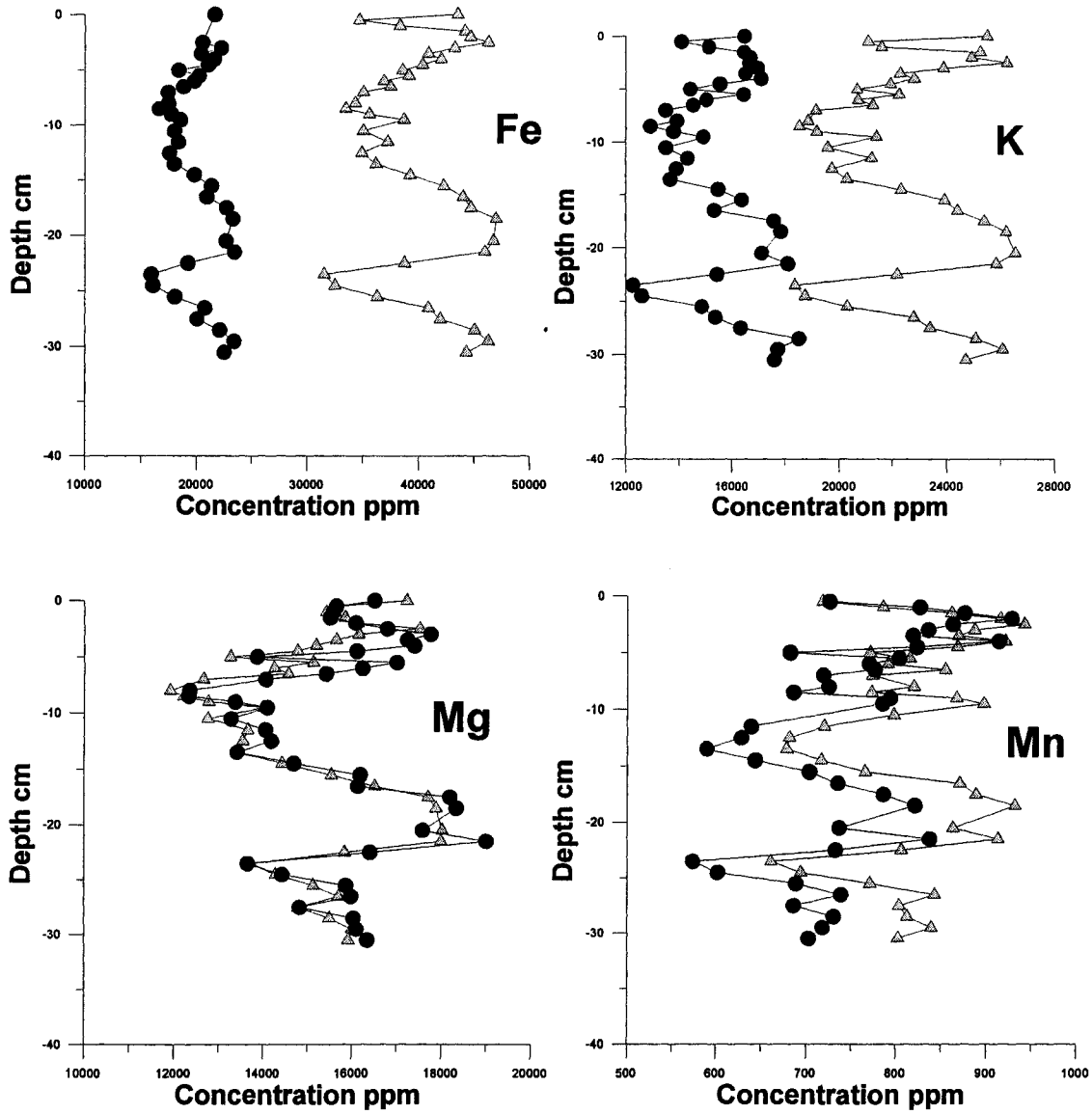

Figure A.1 Comparison of total digestion data obtained by ICP-OES and ICP-MS (△ ICP-OES, • ICP-MS) (Continued)

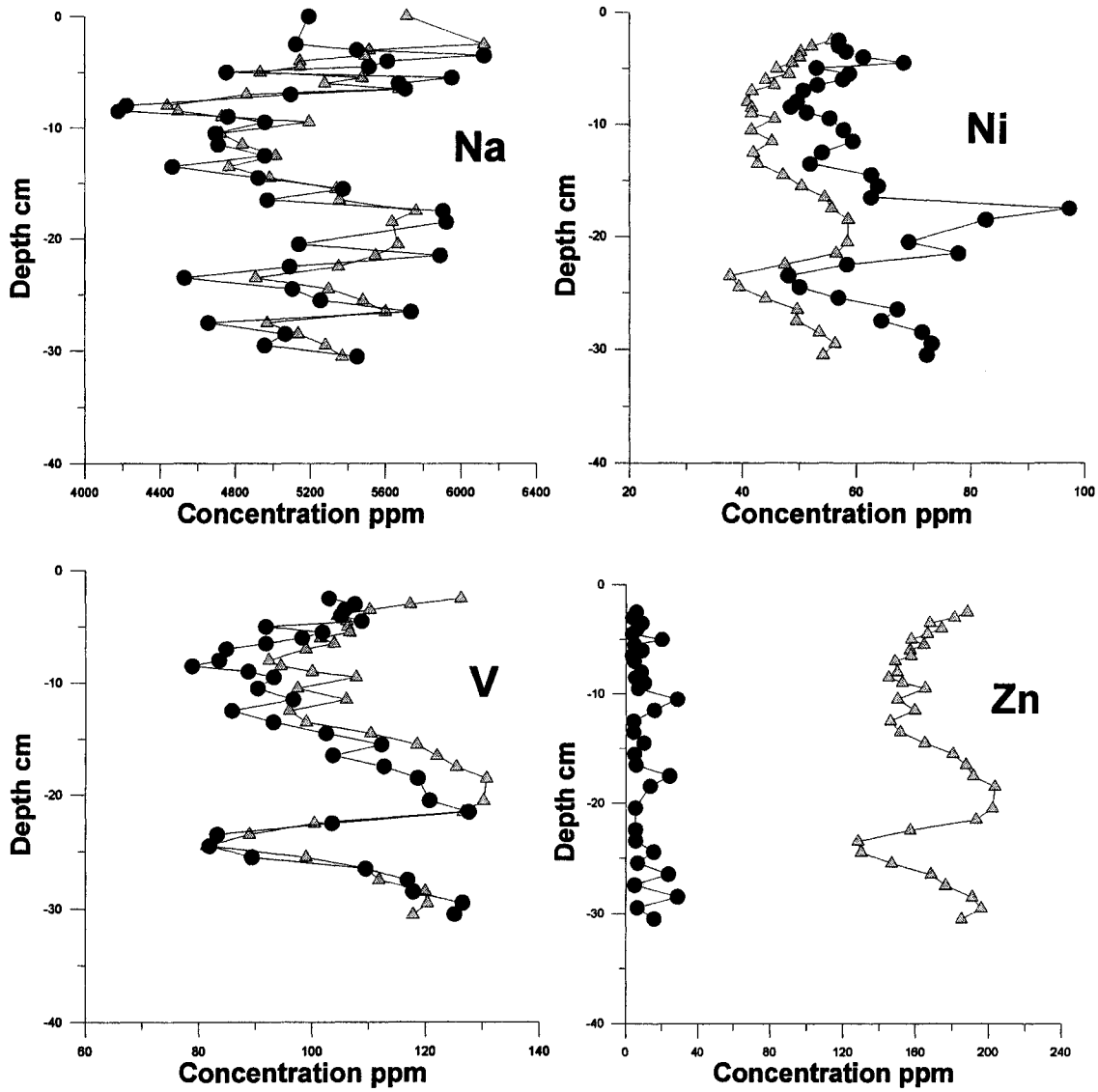

Figure A.1 Comparison of total digestion data obtained by ICP-OES and ICP-MS (△ ICP-OES, • ICP-MS) (Continued)

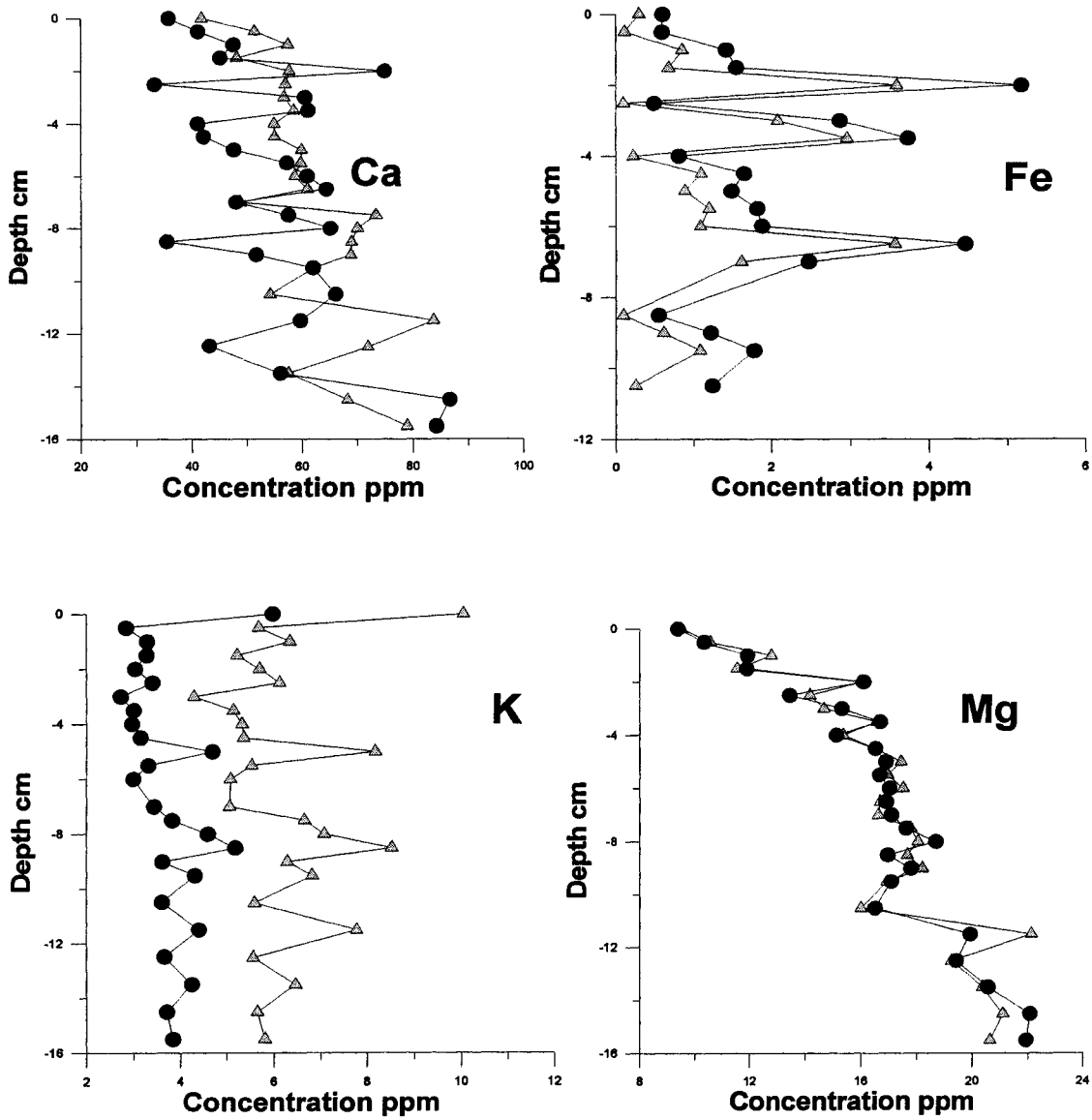

Figure A.2 Comparison of pore water data obtained by ICP-OES and ICP-MS (△ ICP-OES, • ICP-MS)

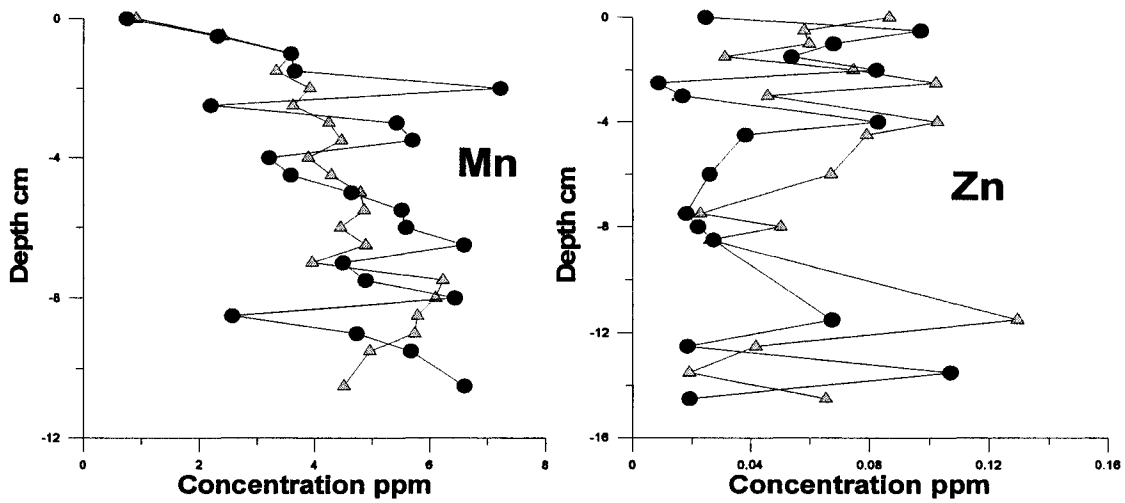

Figure A.2 Comparison of pore water data obtained by ICP-OES and ICP-MS (△ ICP-OES, • ICP-MS)

Table A.1: Results for the total metal content of MESS–3

(ppm unless otherwise stated)

Element	Certified Value (ppm)	ICP-MS (ppm)	ICP-OES (ppm)
Na	1.6 (%)	1.3 (%)	1.4 (%)
Mg	1.6 (%)	1.6 (%)	1.6 (%)
K	2.6 (%)	1.7 (%)	2.4 (%)
Ca	1.47 ± 0.06 (%)	1.32 (%)	1.38 (%)
V	243 ± 10	225.28	231.51
Cr	105 ± 4	95.08	93.9
Mn	324 ± 12	259.92	306.11
Fe	4.34 ± 0.11 (%)	2.06 (%)	4.27 (%)
Co	14.4 ± 2.0	13.38	26.56
Ni	46.9 ± 2.2	60.17	46.27
Cu	33.9 ± 1.6	32.28	28.51
Zn	159 ± 8	10.08	149.33
Cd	0.24 ± 0.01	0.63	
As	21.2 ± 1.1	20.55	
Mo	2.78 ± 0.07	2.63	
U	4	3.37	
Sr	129 ± 11	111.31	

VITA AUCTORIS

NAME	Zhe Song
PLACE OF BIRTH	Tianjin, P.R.China
YEAR OF BIRTH	1971
EDUCATION	M. Sc., University of Windsor, Windsor, Ontario, Canada, 2006
	M. Eng., Nankai University, Tianjin, P.R.China, 1996
	B. Sc., Nankai University, Tianjin, P.R.China, 1993